ACOUSTIC NON-DESTRUCTIVE TESTING FOR WOOD

A thesis by publications presented in fulfillment of the requirements for the

degree of

Doctor of Philosophy

in

Engineering

at Massey University, Albany,

New Zealand.

Adli Hasan Bin Abu Bakar

2023

Abstract

The ability to measure the stiffness of wood is important as it can be used to determine the optimal usage of the timber sample to maximise profitability and increase sustainability. The stiffness of trees and logs is measured in order to segregate them into different grades. Stiffness measurements are also made on juvenile trees and seedlings for breeding trials to improve the stiffness quality of future plantations. The traditional static bending test is considered the gold standard for measuring the stiffness of wood. However, this method is destructive, costly and difficult to use. Non-destructive testing (NDT) techniques have therefore been developed to mitigate these issues. Acoustics is the most common NDT technique used to measure wood stiffness. The time-of-flight method is the only acoustic method which can be used on standing trees. However, literature has shown that stiffness measurements obtained using the time-of-flight method can have a significant overestimation. Studies have reported the potential causes of this overestimation but the exact cause is still not known. In recent years, NDT techniques such as guided wave techniques have been developed for other industries. Guided wave testing is extensively used on metallic structures such as pipes and bars. However, there have been very few studies that utilize guided waves for wood. This thesis investigates the use of guided wave knowledge to identify the cause of the overestimation and to obtain improved NDT measurements. This thesis contains some of the first reported works to perform guided wave measurements on cylindrical wood samples. The results from guided wave experiments show that enhancement and suppression of desired wave modes can be achieved using a ring array of shear transducers. The effects of dispersion on ToF measurements are investigated and it was found that dispersion can be a potential cause of overestimation. Guided wave techniques were developed to obtain acoustic velocity and stiffness measurements for wood. The measurements were compared with the traditional resonance, ToF and static bending methods and improved measurements were obtained. More work can be done to further develop guided wave tools and techniques to be used in the wood industry.

Authors' Declaration

This thesis has been produced according to Massey University's "Doctoral Thesis with Publications" guidelines. Chapters 2 - 4 in this work consist of works that have already been published. Chapter 5 is currently in preparation for submission to a journal. Note that the accepted manuscripts have been used in the chapters in this thesis. Therefore, the contents are the same as the published manuscripts but the chapters may be presented in a different style.

Acknowledgements

There are many friends, family and individuals who have helped me throughout this journey. However, I would like to offer special acknowledgements to those who have helped me the most.

Firstly, I would like to offer my gratitude to my main supervisor Dr Mathew Legg for motivating, encouraging and helping me for the past few years. He has invested so much of his time and energy to help me get through this. I would also like to thank my secondary supervisors Associate Professor Fakhrul Alam and Dr Daniel Konings for giving me advice on how to survive this journey and providing feedback on manuscripts and journal writing. Additionally, I would like to thank Massey University for supporting me throughout my PhD with a doctoral scholarship.

Special thanks to Ruth Brooks who has helped me with administrative things for the past three years. She was a friend and also a mother figure to me. She was someone who was willing to make time to listen to my problems. Her words of encouragement and advice on life have made me stronger throughout the years.

I would also like to sincerely thank my fellow researchers Baden Parr, Tyrel Glass and Nathaniel Faulker for being such wonderful friends. They have helped me navigate through this journey with their experience and never-ending support. Not to forget Gabriel Phang, Kartikay Lal and Blair Dixon for assisting me in the workshop and helping me procrastinate.

On a personal note, I would like to give a huge thanks to my beloved friends Arif Azmi, Halim Fiqri Ishak and Badzlan Khan for their wonderful friendship and for making the year 2022 a wonderful year. Also, thanks to Farah Izzah, Atikah Sulaiman, Hajar Ibrahim and Alya Lee for their wits, humour and company throughout the year. All of them are people who have given me smiles and laughter, provided me with moral support and helped me climb the mountains of life. They are the ones who have helped me maintain my sanity in the final sprint of this journey. Additionally, I want to acknowledge the support of my siblings - Nurul Aqilah, Nurul Afiqah, Adli Husain, Abdul Rahman and Abdul Raif for their encouragement and motivation.

Last but not least, I would like to express my utmost gratitude to my parents Salbiah Hassan

and Abu Bakar Ahmad for giving me the opportunity to live and study in New Zealand. They have sacrificed their time, effort and money for me to be able to do so. Because of their support, I was able to enjoy this beautiful country called Aotearoa. Therefore, I dedicate this to both of you.

Funding

Table of Contents

Chapter 1

Introduction

Background

In New Zealand, the forestry industry provides a gross income of approximately NZD\$6 billion annually and contributes to 1.6% of New Zealand's GDP (Gross Domestic Product). The industry also creates approximately 35,000 jobs in wood production and processing for the country. This has led to wood-based products becoming the third-largest export earner in New Zealand followed by dairy and meat [1]. Therefore, it is important to explore different techniques that can be used to improve the profitability of this industry.

Wood is a complex, inhomogeneous and anisotropic that can be approximated as orthotropic for the wavelengths of the elastic waves used for non-destructive testing. The orthotropic nature of wood means that the mechanical properties are independent in three mutually perpendicular directions: longitudinal, tangential, and radial. The longitudinal axis L is parallel to the fibre grain, the tangential axis T is perpendicular to the grain but is tangent to the growth rings and the radial axis R is normal to the growth rings.

The compliance tensor for wood can be expressed using twelve elastic constants. Three of which are elastic moduli (E_L, E_R, E_T), three shear moduli (G_{LT}, G_{TR}, G_{RL}) and six Poisson's ratios $(\nu_{RL}, \nu_{LR}, \nu_{TL}, \nu_{LT}, \nu_{TR}, \nu_{RT})$. The compliance tensor [2] can be written as
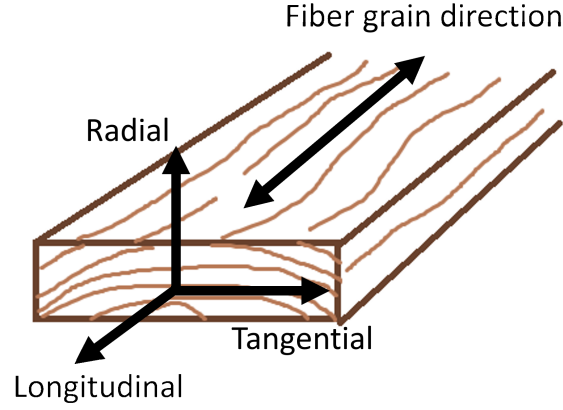
Figure 1.1: Diagram illustration of the three mutually perpendicular axes for wood.

$$\hat{S} = \begin{bmatrix} \frac{1}{E_L} & -\frac{\nu_{RL}}{E_R} & -\frac{\nu_{TL}}{E_T} & 0 & 0 & 0 \\ -\frac{\nu_{LR}}{E_L} & \frac{1}{E_R} & -\frac{\nu_{TR}}{E_T} & 0 & 0 & 0 \\ -\frac{\nu_{LT}}{E_L} & -\frac{\nu_{RT}}{E_R} & \frac{1}{E_T} & 0 & 0 & 0 \\ 0 & 0 & 0 & \frac{1}{G_{RT}} & 0 & 0 \\ 0 & 0 & 0 & 0 & \frac{1}{G_{LT}} & 0 \\ 0 & 0 & 0 & 0 & 0 & \frac{1}{G_{LR}} \end{bmatrix}. \tag{1.1}$$

The stiffness matrix can be obtained by inverting the compliance tensor $\hat{C} = \hat{S}^{-1}$.

The ability to measure the mechanical properties of wood plays a significant role in the foresty industry. It can be used for segregation and pre-sorting of logs and breeding trials for juvenile trees, which can increase sustainability, efficiency and profitability. There are various technologies that can be used to measure wood properties. For example, X-ray computed tomography [3] can be used to measure wood density and moisture content. Pilodyn penetration [4] and Resistograph [5] can be used to measure wood density. Near-infrared (NIR) spectroscopy [6], SilviScan [7], static bending test [8] and acoustics [9] can be used to measure wood stiffness.

The stiffness of wood is one of the main properties of interest for the wood industry. The stiffness of wood is related to the Modulus of Elasticity (MoE) in the longitudinal direction E_L [10]. Stiffness measurements performed on juvenile trees and seedlings are used to help improve the quality of forests through breeding programs [11]. The measurements can also be used for

segregation at the standing tree or log stage which can help increase efficiency and profitability while reducing wood wastage and manufacturing costs [12]. For example, tree growers would be able to estimate the value of the forest before harvesting and sawmills would be able to purchase the right trees before processing in order to maximise grade recovery.

The static bending test is the gold standard that is currently being used to measure the stiffness of wood. The method involves applying a load to a wood sample at a constant rate. The resulting deflection is recorded and the MoE is computed from the load-deflection curve, which is used as a measure of wood stiffness [13]. In addition to being complex and time-consuming, this method can potentially damage or break the sample, which is expensive. To mitigate these issues, non-destructive testing (NDT) techniques have been developed.

Acoustic NDT techniques are widely used in the wood industry as they are inexpensive, non-destructive, fast and simple to use compared to other methods. For acoustic techniques, the stiffness of wood is generally expressed using

$$E_L = \rho \; c_l^2, \tag{1.2}$$

where ρ is the density of the wood sample and c_l is the acoustic velocity in the longitudinal direction. This equation is based on fundamental 1D wave theory and is widely used for stiffness estimation of wood [14].

The two most common acoustic methods are the resonance and time-of-flight (ToF) methods. The ToF method is the only acoustic method that can be used on both standing trees and felled logs whereas the resonance method can only be used on felled logs. The literature has shown that acoustic velocity and stiffness measurements obtained using the ToF method are systematically higher than the resonance and static bending methods [15]. Researchers have suggested potential causes of this overestimation but the exact cause is still not known. Due to this, acoustic measurements obtained using the ToF method on standing trees, seedlings and felled logs are likely to have errors.

Motivation

Within the current literature, the majority of research talks about the "speed of sound" in wood and it is often assumed that the stress waves propagate at a single velocity. This velocity is commonly described using the classical 1D wave theory given by Equation 1.2, which is an approximation and ignores factors such as dispersion. However, there have been several studies that have introduced guided wave theory to explain the wave propagation in elongated wood samples.

Guided wave testing is a NDT technique that is widely used for structural health monitoring of elongated metallic structures. Guided wave testing has been used for defect detection and corrosion monitoring of pipes, beams and rails. Guided waves are expected to propagate in waveguides, which are structures such as rods, beams and plates. Guided waves in rod-like structures are expected to propagate as longitudinal, flexural and torsional wave modes. In guided wave theory, the "speed of sound" used in Equation 1.2 is known as the "rod velocity", which is the velocity of the longitudinal wave mode at zero frequency.

Dispersion is an important aspect of guided wave testing. Dispersion arises from the constrained wave propagation and from the viscoelastic properties of the medium. Dispersion occurs when different frequency components of a wave mode propagate at different velocities in a waveguide. This causes the signal to become distorted as it propagates. Dispersion curves are used to describe the relationship between the frequency and velocity of different wave modes. These can be represented as plots of wavenumber vs frequency, phase velocity vs frequency and group velocity vs frequency. Dispersion can be affected by factors such as material properties and geometric shape. For rod-like structures, dispersion is affected by the diameter. At large diameters, higher order wave modes are expected to propagate at lower frequency ranges.

Currently, there are limited studies pertaining to guided waves for wood. Many of these studies utilise guided wave techniques for structural health monitoring of timber utility poles. There have been some studies that have performed guided wave measurements to obtain dispersion curves and mechanical property measurements for rectangular wood samples. For rectangular

samples, guided waves propagate as Lamb waves, which are different to the rod waves that propagate in rod-like samples. There have been no previous studies that have utilised guided wave knowledge to explain the cause of the ToF overestimation. Additionally, no studies have performed comparisons between the guided wave technique and the acoustic resonance and ToF methods for wood. Could improved NDT measurements of wood properties be obtained through the use of guided wave theory?

This thesis aims to fill some of these gaps in knowledge. In this work, guided wave techniques are investigated and used to identify a potential cause of ToF overestimation and to obtain improved NDT measurements. The scope of this work will be discussed in the following section.

Scope of the study

Wood is highly anisotropic that can be approximated as orthotropic and inhomogeneous material. The stiffness, density and moisture content varies from pith to bark and from top to bottom of the tree. These variations affect the acoustic velocity in wood. The presence of knots, reaction wood, variation in grain angle and temperature can also affect the acoustic velocity [15]. In addition to the fundamental wave modes, higher order guided wave modes would be expected to be able to propagate in larger diameter samples at lower acoustic frequency ranges. These factors make it more complicated to study guided wave propagation in large diameter logs. To study specific guided wave factors such as dispersion, it would be desirable to simplify the wave propagation. This can be achieved by limiting factors that can affect the wave propagation.

In order to better understand guided wave propagation in wood, experiments in this study have mainly been performed on small diameter wooden rod samples. By using a small diameter rod, the effects of inhomogeneity can be reduced. Furthermore, it is possible to only excite the fundamental wave modes in the frequency range of interest. From a practical point of view, the samples used in this study are similar to juvenile trees and seedlings, which are small in diameter. NDT measurements performed on juvenile trees and seedlings can be used for breeding trials to provide future forests with improved stiffness [12; 16]. The outcomes of this study can potentially be applied to these small diameter samples to improve the wood industry.

The findings from this study may also provide some insights into factors that can affect wave propagation in larger diameter wood samples. However, the wave propagation would be more complex in larger samples such as logs and standing trees, which is beyond the scope of this study.

In this study, measurements have only been performed on kiln-dried radiata pine wood samples. The mechanical properties of different types of wood species will vary and can affect guided wave measurements. Furthermore, the acoustic velocity and attenuation in wood are affected by moisture content.

Thesis overview

Chapter 2

Chapter 2 of this thesis investigates the use of ring arrays of shear transducers on a wooden cylindrical rod. This work is the first study to perform ultrasonic guided wave measurements on a wooden rod using a ring array of shear transducers. The 2D FFT method was used to obtain experimental wavenumber dispersion curves of the sample. The study shows that enhancement and suppression of desired wave modes can be achieved using a ring array of transducers or by changing the orientation of the shear transducers. This work was published in a Q1 Journal, Ultrasonics and has the following contributions:

- **Experimental measurement of dispersion curves for a cylindrical wood sample.** Previous guided wave studies for wood had only reported experimental measurements of dispersion curves for rectangular wooden plates. For rectangular plates, guided waves propagate as Lamb waves, which are different to rod waves that propagate in cylindrical rods. This is the first study to obtain experimental dispersion curves for a cylindrical wood sample.

- **Enhancement and suppression of desired wave modes using ring arrays of shear transducers.** There have been previous reports of the usage of ring arrays of transducers for enhancement and suppression of guided waves for wood [17; 18]. However, this is

the first work to use ring arrays of shear transducers. The shear transducer arrays were able to enhance the longitudinal wave mode while suppressing the other wave modes. Additionally, the use of shear transducers also allowed the enhancement of the torsional wave mode which has yet to be investigated in previous studies. This has the potential to be used to obtain the shear strength of the sample.

Chapter 3

The 2D FFT method used in Chapter 2 provided a visual representation of the dispersion curves in the wavenumber domain. The dispersion curve shows that the longitudinal wave mode for the wooden sample is dispersive. However, the 2D FFT method has low resolution, which can lead to high errors when converting from wavenumber to phase velocity. In Chapter 3, we proposed a new method for measuring the rod velocity using guided wave measurements. The proposed method involves obtaining phase velocities directly from guided wave measurements. Experimental dispersion curves were obtained by fitting a dispersion curve through the phase velocity measurements over a range of frequencies. We then obtained the rod velocity which is the phase velocity of the fundamental longitudinal wave mode at zero frequency. Furthermore, the variation and errors in resonance acoustic velocities were found to decrease at higher frequencies due to frequency resolution issues. This could explain the variation in resonance velocities obtained at varying harmonics reported in the literature for wood. The proposed method was also applied to resonance acoustic velocities obtained at a range of harmonics. The guided wave and resonance rod velocities were compared with the traditional resonance and ToF acoustic velocities. The results showed more accurate acoustic velocity measurements were obtained using the proposed method. This work was published in a Q1 Journal, Applied Acoustics and has the following contributions:

- **A new method to obtain the rod velocity and dispersion curve of wood using multi-frequency guided measurements.** This is the first work to measure the rod velocity for wood. This rod velocity was found to produce improved accurate acoustic velocity measurements compared to the traditional resonance and ToF methods.

- **Compare acoustic velocity measurements obtained using guided waves with traditional acoustic methods.** This is the first work to compare acoustic velocity measurements obtained using guided wave techniques with traditional acoustic resonance and ToF techniques.

Chapter 4

The phase velocity dispersion curves obtained in Chapter 3 showed the dispersive nature of the fundamental longitudinal wave mode for wood. In Chapter 4, we investigate the effects of dispersion on ToF measurements obtained using the amplitude threshold First Time of Arrival (FToA) technique. The results showed that dispersion effects can cause signal distortion, particularly at the first arrival of the ToF received signals. This distortion caused ToF velocity measurements to be higher than expected. Using the experimental phase velocity dispersion curves, dispersion compensation was applied to the ToF received signals. Results showed that dispersion compensation was able to mitigate the ToF overestimation. This work was published in a Q1 Journal, Ultrasonics and has the following contribution:

- **The first study to investigate the effects of dispersion on ToF measurements obtained using the FToA amplitude thresholding method.** The results show that dispersion effects can cause the ToF received signals to spread out as it propagates and can also affect the rise time of the signal. This distortion can significantly affect the measured ToF acoustic velocity.

- **The first study to show that dispersion can be a potential cause of ToF overestimation.** No previous research has used guided wave knowledge to explain the cause of the ToF overestimation. There have been some studies that investigated electrical models to approximate the effects of dispersion on acoustic MoE measurements for wood [19; 20]. However, this is the first study to experimentally show that dispersion can cause overestimation in ToF acoustic velocity measurement due to distortion of the ToF received signals.

Chapter 5

In Chapters 2 - 4, we have only focused on comparing acoustic velocity measurements obtained using guided waves with traditional resonance and ToF methods. In Chapter 5, we extend this by obtaining stiffness measurements using the proposed guided wave technique presented in Chapter 3. We then compared the stiffness measurements with the traditional resonance, ToF and static bending methods. This chapter has the following contribution:

- **Compare stiffness measurements obtained using guided waves with resonance, ToF and static bending methods.** Previous guided wave studies for wood have only compared stiffness measurements with static bending methods for rectangular wooden samples. In addition, no previous studies have compared guided wave stiffness measurements with resonance and ToF methods. This is the first work to compare stiffness measurements obtained using all four methods (guided waves, resonance, ToF and static bending) for cylindrical wood samples.

Chapter 6

Chapter 6 concludes the thesis by summarising the main contributions. The chapter also provides some limitations of the current work, improvements that can be made and suggestions for future work.

Note that Chapters 2 - 4 in this thesis are peer-reviewed research journal articles that have been published in Q1 Journals. Chapter 5 is currently in preparation for submission to a journal. A self-contained literature review will therefore be presented in each of the subsequent chapters. Additionally, there is expected to be some repetition in the introduction and methodology of the chapters. Additional notes regarding the published journals have also been added at the start of each chapter.

Appendix 1 contains examples of resonance and ToF velocity calculations. Appendix 2 contains initial guided wave measurements for a 101.67 mm diameter aluminium rod which shows the complexity of wave propagation in large diameter samples. Appendix 3 illustrates the difference

in ToF velocity measurements for aluminum rods with varying diameters. Appendix 4 and Appendix 5 are conference papers that have been published. Appendix 4 contains preliminary results associated with Chapter 2 and Chapter 4. Appendix 5 contains a comparison of the phase velocity measurement technique used in Chapters 3 - 5 with other techniques such as zero-crossing and 2D FFT.

References

[1] Ministry for Primary Industries, Importance of New Zealand Forests, `https://www.mpi.govt.nz/forestry/new-zealand-forests-forest-industry/importance-new-zealand-forests/`, Last accessed on 2022-11-10 (2022).

[2] D. Royer, E. Dieulesaint, Elastic waves in solids I: Free and guided propagation, Springer Science & Business Media, 1999.

[3] Q. Wei, B. Leblon, A. La Rocque, On the use of X-ray computed tomography for determining wood properties: a review, Canadian Journal of Forest Research 41 (11) (2011) 2120–2140.

[4] T. Wang, S. N. Aitken, P. Rozenberg, M. R. Carlson, Selection for height growth and Pilodyn pin penetration in lodgepole pine: Effects on growth traits, wood properties, and their relationships, Canadian Journal of Forest Research 29 (4) (1999) 434–445.

[5] I. Fundova, T. Funda, H. X. Wu, Non-destructive wood density assessment of Scots pine (*Pinus sylvestris* L.) using resistograph and pilodyn, PloS one 13 (9) (2018) e0204518.

[6] S. S. Kelley, T. G. Rials, R. Snell, L. H. Groom, A. Sluiter, Use of near infrared spectroscopy to measure the chemical and mechanical properties of solid wood, Wood Science and Technology 38 (4) (2004) 257–276.

[7] K. J. Jayawickrama, Breeding radiata pine for wood stiffness: review and analysis, Australian Forestry 64 (1) (2001) 51–56.

[8] K. T. Hassan, P. Horáček, J. Tippner, Evaluation of stiffness and strength of Scots pine wood using resonance frequency and ultrasonic techniques, BioResources 8 (2) (2013) 1634–1645.

[9] A. Tsehaye, A. Buchanan, J. Walker, Sorting of logs using acoustics, Wood Science and Technology 34 (4) (2000) 337–344.

[10] X. Wang, Acoustic measurements on trees and logs: a review and analysis, Wood Science and Technology 47 (5) (2013) 965–975.

[11] K. Olaoye, M. Ojo, Non-destructive acoustic assessment of wood quality in trees and logs and the effects of silvicultural treatments: a review, International Wood Products Journal (2022) 1–16.

[12] X. Wang, P. Carter, R. J. Ross, B. K. Brashaw, Acoustic assessment of wood quality of raw forest materials: a path to increased profitability, Forest Products Journal 57 (5) (2007) 6–14.

[13] M. Babiak, M. Gaff, A. Sikora, Š. Hysek, Modulus of elasticity in three-and four-point bending of wood, Composite Structures 204 (2018) 454–465.

[14] R. J. Ross, Nondestructive testing for assessing wood members in structures: A review, US Department of Agriculture, Forest Service, Forest Products Laboratory, 1994.

[15] M. Legg, S. Bradley, Measurement of stiffness of standing trees and felled logs using acoustics: A review, The Journal of the Acoustical Society of America 139 (2) (2016) 588–604.

[16] M. Ivković, W. J. Gapare, A. Abarquez, J. Ilic, M. B. Powell, H. X. Wu, Prediction of wood stiffness, strength, and shrinkage in juvenile wood of radiata pine, Wood Science and Technology 43 (3) (2009) 237–257.

[17] J. El Najjar, S. Mustapha, Understanding the guided waves propagation behavior in timber utility poles, Journal of Civil Structural Health Monitoring 10 (5) (2020) 793–813.

[18] U. Dackermann, Y. Yu, E. Niederleithinger, J. Li, H. Wiggenhauser, Condition assessment of foundation piles and utility poles based on guided wave propagation using a network of tactile transducers and support vector machines, Sensors 17 (12) (2017) 2938.

[19] D. Ouis, On the frequency dependence of the modulus of elasticity of wood, Wood Science and Technology 36 (4) (2002) 335–346.

[20] M. J. Frampton, Acoustic studies for the non-destructive testing of wood., Ph.D. thesis, University of Canterbury (2019).

Chapter 2

Ultrasonic Guided Wave Measurement In a Wooden Rod Using Shear Transducer Arrays

This chapter is republished in accordance with Elsevier's copyright policy. The work presented here is the accepted version of the published article. Therefore, the contents are the same but there may be stylistic differences to the published article.

Additional notes:

- The wood sample was bought off-the-shelf. Therefore, the origin and age of the sample are unknown. In order to support the rods during measurements, two foam pads were placed under the sample near each end.

- The amplitude threshold first time of arrival (FToA) technique was used to determine the propagation time for the ToF method. Refer to Appendix 1 for more details on how the ToF and resonance acoustic velocities were calculated.

- For guided wave method, a transmit signal with a high number of cycles would produce a large temporal wave packet. This can distort the received signal if the transmission of the wave packet has not ended. Additionally, a transmit signal with a low number of cycles would be wideband which can increase dispersion effects. Therefore in this study, a five-cycle sine wave was used as a compromise to obtain a short temporal wave packet

with a narrow bandwidth.

- For processing, the received signals were normalised by the maximum peak amplitude. When using multiple receivers, the average of the normalised received signals from all the receivers was used.

- The calculated wavenumber and frequency resolutions for the wavenumber-frequency plots are 6.22 m^{-1} and 0.1 kHz respectively.

Ultrasonic Guided Wave Measurement in a Wooden Rod using Shear Transducer Arrays

Adli Hasan Abu Bakar, Mathew Legg*, Daniel Konings, Fakhrul Alam

Department of Mechanical and Electrical Engineering, Massey University, Auckland, New Zealand

Abstract

Research related to acoustic/ultrasonic guided wave testing in wood is still at an early stage. This paper describes the first study to perform ultrasonic guided wave measurements in a wooden rod using arrays of shear transducers. Enhancement of either longitudinal L(0,1) or torsional T(0,1) wave modes and suppression of other modes was able to be achieved using these arrays. At low frequencies, it was found that the L(0,1) wave mode had a similar speed to that obtained using the traditional resonance and time of flight methods. The torsional T(0,1) wave mode has not been used before for non-destructive testing of wood. Since it is non-dispersive, it would appear to be suitable for wood property estimation and structural health monitoring of wooden structures. These results indicate that ultrasonic guided wave testing techniques have strong potential to be used to provide improved measurement of wood properties and structural health monitoring of wooden structures.

Keywords: Wood, guided waves, ultrasonic, acoustic, dispersion curves, rod, radiata pine, aluminium, ToF, resonance.

1. Introduction

The ability to measure wood properties is important for a range of industries. In forestry, measurement of wood properties such as stiffness allows segregation and presorting to be performed before the logs are processed. This can directly increase the quality of the processed wood and result in higher profitability [1]. Structural health monitoring of wooden structures such as bridges, utility poles, and piles is also performed to detect decay [2]. There are a range of techniques that can be used to measure wood properties, such as mechanical bending tests, Near Infrared (NIR), computer tomography (CT) scans, and acoustics [3].

Acoustic testing is one of the most commonly used Non-Destructive Testing (NDT) methods as it is simple to use and is generally inexpensive compared to other approaches. Stiffness is the main wood

---

*Corresponding author
Email addresses: A.Hasan@massey.ac.nz (Adli Hasan Abu Bakar), M.Legg@massey.ac.nz (Mathew Legg),
D.Konings@massey.ac.nz (Daniel Konings), F.Alam@massey.ac.nz (Fakhrul Alam)

property measured using acoustics. It is related to the Modulus of Elasticity (MoE) in the longitudinal direction (direction along the grain). This is generally estimated using

$$E_L = \rho \; c_l^2 \tag{1}$$

where c_l is the acoustic velocity in the longitudinal direction and ρ is the density of the material. The two common methods to measure the acoustic velocity of wood is resonance and Time of Flight (ToF) [4].

The acoustic technique described above uses theory based on the assumption of 1D wave propagation in an infinitely thin, homogeneous, isotropic rod [5]. However, wood is orthotropic (speed of sound varies with direction) and a log or timber sample will have a finite diameter. For an elongated structure like a rod or log, guided waves would be expected to occur. We hypothesize that further research into guided waves in wood can lead to improved measurement of wood properties.

Guided waves are generally composed of different types of vibrations, which are referred to as wave modes. These are generally dispersive in nature. This means that different frequency components of the signal propagate at different speeds along the structure. This causes the signal to spread out as it propagates. Dispersion curves plot the variation in the speed of the wave modes with frequency. These can be represented as either phase velocity, group velocity, or wavenumber plotted as a function of frequency [6].

There have been extensive studies on guided waves in metal structures [7, 8]. Metal structures are generally isotropic and homeogeneous. In contrast, wood is highly inhomeogeneous, orthotropic, and has strong attenuation which increases with frequency. Because of this, wave propagation in wood is more complex. This might explain why there have been relatively few studies using acoustic/ultrasonic guided waves for wood.

Several studies have performed experimental measurement of guided waves in timber samples. Veres et.al [9] measured phase velocity dispersion curves for a rectangular wooden bar using a laser vibrometer and the 2D Fast Fourier Transform (FFT) method described Alleyne and Crawley [10]. Additionally, Dahmen et.al [11] utilized air-coupled capacitive transducers to experimentally measure dispersion curves for a wooden plate. The phase velocities obtained from the dispersion curves were then used to estimate the elastic constants for the wood sample. However, no previous studies have been found which have performed experimental measurement of dispersion curves for wooden circular rods, poles, or logs.

Fathi et.al also used guided waves to measure the properties of small wooden plates. They measured the velocity of the asymmetric Lamb wave mode (A0) Lamb wave by measuring the phase difference at different receiver positions [12, 13]. Machine learning techniques were used to combine measurement of A0 Lamb wave speed, moisture content, and density to predict the MoE and Modulus of Rupture (MoR) of wood [14].

Guided waves have also been investigated for nondestructive evaluation of decay below ground level in wooden utility poles and piles. Finite Element Modelling (FEM) has been performed to investigate wave propagation in timber utility poles [15, 16]. This includes simulated dispersion curves. Holt et al. developed

a technique for using a dispersive flexural wave mode generated by a hammer hit to measure the length of undecayed poles in the ground [17]. A similar method was used by Sriskantharajah et.al [18].

Subhani performed simulations which suggested that multiple transducers could be arranged around a pole to enhance reception of longitudinal and flexural wave modes [19]. Similarly, Dackermann et.al used a ring of tactile transducers which aimed to enhance the excitation of the longitudinal wave mode compared to other modes in timber utility poles [20]. Najjar and Mustapha were able to enhance the longitudinal wave mode and suppress flexural wave modes by using a ring of Micro Fiber Composites (MFC) actuators attached onto a timber utility pole both experimentally and numerically using simulations [21].

The transducers that were used in the above studies appear to have been compressional transducers. These generate and/or receive vibration mainly in a direction normal to the surface of the transducer. To the best of the authors' knowledge, the only previous study to have used shear transducers for generating/receiving guided waves in wood is that presented by Legg and Bradley [22]. In that study, the authors showed that vibrations with different speeds could be generated by aligning the shear transducers in either the torsional or longitudinal direction. It was believed that this was caused by different types of guided wave modes being generated/received. However, more work was required to confirm this.

This paper builds on the findings of [22]. Guided wave measurements were made using shear transducer on a 16 mm diameter wooden rod. Experimental dispersion curves were measured. Enhancement of specific wave modes was able to be achieved by varying the alignment of the shear transducers and using a ring array of transducers. For comparison, the same experimental measurements are repeated for an aluminium rod of similar dimensions, whose dispersion curves were known.

The work presented in this paper offers the following contributions. To the best of the authors' knowledge, it is the first work to:

(1) Experimentally measure guided wave dispersion curves for a wooden cylindrical rod.

(2) Provide a comparison between traditional resonance and ToF speed measurements in wood with the measured dispersion curves.

(3) Use a ring of shear transducers to enhance the excitation and reception of desired guided wave modes in wood while suppressing the other wave modes.

This remainder of the paper is configured as followed. Section 2 describes the methodology and samples used. The experimental results are provided in Section 3. Experimentally measured dispersion curves are shown and the effect of using a ring array of transducers are outlined. Finally the conclusion is provided in Section 4.

2. Materials and Methods

2.1. Wood and aluminium rod samples

A kiln-dried radiata pine rod with a diameter of 16 mm and length of 2460 mm was used in this study. The sample was selected such that it did not contain any obvious defects or knots. For comparison purposes, a 6061-T6 aluminium rod with a diameter of 16 mm and length of 2510 mm was used.

Theoretical dispersion curves for the aluminium rod are shown in Figure 1. These were obtained using GUIGUW [23] assuming a density of 2710 kg/m^3, Young's Modulus of 68.9 GPa and Poisson's ratio of 0.33. The dispersion curves show that no higher-order wave modes exists for frequencies below 100 kHz. They also show that the flexural F(1,1) and to a lesser extent the longitudinal L(0,1) wave modes are dispersive in this frequency range whereas the torsional T(0,1) is non-dispersive.
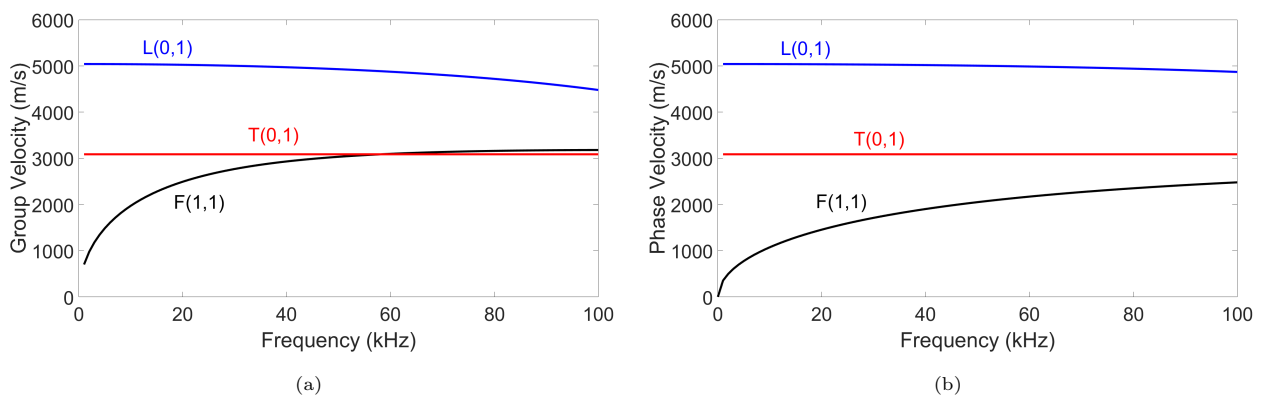

Figure 1: Theoretical dispersion curves for a 16 mm aluminium rod using GUIGUW showing (a) group velocity and (b) phase velocity.

2.2. Hardware

Shear transducers from Plant Integrity Ltd (TWI) UK were used for both transmission and reception [24]. These transducers have a shear piezoelectric ceramic on their contact face which was aligned to excite/receive vibration in a direction parallel to the contact face, as shown in Figure 2(a). These are dry-coupled transducers which were pushed against the samples using springs, see Figure 2(b). For longitudinal and torsional transmission and reception, the transducers were respectively aligned either parallel or at right angles to the wood grain direction of the rod. The orientation of the transducers can be seen in Figure 3. An array of four transducers could also be mounted around the sample using the mounting system shown in Figure 4. Each transducer was pushed against the sample using springs.

An acoustic/ultrasonic signal could be generated on the samples using a hammer hit. However, more control over the signal generated was able to achieved by transmitting a signal on one or more transducers. An arbitrary signal such as a sine or chip signal was generated using MATLAB and outputted from an
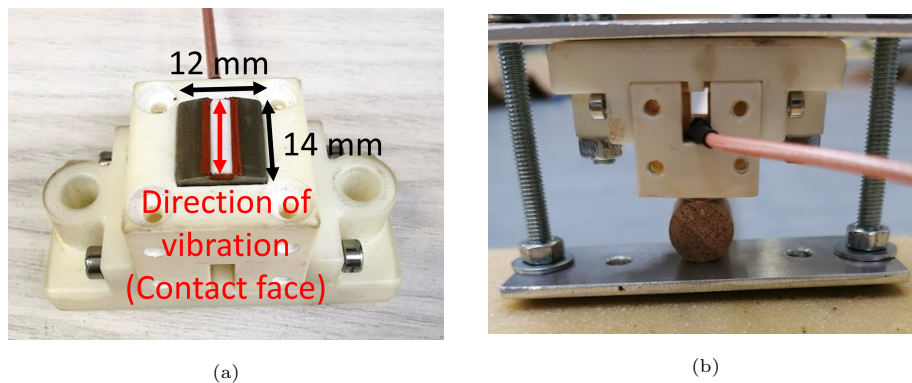
Figure 2: Photo (a) shows one of the shear transducers used in the experiment. Photo (b) shows the setup used to push a single transducer against the wooden sample.

Agilent 33220A Function Generator which has a sampling rate of 20 MHz and resolution of 16 bits. The resulting signal was amplified using a custom built linear power amplifier. This could output signals with a amplitude of up to 400 Vpp. If an array of transducers were to be used for transmission, these could be wired in parallel so that the same signal was transmitted on all the transducers.

The resulting acoustic/ultrasonic signal could be measured using either a GRAS 46BF-1 microphone (for resonance tests) or using one or more transducers. The signal from each transducer was able to be amplified using a custom designed preamp circuit. The signal from each transducer was then sampled using a separate Analog to Digital Converter (ADC) channel of a Data Translation DT9832A module. A sampling rate of 2 MHz and a resolution of 16 bits were used. The sampled signal was then processed using MATLAB.

2.3. Experimental procedure

2.3.1. ToF and resonance tests

Resonance and ToF speed of sound measurements were performed so that the results can be compared to guided wave measurements to determine any correlation between them. Note that the modulus of elasticity obtained using the resonance speed of sound in wood has been reported to have good correlations with
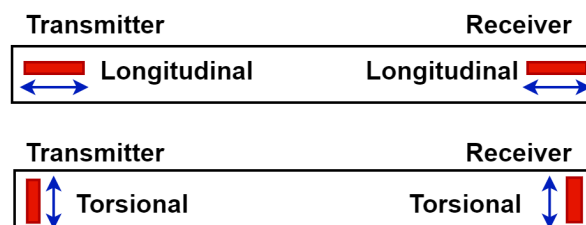

Figure 3: Diagram showing the transducer alignment in either the longitudinal or torsional direction on the rod. The red rectangle shows the contact face of the transducer and the blue arrows shows the direction of vibration.
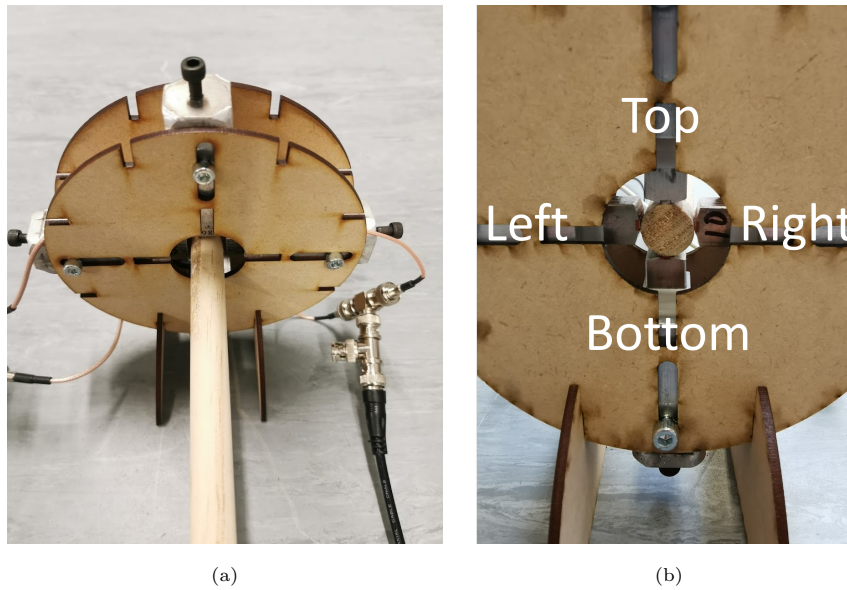
(a)   (b)

Figure 4: Photos of the transducer array mounting system used to position the transducers in a ring around the sample.

mechanical bending tests.

Measurements were obtained to calculate the resonance speed of sound for the sample. A GRAS 46BF-1 microphone was placed near one end of the sample and the opposite end was hit with a hammer. The resulting signal was sampled and resonant frequencies were obtained using the Fast Fourier Transform (FFT). The resonance speed was then calculated using

$$c_{res} = \frac{2Lf_n}{n} \tag{2}$$

where L is the length of the sample and f_n is the nth resonant frequency (where $n = 1, 2, 3..$).

ToF measurements were also obtained. A transducer was positioned at each end of the sample. A hammer hit was performed at one end of the sample and the received signal from both transducers were recorded. The time T taken for the signal to first propagate between the two receiver transducers was obtained. A ToF speed was then calculated using

$$c_{tof} = \frac{\Delta d}{T}, \tag{3}$$

where Δd was the separation between the transducers. The average of 10 samples was taken as the ToF velocity.

2.3.2. Pitch catch and dispersion curve measurements

Pitch-catch measurements are often used for guided wave testing. In a pitch-catch configuration, one transducer acts as a transmitter and another transducer acts as a receiver. Pitch-catch measurements were

made where the transmit and receive transducers were placed at opposite ends of the rod. A 20 kHz five cycle sine wave was used as the transmit signal and the resulting signal was saved to file. Measurements were initially made using a single transmit and a single receive transducers. This was then repeated using the transmit and receive arrays.
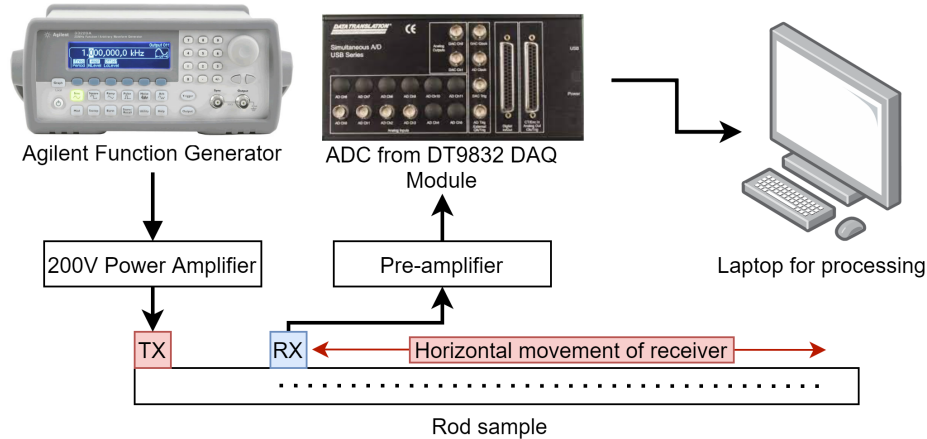

Figure 5: Experimental setup for obtaining the wavenumber plot

Guided wave dispersion curve measurements were performed using the experimental setup shown in Figure 5. A transmit transducer was attached at one end of the rod and a receiver transducer was attached 1000 mm away in a pitch-catch configuration. A chirp signal ranging from 5 to 100 kHz was transmitted on the transducer and the resulting signal was recorded. The receiver was then displaced 5 mm away from its initial position and the process was repeated for a total of 201 measurements. This experiment was repeated using the transmit and receive arrays.

Experimental dispersion curves were then obtained from this data using the method described in reference [10]. The sampled signal from all the measurement positions were formed into a $201 \times N$ matrix, where N is the number of samples. A 2D FFT was then performed on this matrix and the result was plotted. This converts the matrix from the space-time domain to the wavenumber-frequency domain. The theoretical phase velocity v_{ph} for the aluminium rod could be overlaid on the wavenumber - angular frequency plot using the relationship

$$v_{ph} = \frac{\omega}{k} \tag{4}$$

where ω is the angular frequency and k is the wave number. This was rearranged to give

$$k = \frac{\omega}{v_{ph}}. \tag{5}$$

On the wave number-frequency plot, a non-dispersive wave mode will result in a straight line passing through the origin with a slope of $1/v_{ph}$. A dispersive wavemode will result in a curved line. Note that the group

velocity is the rate of change of the angular frequency with respect to the wavenumber

$$v_{gr} = \frac{\delta\omega}{\delta k}. \tag{6}$$

3. Results

3.1. Resonance and time of flight

Resonance and TOF measurements were made using the methodology described in Section 2.3.1. The resonance and ToF speed of sound measurements are given in Table 1. There is a good correlation between the measured average resonance and ToF velocity for wood and aluminium rods. The difference is approximately 0.6% and 2.4% respectively, which is roughly within the measurement error.

Table 1: Average resonance and ToF velocity for wood and aluminium rod samples

Material	**Resonance velocity (m/s)**	**ToF velocity (m/s)**
Wood	4456 ± 58	4428 ± 116
Aluminium	5068 ± 78	5197 ± 32

3.2. Effect of transducer orientation and placement

Pitch catch measurement were performed using the method described in Section 2.3.2. The transducers were aligned in different directions to generate vibrations in the longitudinal and torsional direction respectively.
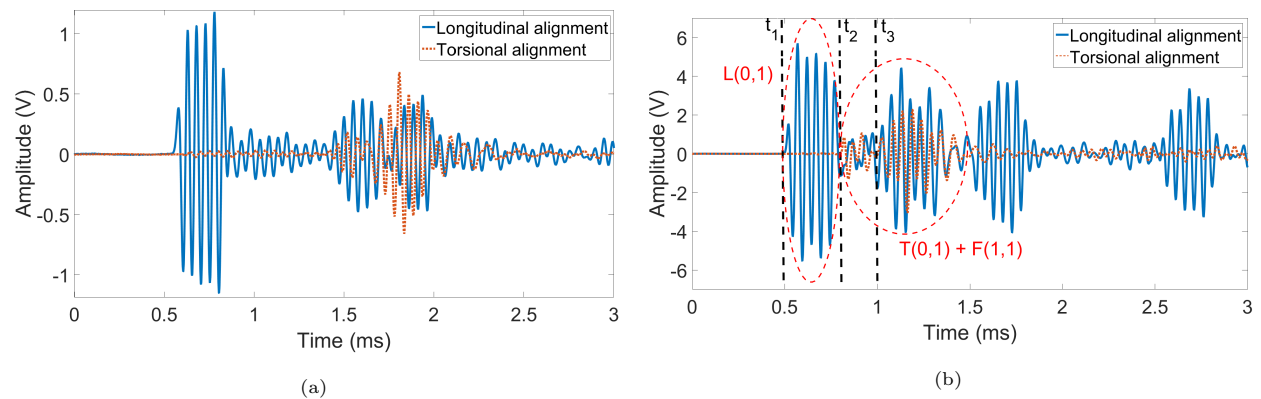

(a)

(b)

Figure 6: Plots of received signal for a 20 kHz 5 cycle sine wave excitation using different transducer orientation for (a) wood and (b) aluminium samples.

Figure 6 shows an example of the received signal for wood and aluminium using a single transmit and receive transducer. The labels t_L, t_F and t_T for the aluminium rod plot are the expected arrival times of the

longitudinal, flexural, and torsional wave modes respectively. These are obtained from the dispersion curves from Figure 1(a). These plots shows that when the transducers were aligned in the torsional direction, the arrival of the received signal is slower compared to the longitudinal direction. This was observed for both wood and aluminium.

These pitch catch measurements were repeated using a single transmit transducer and four receiver transducers configured in a ring array. Figure 7 shows the normalized received signal for wood with all transducers orientated in the longitudinal and then torsional directions. It can be seen that part of the signal from the individual transducers are in phase but other parts are out of phase.
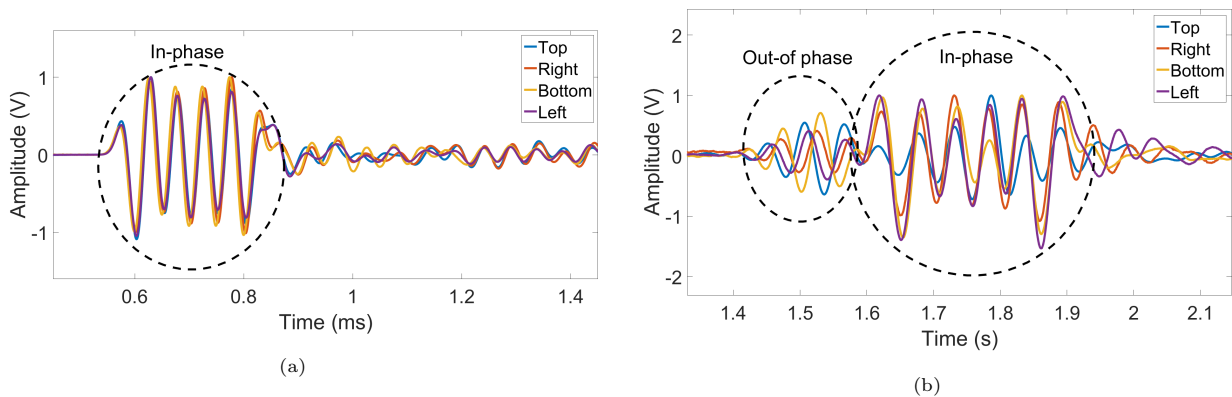

Figure 7: Plots showing the received signal for for a 20 kHz 5 cycle sine wave with four receivers attached onto different positions of the wood sample where the transducers are orientated in the (a) longitudinal and (b) torsional directions.

The measurements above were repeated for the aluminium rod. Using the theoretical dispersion curves, it was observed that the fundamental longitudinal $L(0,1)$ and torsional $T(0,1)$ wave modes were in phase respectively when the transducers were aligned in the longitudinal and torsional directions. However, the flexural wave mode was out of phase. This is what we would expect for a ring of transducers. By summing the signal from all four transducers, longitudinal or torsional wave modes can be enhanced depending on the orientation of the shear transducers while the out of phase flexural wave mode is suppressed. This feature has been used in guided wave testing of structures such as pipes to try to improve the accuracy of measurements by using single wave mode excitation and reception, mainly using the non-dispersive $T(0,1)$ wave mode [25]. However, this had not been investigated before for wooden rods/poles. The results presented here show that there is strong potential for guided wave techniques, which have been developed in other industries, to be applied for improving nondestructive measurement of wood.

3.3. Measured dispersion curves

Experimentally measured dispersion curves were obtained using the 2D FFT method described in Section 2.3.2. Results for the aluminium rod are shown first so that we can correlate results with theory. Results for wood are then presented.
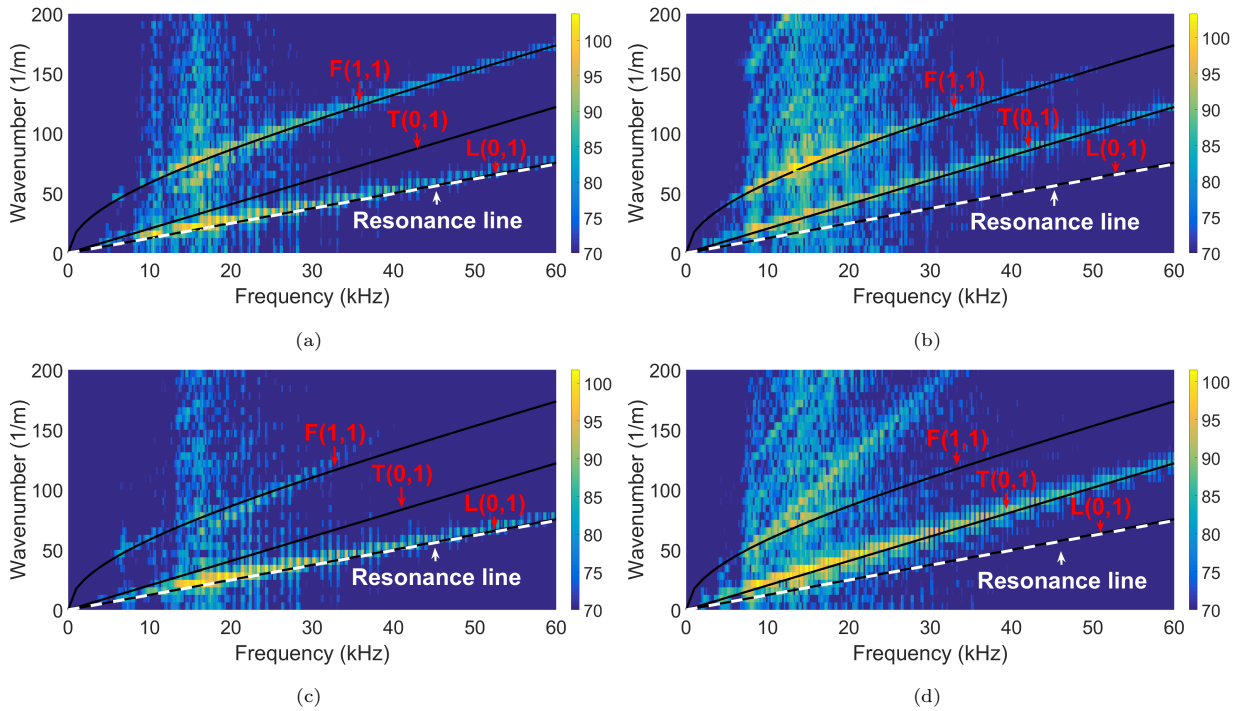
3.3.1. Aluminium

(a)

(b)

(c)

(d)

Figure 8: Wavenumber-frequency plots for the aluminium rod showing the effect of using one transmitter oriented in the (a) longitudinal direction and (b) torsional direction and four transmitters oriented in the (c) longitudinal direction and (d) torsional direction. A single receiver was used which was aligned in the same direction as the transmitter. Overlaid are theoretical dispersion curves.
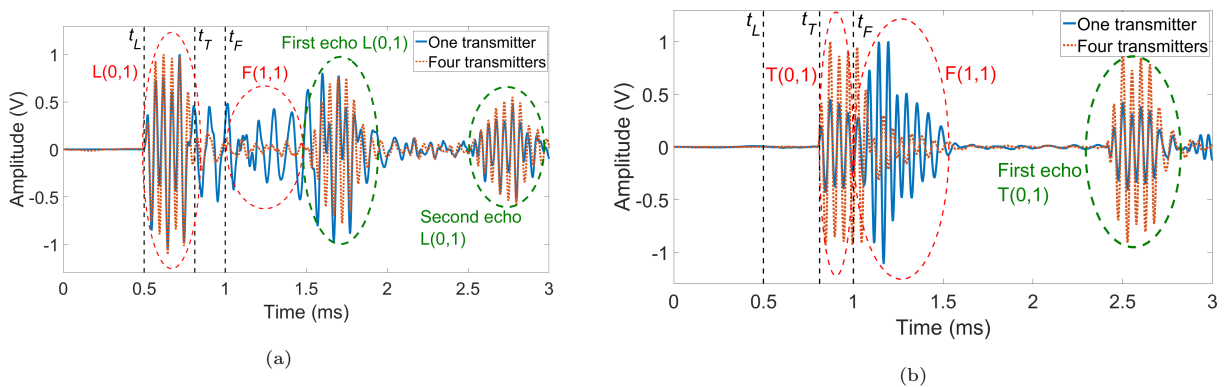

(a)

(b)

Figure 9: Amplitude normalised pitch catch received signal plots for the aluminium rod showing the effect of using one and four transmitters which are all orientated in either the longitudinal (a) or torsional (b) direction.

Figure 8 shows the experimental wavenumber-frequency plots for the aluminium sample using one and four transmitters where all transducers were either aligned in the longitudinal or torsional direction. Theoretical dispersion curves for the aluminium sample were obtained using GUIGUW and overlaid over the

experimental plots. Equation 5 was used to overlay a line which corresponds to the the measured resonance speed (see Table 1). It can be seen that the resonance speed line approximately aligns with the longitudinal L(0,1) wave mode. Note that there are linear features in the wavenumber plots which do not correspond to the theoretical dispersion curves. These appear to be due to mode conversion of the signal when reflections occur. This could be mitigated by windowing the data to remove multiple echoes being processed by the 2D FFT. Using a sample with a longer length would be beneficial for this.

Figure 8(a) show that when a single transmit and a single received transducer are aligned in the longitudinal direction, two dispersion curves are observed which align with the F(1,1) and L(0,1) wave modes. However, when four transmit transducers are used with longitudinal alignment, only the L(0,1) wave mode was observed, as shown in Figure 8(c). Similarly, we can see in Figure 8(b) that using one transmit and one receive transducer aligned in the torsional direction resulted in both the T(0,1) and F(1,1) wave modes being observed. However, when four transmitters were used, the F(1,1) mode was suppressed, see Figure 8(d). This can also be seen in the time domain plots shown in Figure 9.
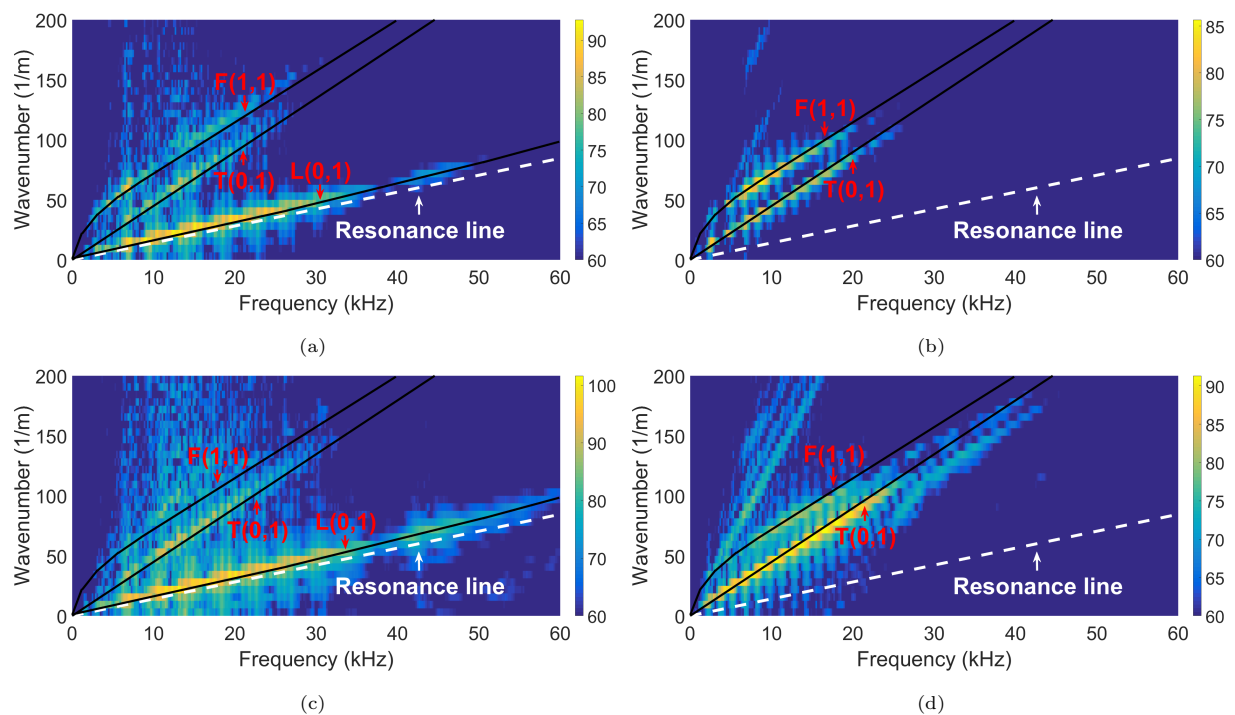
3.3.2. Wood

Figure 10: Wavenumber-frequency plots for the wooden rod showing the effect of using one transmitter oriented either in the (a) longitudinal direction or (b) torsional direction and four transmitters oriented in either the (c) longitudinal direction or (d) torsional direction.

Figure 10 shows the wavenumber-frequency plots obtained for the wood sample with varying alignment

and number of transducers. The mechanical properties of the wooden sample were not known and hence theoretical dispersion curves were not simulated. Curves have therefore been overlaid onto the wavenumber-frequency plots to show the wave modes. Given the dimensions of the sample, three dispersion curves which represents the fundamental flexural, torsional and longitudinal modes are expected to be observed.

There are similarities between the plots obtained for the wood sample in Figure 10 and the aluminium sample in Figure 8. The resonance speed line aligns with the longitudinal wave mode at frequencies below 30 kHz. Different wave modes are excited when the transducers are aligned in the longitudinal and torsional direction. Using a ring array of four transmitters, which are aligned in either the longitudinal or torsional directions, helps to enhance the L(0,1) or T(0,1) modes and suppress other modes as seen in Figure 10(c) and (d). The use of shear transducers in a ring array can potentially be used for single mode excitation/reception in wood. This is desirable for nondestructive testing using guided waves as it enables more accurate measurements to be made.

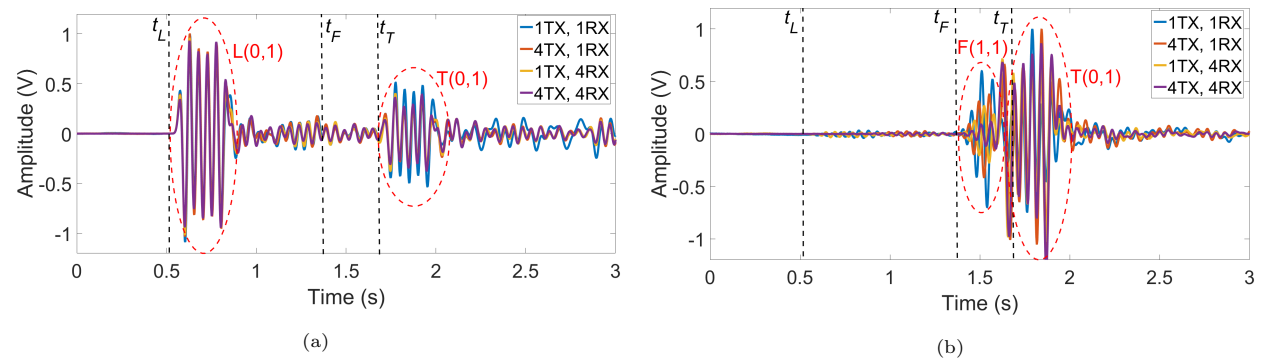### 3.4. Multiple transducers for transmit and receive

Figure 11: Amplitude normalised received signal plots for the wooden rod showing the effect of varying the number of transmitters and receivers orientated in the (a) longitudinal and (b) torsional directions.

The effect of using a different number of transmit and receive transducers configured in a ring array was investigated using pitch catch measurements on the wooden sample. The results are shown in Figure 11. The received signal was normalised according to the maximum amplitude of the signal. This was done so that relative comparisons can be made. The labels t_L, t_F and t_T are the expected arrival times of the longitudinal, flexural and torsional wave modes respectively and were calculated using the tangent/slope of the wave mode at the frequency of interest in the wavenumber-frequency plot in Figure 10 and converting this to group velocity using Equation 6. It can be seen from Figure 11 that the use of a ring array enable more control over the wave modes being excited and received. This is illustrated in Table 2. For example, with longitudinal alignment, the Root Mean Squared (RMS) of the torsional T(0,1) wave mode dropped from 56% to 39% relative to the L(0,1) wave mode when the transmit and receive ring arrays were used.

26

Table 2: Table showing the percentage (%) reduction of wave modes relative to L(0,1) when the transducers were aligned in the longitudinal direction and relative to T(0,1) when the transducers were aligned in the torsional direction for varying number of transmitters (TX) and receivers (RX).

	Longitudinal alignment		Torsional alignment	
	F(1,1)	**T(0,1)**	**L(0,1)**	**F(1,1)**
1TX, 1RX	9.2	56	4.6	86
4TX, 1RX	9.5	38	0.4	33
1TX, 4RX	9.3	40	3.0	26
4TX, 4RX	9.6	39	0.3	12

Similarly, for torsional alignment of the transducers, the flexural F(1,1) wave mode was reduced from 86 to 12% relative to the torsional T(0,1) wave mode when the arrays were used.

3.5. Comparison between the resonance speed and dispersion Curves

Figure 12 shows the dispersion curves for the longitudinal wave mode L(0,1) and the resonance speed line for both aluminium and wood. For aluminium, the resonance speed line aligns well with L(0,1) for frequencies below 100 kHz but starts deviating afterwards, as seen in Figure 12(a). The straight line represents the non-dispersive region of the L(0,1) whereas the curved line corresponds to the dispersive region of the wave mode. Similarly, we can see in Figure 12(b) for the wood sample. The resonance speed line aligns with L(0,1) mode but at a lower frequency ($\approx$30 kHz) compared to aluminium.

4. Conclusion

Guided wave measurements have been performed on a 16 mm diameter wooden cylindrical rod using shear transducers. For comparison, the experiments were repeated on an aluminium rod with similar dimensions. Experimental dispersion curves were obtained using a 2D FFT method. Results showed that the amplitude of the wave modes could be controlled by orientating the shear transducers in either the longitudinal or torsional directions. Further control of the wave modes was able to be achieved using ring arrays of shear transducers. This was most noticeable for torsional alignment of the transducers where it was able to significantly suppress the flexural wave mode. It was found that the resonance speed aligns well with the speed of the longitudinal L(0,1) wave mode at low frequencies.

In future work, we plan to perform experiments on samples of different diameters to investigate the correlation between diameter of the sample with the resonance speed, ToF speed and guided wave measurements. Additionally, future work is planned to be performed to investigate the correlation between the different
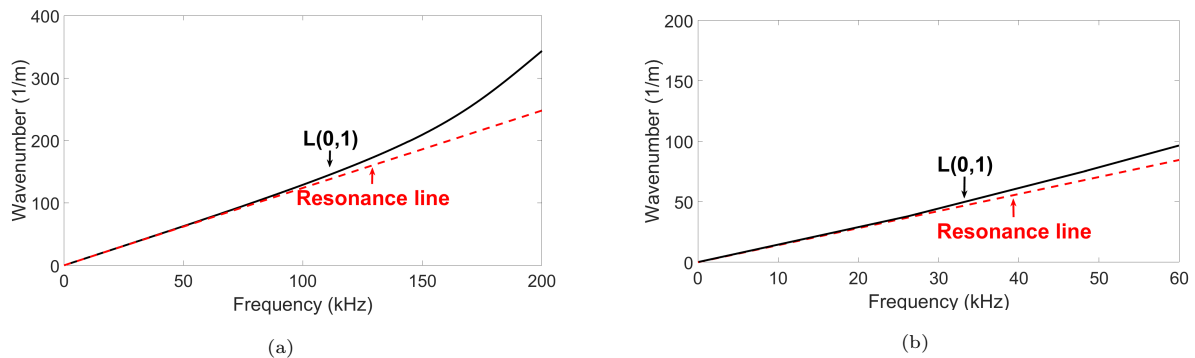
Figure 12: Plot of dispersion curves for longitudinal wave modes and resonance velocity for (a) aluminium and (b) wood

wave modes and mechanical properties of wood. For example, the torsional wave mode should be related to the shear modulus.

To the best of the authors' knowledge, no previous studies have been performed using the torsional wave mode for non-destructive testing of wood. The torsional wave mode is non-dispersive and hence does not spread out as it propagates. This might make it suitable for not only wood property estimation but also structural health monitoring of structures such as wooden utility poles. More research is needed into guided waves in wood to see if these can be used to provide improved measurement of wood properties and structural health monitoring of wood structures.

References

[1] A. C. Matheson, R. L. Dickson, D. J. Spencer, B. Joe, J. Ilic, Acoustic segregation of *Pinus radiata* logs according to stiffness, Annals of Forest Science 59 (5-6) (2002) 471–477.

[2] M. Krause, U. Dackermann, J. Li, Elastic wave modes for the assessment of structural timber: Ultrasonic echo for building elements and guided waves for pole and pile structures, Journal of Civil Structural Health Monitoring 5 (2) (2015) 221–249.

[3] L. Schimleck, J. Dahlen, L. A. Apiolaza, G. Downes, G. Emms, R. Evans, J. Moore, L. Pâques, J. Van den Bulcke, X. Wang, Non-destructive evaluation techniques and what they tell us about wood property variation, Forests 10 (9) (2019) 728.

[4] M. Legg, S. Bradley, Measurement of stiffness of standing trees and felled logs using acoustics: A review, The Journal of the Acoustical Society of America 139 (2) (2016) 588–604.

[5] J. Achenbach, Wave propagation in elastic solids, Elsevier, Amsterdam, Netherlands, 2012.

[6] J. L. Rose, Ultrasonic guided waves in solid media, Cambridge University Press, Cambridge, UK, 2014.

[7] J. L. Rose, A baseline and vision of ultrasonic guided wave inspection potential, Journal of Pressure Vessel Technology 124 (3) (2002) 273–282.

[8] C. Lissenden, Ultrasonic Guided Waves, MDPI, 2020.

[9] I. A. Veres, M. B. Sayir, Wave propagation in a wooden bar, Ultrasonics 42 (1-9) (2004) 495–9.

[10] D. Alleyne, P. Cawley, A two-dimensional Fourier transform method for the measurement of propagating multimode signals, The Journal of the Acoustical Society of America 89 (3) (1991) 1159–1168.

[11] S. Dahmen, H. Ketata, M. H. B. Ghozlen, B. Hosten, Elastic constants measurement of anisotropic Olivier wood plates using air-coupled transducers generated Lamb wave and ultrasonic bulk wave, Ultrasonics 50 (4-5) (2010) 502–507.

[12] H. Fathi, S. Kazemirad, V. Nasir, A nondestructive guided wave propagation method for the characterization of moisture-dependent viscoelastic properties of wood materials, Materials and Structures 53 (6) (2020) 1–14.

[13] H. Fathi, S. Kazemirad, V. Nasir, Lamb wave propagation method for nondestructive characterization of the elastic properties of wood, Applied Acoustics 171 (2021) 107565.

[14] H. Fathi, V. Nasir, S. Kazemirad, Prediction of the mechanical properties of wood using guided wave propagation and machine learning, Construction and Building Materials 262 (09 2020). `doi:10.1016/j.conbuildmat.2020.120848`.

[15] M. Subhani, J. Li, H. Gravenkamp, B. Samali, Effect of elastic modulus and Poisson's ratio on guided wave dispersion using transversely isotropic material modelling, Advanced Materials Research 778 (2013) 303–311. `doi:10.4028/www.scientific.net/AMR.778.303`.

[16] Y. Yu, N. Yan, Numerical study on guided wave propagation in wood utility poles: Finite element modelling and parametric sensitivity analysis, Applied Sciences 7 (10) (2017) 1063.

[17] J. Holt, S. Chen, R. Douglas, Determining lengths of installed timber piles by dispersive wave propagation, Design and Construction of Auger Cast Piles, and Other Foundation Issues 1447 (1994) 110.

[18] B. Sriskantharajah, E. Gad, S. Bandara, P. Rajeev, I. Flatley, Condition assessment tool for timber utility poles using stress wave propagation technique, Nondestructive Testing and Evaluation 36 (3) (2021) 336–356.

[19] M. Subhani, A study on the behaviour of guided wave propagation in utility timber pole, Ph.D. thesis, Faculty of Engineering and Information Technology, University of Technology Sydney (11 2014).

[20] U. Dackermann, Y. Yu, E. Niederleithinger, J. Li, H. Wiggenhauser, Condition assessment of foundation piles and utility poles based on guided wave propagation using a network of tactile transducers and support vector machines, Sensors 17 (12) (2017) 2938.

[21] J. El Najjar, S. Mustapha, Understanding the guided waves propagation behavior in timber utility poles, Journal of Civil Structural Health Monitoring 10 (5) (2020) 793–813.

[22] M. Legg, S. Bradley, Experimental measurement of acoustic guided wave propagation in logs, in: 19th International Nondestructive Testing and Evaluation of Wood Symposium, Rio de Janeiro, Brazil, 2015, pp. 681–688.

[23] GUIGUW, `www.guiguw.com`, last access Aug. 2021.

[24] B. A. Engineer, The mechanical and resonant behaviour of a dry coupled thickness-shear PZT transducer used for guided wave testing in pipe line, Ph.D. thesis, Brunel University, [`http://bura.brunel.ac.uk/handle/2438/13910` (2013)].

[25] H. Miao, Q. Huan, Q. Wang, F. Li, Excitation and reception of single torsional wave T(0, 1) mode in pipes using face-shear d24 piezoelectric ring array, Smart Materials and Structures 26 (2) (2017) 025021.

Chapter 3

Estimation of the Rod Velocity in Wood using Multi-Frequency Guided Wave Measurements

This chapter is republished in accordance with Elsevier's copyright policy. The work presented here is the accepted version of the published article. Therefore, the contents are the same but there may be stylistic differences to the published article.

Additional notes:

- The equation used to generate dispersion curves in this chapter is based on the correction for the Rayleigh-Bishop theory that is used for circular isotropic rods. The constants α_1 and α_2 are related to the Poisson's ratio and the radius of gyration of the sample. Wood is anisotropic hence it does not have a single Poisson's ratio. The experimental values for α_1 and α_2 for wood obtained in this study are 4.78×10^{-5} and 0.303 respectively. Additionally, the experimental α_1 and α_2 values for the aluminium rod sample are 7.83×10^{-6} and 0.349 respectively.

- The difference between the measured rod velocities for the 16 mm and 40 mm diameter wooden rod samples (5485 m/s and 4526 m/s) may be due to the difference in density. The measured density for the 16 mm and 40 mm samples are 439 kg/m^3 and 567 kg/m^3 respectively.

- Traditionally, the resonance acoustic velocity for wood is obtained using either the fundamental or second harmonic. To mitigate this error in this work, the average between the fundamental and second harmonic was taken as the average traditional resonance velocity.

- The variation in the measured resonance frequency harmonic at low frequency for the aluminium sample may be due to the frequency resolution.

Estimation of the Rod Velocity in Wood using Multi-frequency Guided Wave Measurements

Adli Hasan Abu Bakar, Mathew Legg*, Daniel Konings, Fakhrul Alam

Department of Mechanical and Electrical Engineering, Massey University, Auckland, New Zealand

Abstract

This study presents a new approach for measuring the acoustic "rod velocity" in wood using guided wave measurements. The approach fits the acoustic guided wave longitudinal L(0,1) wave mode dispersion curve, through experimental guided wave phase velocity measurements taken over a range of frequencies. The rod velocity is obtained by measuring the phase velocity of the fitted L(0,1) wave mode dispersion curve at zero frequency. This technique is used to obtain rod velocity measurements for cylindrical wood and aluminium samples. The same approach was also performed on resonance measurements at a wide range of harmonics. These rod velocities are then compared to acoustic velocities obtained using the traditional time of flight and resonance methods.

Keywords: Wood, aluminium, ToF, resonance, guided waves, dispersion curves

1. Introduction

The ability to measure the properties of wood such as stiffness is important for the forestry industry. For example, segregation of logs according to stiffness before processing can lead to an increase in profitability and efficiency [1, 2]. The static bending test is the gold standard technique for measuring the stiffness of timber [3]. However, ideally the stiffness of wood should be known before it is processed to ensure it is suitable for the desired product. Various Non Destructive Testing (NDT) techniques have therefore been developed to measure the stiffness of wood such as Near Infrared (NIR) spectroscopy [4], SilviScan [5], and acoustics [6].

Acoustics is the main technique used for measuring the stiffness of wood as it is inexpensive, simple to use and non-destructive. The stiffness of wood is related to the Modulus of Elasticity (MoE) in the longitudinal direction. The relationship between acoustic velocity c_l in the longitudinal direction and the elastic modulus

---

*Corresponding author

Email addresses: `A.Hasan@massey.ac.nz` (Adli Hasan Abu Bakar), `M.Legg@massey.ac.nz` (Mathew Legg), `D.Konings@massey.ac.nz` (Daniel Konings), `F.Alam@massey.ac.nz` (Fakhrul Alam)

E_L is commonly described using the classical 1D wave equation

$$c_l = \sqrt{\frac{E_L}{\rho}}, \tag{1}$$

where ρ is the density. This is often referred to as the rod velocity.

The Time-of-Flight (ToF) method is the common method used for measuring the acoustic velocity in standing trees. It can also be used with felled logs and timber samples [7]. Two probes are typically inserted into a sample and separated by a distance Δd. These are used to measure stress waves generated by either a hammer hit or an ultrasonic transducer which propagate along the sample. The acoustic velocity is then measured using

$$c_{tof} = \frac{\Delta d}{T}, \tag{2}$$

where T is the time taken for the signal to propagate between the two probes. This "time of flight" is predominantly measured using the amplitude threshold method. This uses a threshold to determine when the signal first goes above a threshold voltage at each transducer. The First Time of Arrival (FToA) technique only looks at the very start of the signal and ignores the rest of the signal. This technique will be referred to here as the traditional ToF method. This method has been shown to result in measurements of acoustic velocities that vary with the threshold value used, the hammer hit strength, and the noise level in the signal [8, 9].

The acoustic resonance method is the main method used to measure the acoustic velocity for felled logs and timber samples, but cannot be used for standing trees. This technique predominantly uses stress waves generated by a hammer hit at one end of the log or timber specimen in the direction parallel to the grain. The stress waves are reflected from the ends of the sample multiple times resulting in standing waves. A device at one end of the sample records the signal and the spectrum is measured. The longitudinal resonance acoustic velocity can then be calculated using

$$c_{res} = \frac{2Lf_n}{n}, \tag{3}$$

where f_n is the nth resonant frequency, n is an integer $(1, 2, 3\ldots)$ and L is the length of the specimen. This will be referred to here as the traditional resonance method. The second harmonic is commonly used for acoustic velocity determination in logs [10]. However, the fundamental frequency have also been used [6]. Note that flexural vibration techniques have also been used by researchers where a hammer hit is performed normal to the grain [11].

Studies have also shown that the acoustic velocity obtained using the ToF method has higher noise and is systematically higher than that of the resonance method [6, 12–14]. This reported overestimation can be up to 36% and vary with factors such as the diameter, age, and slenderness of the tree stem. This results in the ToF method having a systematic overestimation in stiffness measurements compared to those

obtained using both resonance and static bending tests. There have been some suggestions made as to why this overestimation may be occurring [6, 14]. For example, it is believed that the overestimation may be due to the ToF technique using bulk waves while the resonance technique measures the slower "rod waves". However, this topic still remains a key area where more fundamental research is needed.

Another area where questions have been raised by researchers is related to the harmonics used for obtaining the resonance acoustic velocity. Studies have reported that the measured resonance velocity varies depending on which harmonic frequencies are used. Andrews [12] reported measuring resonance frequencies that were not integer-multiple harmonics of each other. Chauhan and Walker [15] reported that the measured resonance velocities obtained using the first and second harmonic could differ by as much as 11%. Similarly, Hansen [16] reported differences in the velocities of up to 9% between the first five harmonics for pine and eucalyptus samples. Andrews [12] suggested that the tapered shape of the log could be the cause of the variation. However, the exact cause is still not known and more research is needed in this area.

Ultrasonic guided wave testing is a technique that is extensively used for structural health monitoring of metal structures such as oil and gas pipelines [17–20]. However, the use of acoustic/ultrasonic guided waves in wood is still in very early stages. Several lab-based studies have used measurements of the phase or group velocity of the guided wave modes to measure wood properties [21–25]. These studies were performed on rectangular cross-section timber samples which generate Lamb waves, which is different to the rod waves generated in cylindrical rods used in this study. Also, previous studies have not investigated the relationship between acoustic velocity measurements obtained using acoustic/ultrasonic guided waves and those obtained using the traditional ToF and resonance methods. Bakar et al. [26] showed that the ToF and resonance acoustic velocities in wooden and aluminium rods were roughly correlated with the longitudinal L(0,1) wave mode at low frequencies in the experimentally measured wavenumber-frequency dispersion curves plots. However, guided wave velocity measurements were not calculated from these wavenumber dispersion curves due to the low resolution of the 2D Fast Fourier Transform (FFT) method used [27].

This work presents a new approach that uses multi-frequency fitting of the guided wave L(0,1) wave mode measurements to provide more accurate acoustic velocity measurements for wood property estimation. To the best of the author's knowledge, this is the first time this method has been used on resonance and guided wave measurements for wood. This work also compares acoustic velocity measurements obtained using the ToF, resonance and guided waves techniques for 16 mm diameter cylindrical aluminium and wood samples. We are not aware of any previous studies which have compared all three techniques for any type of material.

The remainder of the paper is organised as follows. Section 2 provides background theory. Section 3 describes the methodology and experimental procedure. Section 4 presents the experimental results. Lastly, Section 5 provides a conclusion and suggestions for future works.

2. Background Theory

The classical 1D wave theory which is given by Equation 1 is widely used due to its simplicity and gives good approximations at low frequencies. It ignores dispersion and suggests that the longitudinal wave mode propagates at a single velocity called the "rod velocity". An acoustic signal propagating through a rod-like sample should initially propagate as bulk waves. However, the signal may become a guided wave after travelling a sufficient distance along the sample if the diameter is small enough relative to the wavelength. These guided waves propagate as different types of vibrations called wave modes, which propagate at different velocities and are generally dispersive. Dispersion is caused by different frequency components in a wave mode propagating at different velocities, resulting in the signal spreading out as it propagates.

Dispersion of waves propagating in rod-like structures occurs due to the geometric and viscoelastic properties of the material [28]. There are three types of wave modes for a rod-like structure: longitudinal, flexural and torsional modes. Dispersion curves describe the propagation speed in a medium and can be represented by plotting the phase velocity, group velocity or wavenumber as a function of frequency [29]. Dispersion curves can be obtained by solving the Pochammher-Chree (PC) equation [30–32] which is considered the exact theory. The exact solution to the PC equation describes the three dimensional wave propagation of the longitudinal, torsional and flexural in cylindrical rods of infinite length. The solution is complex and is restricted to bars of circular cross-section and infinite length [33].

Since the longitudinal wave mode is widely used for engineering applications [34], several approximate theories have been developed to describe the wave propagation of the longitudinal wave mode. Examples of these approximate theories include the Rayleigh-Love [35], Rayleigh-Bishop [36] and Mindlin-Hermann [37] theories. These theories represent dispersive systems where the phase velocity of the longitudinal L(0,1) wave mode is a function of frequency. The exact solution to the PC equation is normally used as a reference to determine the accuracy of these approximate theories.

As an alternative to the exact theory, analytical methods have been developed to model the wave propagation in a material. Among them, the Semi-Analytical Finite Element (SAFE) method is widely used and is accurate [38]. GUIGUW [39] is an example of a free software which uses the SAFE method to obtain dispersion curves. Figure 1 shows the theoretical dispersion curves obtained using GUIGUW for a 16 mm diameter aluminium rod with an assumed density of 2,710 kg/m^3, Poisson's ratio of 0.33 and Young's Modulus of 68.9 GPa. These dispersion curves show that for the frequency range shown here, only the fundamental longitudinal L(0,1), torsional T(0,1) and flexural wave F(1,1) modes are present. (Note that higher order wave modes may start propagating if either the frequency or diameter is increased). The fastest wave mode is the longitudinal wave mode. At low frequencies, the longitudinal wave mode propagates at the rod velocity given by Equation 1. The rod velocity in cylindrical rods corresponds to the velocity of the fundamental longitudinal wave mode L(0,1) at zero frequency [32, 40–42]. As the frequency increases, the
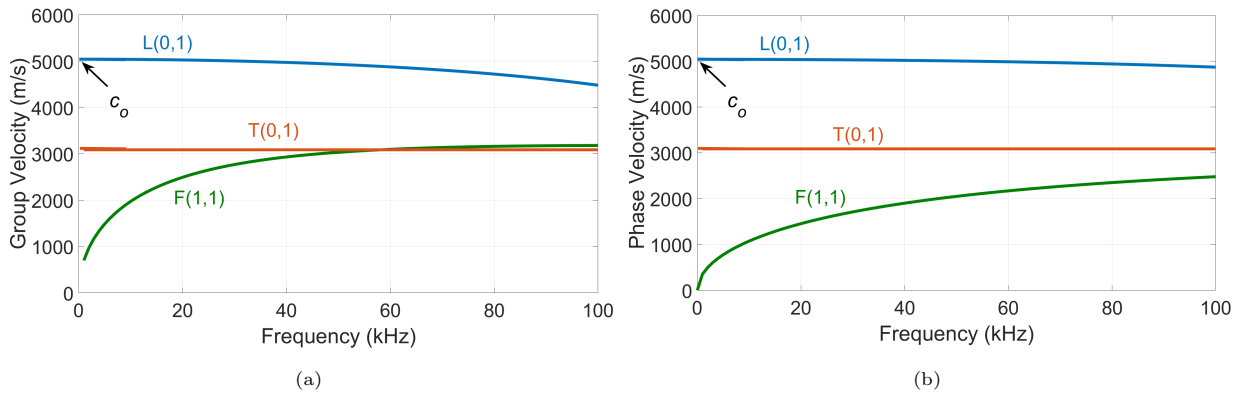
Figure 1: Theoretical dispersion curves for a 16 mm diameter aluminium rod showing the (a) group and (b) phase velocities. Also shown is the rod velocity c_o, which is the longitudinal velocity as the frequency goes to zero.

measured acoustic velocity will be lower than the rod velocity c_o due to dispersion.

If the L(0,1) wave mode was able to be excited at very low frequencies, its phase velocity should ideally correspond to the rod velocity allowing one to calculate the MoE by rearranging Equation 1 to give

$$E_L = \rho \; c_o^2. \tag{4}$$

However, the guided wave phase velocity measurements for higher frequencies should produce a phase velocity that is lower than the rod velocity c_o due to dispersion. This could lead to an underestimation in the calculated MoE. This underestimation should depend on the radius and Poisson's ratio for an isotropic cylindrical sample. However, it should be noted that the wave propagation is more complex for wood, which is orthotropic and hence has more than one Poisson's ratio [14].

Acoustic resonance has been used, mainly in early works, to measure dispersion curves for metal rods [43–47]. Equation 3 is used over a wide range of resonant frequencies to obtain experimental measurements of the L(0,1) phase velocity dispersion curve. Brizard [47] reported that at the lower frequencies, the resonance technique is prone to larger errors due to frequency resolution issues. Brizard used fitting of multi-frequency resonance measurements to obtain rod velocity and Poisson's ratio measurements for a steel bar in Split Hopkinson Bar (SHB) testing. This technique has not been used before for wood. Additionally, we have not found any previous papers that have used multi-frequency guided wave measurements to obtain the rod velocity for wood. Shin [48, 49] also obtained rod velocity and Poisson's ratio measurements for steel rods but this was related to a dispersion correction technique in SHB measurements.

In this work, we used a somewhat similar approach to the one presented by Brizard [47]. The resonance velocities for a wood sample were calculated using Equation 3 for a range of harmonic frequencies and a curve was fitted across the measurements to obtain the rod velocity c_o. Additionally, this work extends the work presented by Brizard by obtaining the rod velocity of wood using guided wave phase velocity measurements

where narrow bandwidth signals are used to excite the fundamental L(0,1) wave mode. These rod velocities are compared with the acoustic velocities obtained using traditional resonance and ToF methods.

3. Methodology

Kiln-dried radiata pine rods with diameters of 16 and 40 mm that were 2460 mm in length were obtained. The samples were selected such that they were defect-free and did not have any observable knots, cracks or damage. Additionally, a T6 temper 6061 aluminium rod with a diameter of 16 mm and a length of 2510 mm was also used to provide a comparison.

Figure 1 shows the theoretical dispersion curves for a 16 mm diameter aluminium rod. The figure shows that at frequencies below 100 kHz, no higher order wave modes are present and only the fundamental longitudinal L(0,1), flexural F(1,1) and torsional T(0,1) wave modes exist. Both the longitudinal and flexural wave modes are observed to be dispersive whereas the torsional wave mode is not. Using the above parameters, the calculated bulk wave speed for aluminium is approximately 6,175 m/s, [14], which is significantly higher than the rod velocity.

Theoretical dispersion curves for wood are not provided here since the mechanical properties of the sample were not known. Refer to our previous article [26] for examples of wavenumber dispersion curve measurements for both the aluminium and wood samples where the same three wave modes were generated in both aluminium and wood samples.

3.1. Resonance measurements

For resonance measurements, a hammer hit was performed parallel to the grain at one exposed end of the sample to generate longitudinal vibrations. At the opposite end of the sample, a GRAS 46BF-1 microphone [50] that has a bandwidth of 4 Hz - 100 kHz was used to measure the received signal. The microphone was connected to a GRAS 26A-1 pre-amp and powered by a GRAS 12AK power module. The received signal from the microphone was sampled at 2 MHz using the Analog to Digital Converter (ADC) channel from a Data Translation DT9832 data acquisition module. This setup can be seen in Figure 2.
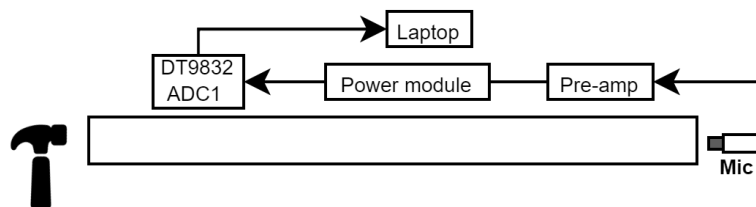

Figure 2: Experimental setup resonance measurements.

An FFT was performed on the sampled data and the resonant frequencies were identified. Resonance acoustic velocities were calculated from each resonance frequency peak over a wide frequency range using

Equation 3. As discussed in the previous section, this should provide an experimental measurement of the longitudinal L(0,1) phase velocity dispersion curve for the aluminium and wood samples.

3.2. ToF measurements

For wood related studies, probes are traditionally inserted into a wood sample to penetrate the bark. This allows good coupling between acoustic signals and the wood sample. However, in this work, shear PZT transducers produced by The Welding Institute (TWI), UK were directly coupled onto the sample by clamping them using springs as shown in Figure 3. The transducers are broadband and have a relatively flat frequency response for the frequency range used in this study [51].

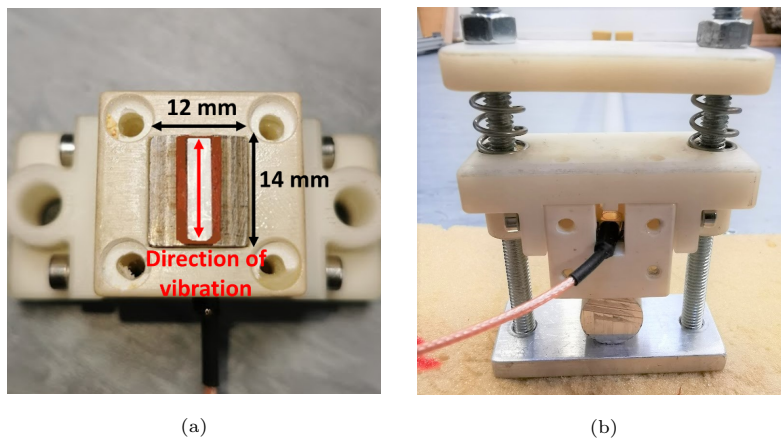(a)   (b)

Figure 3: Photo (a) shows one of the transducers used in this experiment. Photo (b) shows the transducer being pushed against an aluminium rod sample using springs.
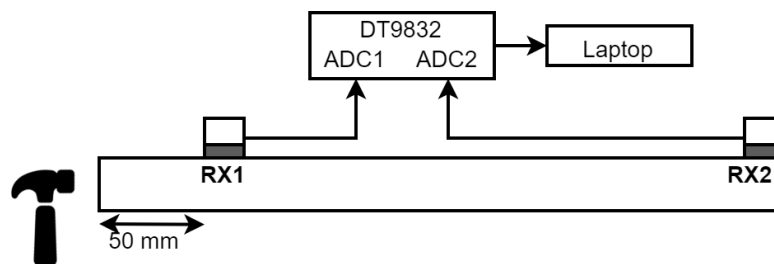

Figure 4: Experimental setup ToF measurements.

Two shear transducers were used to receive vibrations and were positioned as shown in Figure 4. The contact face of the transducers were oriented parallel to the wood grain to enhance the reception of longitudinal vibrations. A hammer impact was performed parallel to the grain at one end of the sample. The recording of the received signal was initiated by a keyboard button press just before the hammer hit was performed. Transducers RX1 and RX2 were directly connected to the ADC channels of the DT9832 module

and sampled at 2 MHz. The received signal was saved to file for further post-processing. Amplitude thresholding was used to determine the First Time of Arrival (FToA) of the received signals. The ToF velocity was then calculated using Equation 2.
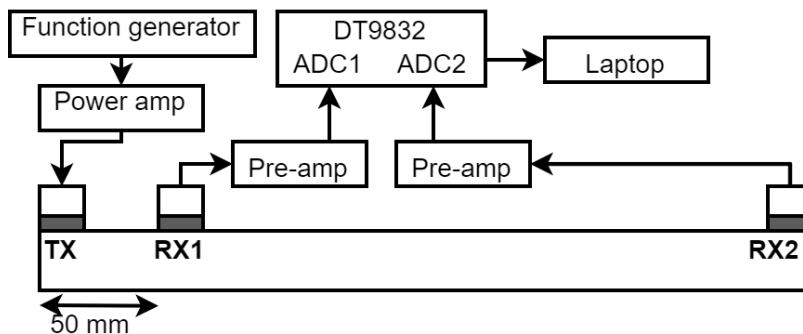
3.3. Guided wave measurements

Figure 5: Experimental setup for guided wave measurements.

For guided wave measurements, three shear transducers were used and positioned as seen in Figure 5. The contact faces of the transducers were oriented parallel to the grain to enhance the excitation and reception of longitudinal vibrations. The transducers were directly clamped onto the sample using springs. The excitation signal applied to the transmit transducer (TX) was created in MATLAB. For transmission, five cycles of a Hanning windowed sine wave with central frequencies f_o ranging from 15 kHz to 50 kHz were used and outputted using an Agilent 33220A Function Generator. A custom-made linear power amplifier was then used to amplify the outputted signal to amplitudes of up to 400 Vpp. The receivers were connected to pre-amps and the received signal at RX1 and RX2 were sampled at 2 MHz using the ADC channels from the DT9832 module and saved to file.

Phase velocity measurements were performed using the guided wave measurements to obtain the phase velocity dispersion curve for the L(0,1) wave mode. The phase velocities were obtained using a frequency-domain shifting technique. For each transmission, the received signal at RX1 was converted into the frequency domain using a FFT. Equation 5 below was then used to simulate the propagation of the frequency-domain received signal $G(\omega)$ by a distance d using an initial phase velocity $v_{ph}(\omega)$ and attenuation $\alpha(\omega)$.

$$Y(\omega) = G(\omega)e^{-j\,\frac{w}{v_{ph}(\omega)}\,d\,-\,\alpha(\omega)\,d}.\tag{5}$$

The distance between RX1 and RX2 receivers was used as the distance d. The propagated signal $Y(\omega)$ was then converted back into the time-domain using an Inverse Fast Fourier Transform (IFFT). The Root Mean Squared Error (RMSE) between the propagated time-domain signal RX1 and RX2 was calculated. The

phase velocity v_{ph} was adjusted by 1 m/s until a minimum RMSE was obtained. This process was repeated for a range of central transmit frequencies f_o.

3.4. Rod velocity estimation

Equation 4 allows us to calculate the MoE from the rod velocity c_o, which is the phase velocity of the L(0,1) wave mode at low frequencies. However, as discussed in Section 2, at higher frequencies, the phase velocity of this wave mode will be lower than the rod velocity leading to an underestimation in the estimated MoE using this equation. A fitting technique was used that estimates the rod velocity at zero frequency using experimental measurements of the phase velocity of the L(0,1) wave mode at a range of frequencies. This technique is used for both the resonance and guided wave measurements. In this paper, the terms resonance rod velocity and guided wave rod velocity corresponds to the phase velocity at zero frequency that is obtained by fitting a dispersion curve through the experimental resonance or guided wave measurements. A curve of best fit was obtained using the following equation

$$c_l = c_o \sqrt{\frac{1 + \alpha_1 \ \alpha_2 \ k^2}{1 + \alpha_1 \ k^2}}, \tag{6}$$

where c_o is the rod velocity, α_1 and α_2 are constants and k is the wavenumber. The optimum values for variables c_o, α_1 and α_2 were obtained using a non-linear least squares fitting technique performed in MATLAB. The equation is based on the correction for the Rayleigh-Bishop theory [52]. The equation was chosen as it is simple to use and gives good approximations at "low" to "medium" wavenumbers. More accurate approximations at "large" wavenumbers can be obtained using higher-order rod approximations such as the Mindlin-McNevin theory [53] or the one proposed by Anderson [54]. These approximations are more accurate over larger range of wavenumbers but are much more complex. Equation 6 should be sufficient to characterize the dispersion curve of the L(0,1) wave mode for the frequency range of interest in this current work.

4. Results

Figure 6 shows a comparison of the acoustic velocities obtained using the different methods at varying frequencies for the 16 mm diameter aluminium and wood samples. The theoretical L(0,1) dispersion curve for the aluminium sample obtained using GUIGUW was overlaid onto the figure. However, the same could not be done for the wood sample as the mechanical properties are not known. Note that the experimental frequency range for the wood sample is lower than the aluminium sample because wood suffers from a stronger degree of attenuation at higher frequencies. The hammer hit ToF measurements are not frequency dependent hence these measurements have been represented in these plots as a grey shaded region, which shows the variation of the ToF acoustic velocities.
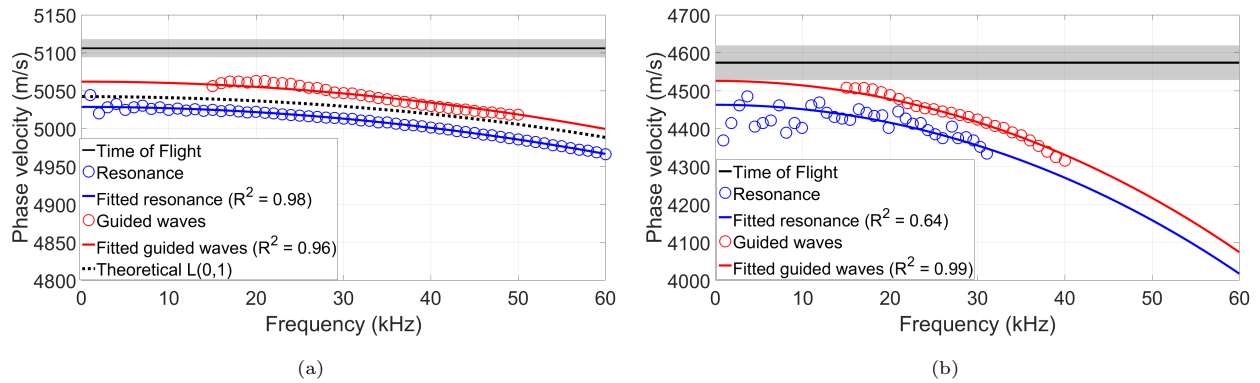
Figure 6: Plot of acoustic velocity measured using resonance, ToF and guided waves plotted as a function of frequency for the 16 mm diameter (a) aluminium and (b) wooden samples. Overlaid are the fitted dispersion curves which are used to estimate the rod velocity. For the aluminium sample, the theoretical L(0,1) dispersion curve has also been overlaid.

Table 1: Acoustic velocity measurements for 16 mm diameter aluminium and wood samples using different methods.

Method	Acoustic velocity (m/s)	
	Aluminium	Wood
Average traditional ToF	5106 ± 12	4574 ± 46
Average traditional resonance	5031 ± 13	4392 ± 24
Fitted resonance rod velocity	5029	4463
Fitted guided wave rod velocity	5062	4526

Table 1 shows the average acoustic velocity and uncertainties for each method. The traditional ToF velocities are obtained from the average of 100 measurements per sample using a threshold value of 0.05 V. Traditionally, the resonance acoustic velocity for wood is obtained using either the fundamental or second harmonic. In this work, the average between the fundamental and second harmonic was taken as the average traditional resonance velocity.

For aluminium, the maximum error between the measured phase velocities for guided wave and resonance measurements compared with those obtained from the theoretical L(0,1) wave mode, as shown in Figure 6, is approximately less than 0.8%. This shows that the L(0,1) wave mode is being excited and measured in this study. The same is expected for the wood sample. A discussion of the results for each method is presented in the subsections below.

4.1. Traditional Time of Flight

Figure 7 shows an example of the received signal obtained using the ToF method for both 16 mm diameter aluminium and wood sample. An amplitude threshold of 0.05V was used as it was approximately 3 times the standard deviation of the noise and did not result in false positives. Note that the difference in arrival
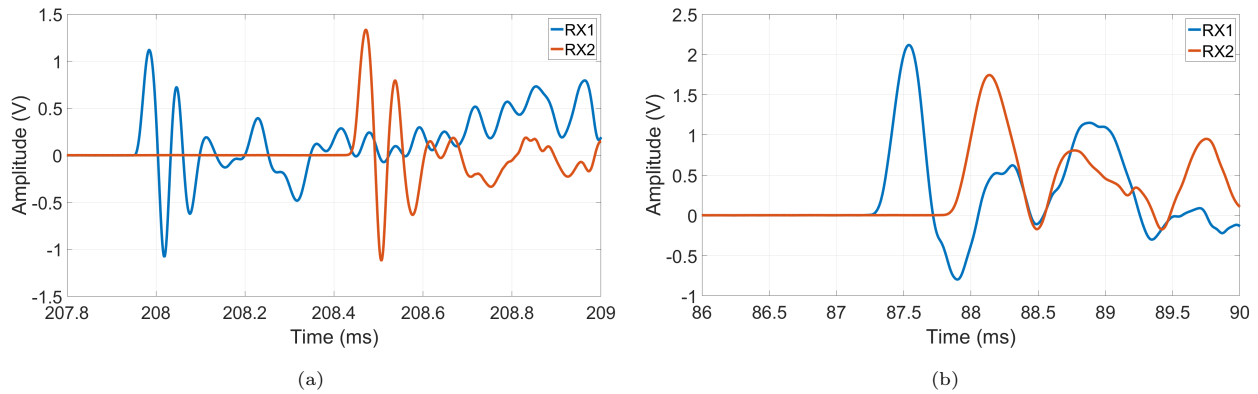
41

Figure 7: Plot of received signal for ToF experiment for (a) aluminium and (b) wood samples.

times is because the recording of the received signals was initiated manually through a button press.

The ToF measurements used in this work are obtained using the amplitude thresholding method, which measures the FToA of the signal. It will therefore obtain velocity measurements using the frequency component of the signal with the fastest phase velocity. If we assume that only the longitudinal L(0,1) wave mode is propagating, this speed should ideally correspond to the rod velocity at zero frequency. However, the traditional ToF velocities are observed to be higher than the traditional resonance velocities and the fitted resonance and guided wave rod velocities. It does not appear that this is due to the ToF technique measuring the bulk wave speed in this case, as we know that the bulk wave speed for aluminium (6175 m/s) is much higher than the results we obtained. Instead, this is most likely due to the first part of the received signal being distorted due to dispersion effects [55, 56]. This could potentially affect ToF measurements obtained using the amplitude threshold method.

4.2. Resonance

Figure 8 shows the measured resonance frequencies for the 16 mm diameter aluminium and wood samples. The wood sample has high attenuation, which results in a limited frequency range compared to the aluminium sample.

The results presented in Figure 6 show that the resonance velocity decreases with increase in frequency and follows a curve. The figure also shows that there is some variation in the measured resonance velocities, which decreases at higher frequencies. One factor that could be causing this is the resolution of the measured resonance velocity. The frequency resolution (resolution of the FFT) is defined as $\Delta f = f_s/N$ where f_s is the sampling frequency and N is the number of samples. Substituting this into Equation 3, the resolution (quantisation) of the measured resonance velocity can be calculated as

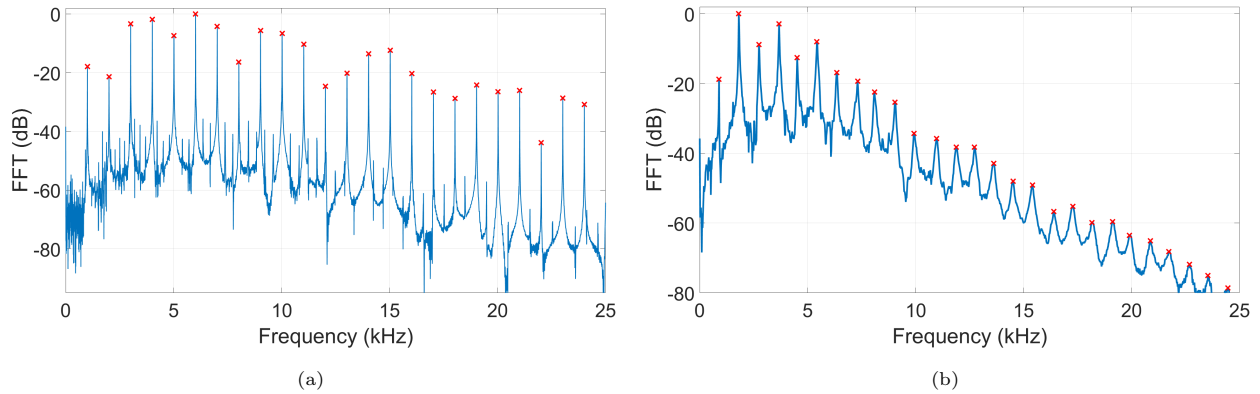$$\Delta c = \frac{2\ L\ f_s}{n\ N}. \tag{7}$$

42

Figure 8: Plot showing the resonance frequencies (marked red) for the 16 mm (a) aluminium sample and (b) wood sample.

The resolution of the measured resonance velocity is therefore inversely proportional to the harmonic integer n. As the harmonic integer increases, the resolution of the resonance velocity decreases asymptotically. This explains why the variation in resonance measurements decreases with increase in frequency. This can be mitigated by using a longer recording time of the received signal. As the recording time increases, the number of samples N also increases hence the resolution of the measured resonance velocity Δc decreases. However, increasing the recording time could cause high frequency components to be reduced due to attenuation. It can also be seen that there is more variation in the measured resonance velocities for wood compared to those obtained for the aluminium sample. This may be because of higher attenuation rates or because wood is orthotropic and inhomogeneous.

4.3. Guided Waves

Figure 6 shows that the longitudinal L(0,1) guided wave velocity measurements for 16 mm diameter wood and aluminium samples decrease with increase in frequency and roughly follow the traditional resonance measurements. However, the guided wave phase velocity values are systematically slightly higher than those for resonance at a given frequency. The similarity in the curve produced between the guided wave measurements for the 16 mm diameter aluminium and wood gives us the confidence that the measurements performed on wood are reliable. The phase velocities for frequencies below 15 kHz could not be reliably measured as the received signals were highly distorted due to the long wavelengths and reflections from the ends of the samples. Using samples with a longer length could allow lower frequencies to be used as the signal would have time to finish transmission before reflections occur.

The phase velocity measurements obtained using the guided wave method were very repeatable. The measured guided wave phase velocities were found to be independent of the amplitude of the transmit signal. This is because the method matches the peaks of the entire waveform. No difference in the measured velocity was observed for each sample when velocity measurements were repeated across multiple recordings for a

given transmission frequency. It therefore provides more consistent results than the traditional ToF method but produces acoustic velocities that vary with frequency.

4.4. Resonance and Guided Wave Rod Velocity

As discussed above, both the resonance and guided wave phase velocity measurements follow the L(0,1) wave mode dispersion curve and hence vary with frequency. A curve was fitted through the experimental resonance measurements using Equation 6 to obtain the rod velocity. A resonance rod velocity of 5029 m/s and 4463 m/s was obtained for the aluminium and wood samples respectively. The difference between the traditional resonance velocity and the resonance rod velocity is approximately 0.03% and 1.61% for the aluminium and wood samples respectively.

In order to quantify the goodness-of-fit of the fitted dispersion curve, the coefficient of determination or R^2 value is used. The R^2 value indicates the proportion of variance in the dependent variable that can be explained by the independent variable. In this study, the R^2 measures the amount of variation in the experimental data that can be explained by the fitted regression model. The R^2 values (0.98 for aluminium and 0.64 for wood) show that the fitted dispersion curves matches well with the experimental traditional resonance measurements. The R^2 value for the wood sample is smaller than the aluminium sample as there is more variation in resonance measurements for the wood sample. This may be due to the highly attenuative nature of wood or because wood is orthotropic and inhomogeneous.

Dispersion curves were also fitted through the experimental guided wave phase velocity measurements for both aluminium and wood samples. For the aluminium sample, at the frequency range of interest, the fitted dispersion curves are observed to be close to the theoretical L(0,1) dispersion curve, as seen in Figure 6. The maximum difference between the fitted resonance and guided wave dispersion curves relative to the theoretical L(0,1) dispersion curve for the aluminium sample are 0.4% and 0.3% respectively. The theoretical dispersion curve for the wood sample could not be obtained as the mechanical properties are not known. Guided wave rod velocities of 5062 m/s and 4526 m/s were obtained for the aluminium and wood samples respectively. The measured guided wave rod velocities are observed to be lower than the acoustic velocities obtained using the traditional ToF method but are slightly higher compared to the traditional resonance method. High R^2 values (0.96 for aluminium and 0.99 for wood) were obtained from the fitted dispersion curves using the guided wave phase velocity measurements. This shows that Equation 6 provides a good approximation of the L(0,1) phase velocity dispersion curve for the samples used in this study in the frequency range of interest.

4.5. Results on larger diameter wood sample

Resonance, ToF and guided wave measurements were also performed on a 40 mm diameter wood sample. Figure 9 shows a comparison of acoustic velocities obtained using these methods at varying frequencies for
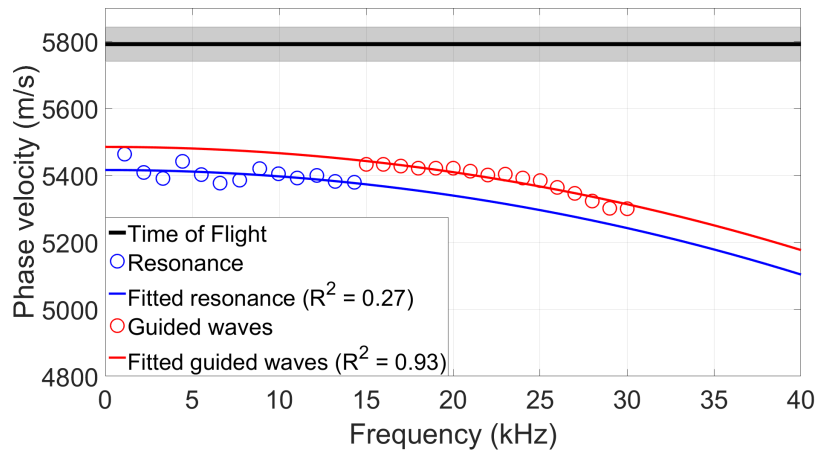
Figure 9: Plot of acoustic velocity using ToF, resonance and guided wave plotted as a function of frequency for a 40 mm diameter wood sample. Overlaid is the fitted dispersion curve for the guided wave measurements.

the 40 mm diameter wood sample. ToF acoustic velocities are observed to be significantly higher compared to the resonance and guided wave velocities. The frequency range where measurements were able to be reliably obtained were lower for both resonance and guided wave measurements compared to the 16 mm wood sample. There appears to be higher attenuation rates at higher frequencies for this sample relative to the 16 mm diameter wood sample. The resonance and guided wave phase velocity measurements decreases with an increase in frequency and follows a curve which is similar to the 16 mm diameter wood sample. Dispersion curves are fitted using the method described in Section 3.4 through the measurements and a high R^2 value (0.93) is obtained for the fitted dispersion curve for guided wave phase velocity measurements. However, a low R^2 value (0.27) is obtained for the resonance measurements which may be due to the measurement variations.

Table 2: Average acoustic velocity obtained using different methods for a 40 mm diameter wood sample

Method	Acoustic velocity (m/s)
Average traditional ToF	5792 ± 51
Average traditional resonance	5435 ± 37
Fitted resonance rod velocity	5416
Fitted guided wave rod velocity	5485

Table 2 shows a comparison of acoustic velocities obtained using different methods for the 40 mm diameter wood sample. The traditional ToF acoustic velocity is approximately 6.5% higher compared to the traditional resonance method. This ToF overestimation is significantly higher compared to the 16 mm diameter wood sample. The fitted guided wave rod velocity is closer to the traditional resonance velocity

compared to the traditional ToF velocity. The results show that the fitting technique and guided wave phase velocity measurements can be used as an alternative to the traditional ToF method to obtain more accurate acoustic velocity measurements for wood.

5. Conclusion

The traditional acoustic resonance technique is commonly used for wood stiffness measurements as it is accurate and easy to use. However, it cannot be used on standing trees. In contrast, the traditional ToF method works on both standing trees and cut logs but literature has reported an overestimation using this measurement technique. This study investigated a new technique for obtaining the rod velocity of wooden samples using ultrasonic guided waves which can potentially be used for both standing trees and cut timber/logs.

The acoustic/ultrasonic guided wave phase velocity of the L(0,1) wave mode theoretically starts at the rod velocity at zero frequency and then decreases as the frequency increases. Therefore, to measure the rod velocity, the proposed technique performs measurements of the L(0,1) phase velocity at a range of frequencies and fits a curve through them to obtain an estimate of the phase velocity at zero frequency. This will correspond to the rod velocity of the sample. The same rod velocity fitting technique is also used with resonance velocity measurements made using a range of resonance harmonics.

To test the proposed method, resonance, ToF and guided wave measurements were performed on cylindrical wooden rods with diameters of 16 mm and 40 mm and length of 2460 mm each. These measurements were repeated on a 16 mm diameter aluminium rod with a similar length for comparison. The guided wave longitudinal L(0,1) phase velocity measurements in the rod samples decreases with an increase in frequency. The fitted phase velocity dispersion curves matched well with the experimental phase velocity measurements for both aluminium and wood samples. The R^2 values of the fits were 0.99 and 0.93 for the wood samples and 0.96 for the aluminium sample. The fitted rod velocities matched well with the traditional resonance velocities. In contrast, the measured ToF velocities were higher compared to both the guided wave rod velocities and traditional resonance velocities, as shown in Table 3.

Table 3: Difference in measured acoustic velocity obtained using traditional ToF and the rod velocity obtained using the guided wave method relative to the traditional resonance velocity for wood.

Wood sample	Difference relative to resonance	
	Traditional ToF	Rod velocity
16 mm diameter	4.1%	3.0%
40 mm diameter	6.5%	0.9%

This same fitting technique was also used for the phase velocity measurements obtained using the multi-

frequency resonance method. These measurements decreased with increased frequency and follow the phase velocity dispersion curve of the L(0,1) wave mode. The fitting technique was used to obtain the rod velocity in a similar manner to the guided wave measurements. The R^2 values of the fitting were lower than for the guided wave measurements (0.64 and 0.27 for the wood samples). This is related to the larger variance in the resonance measurements at lower frequencies, which appears to be related to the resolution of the FFT. Since the fitting technique uses higher frequency harmonics, this technique can be used to provide more accurate results compared to the traditional resonance technique, which only uses a single lower frequency resonance peak where the variances are larger. However, more work is needed to see if the higher frequency harmonics can be measured with samples that have a larger diameter and higher moisture content which may have higher attenuation rates.

Ultrasonic guided waves have previously been used on logs with large diameters [57]. Therefore, the guided wave technique presented in this study has the potential to be used as an alternative to the traditional ToF method to obtain acoustic velocity measurements for logs, standing trees and seedlings. Initial results from this study show that the guided wave fitting technique was more accurate compared to the traditional ToF method. This can result in more efficient segregation and sorting of logs before harvesting which could improve the sustainability and profitability of the forestry industry. This work shows that guided wave techniques can be used to obtain improved measurements of wood properties. Additionally, there is potential for the fitted resonance technique to provide more accurate rod velocity measurements for timber and log samples compared to the traditional resonance technique, which is considered to be the gold standard in acoustic non-destructive stiffness measurements for wood.

Future works should investigate the use of more accurate approximations of the longitudinal L(0,1) wave mode, as these might provide more accurate rod velocity measurements. Stiffness measurements obtained using the presented approach should also ideally be compared with those obtained using static bending tests. Also, measurements should be performed on larger diameter samples such as logs. This will allow the effect of higher order wave modes and potentially the presence of bulk waves to be evaluated.

References

[1] A. Achim, N. Paradis, P. Carter, R. E. Hernández, Using acoustic sensors to improve the efficiency of the forest value chain in Canada: A case study with laminated veneer lumber, Sensors 11 (6) (2011) 5716–5728.

[2] X. Wang, P. Carter, R. J. Ross, B. K. Brashaw, Acoustic assessment of wood quality of raw forest materials: a path to increased profitability, Forest Products Journal 57 (5) (2007) 6–14.

[3] P. H. Hai, B. Hannrup, C. Harwood, G. Jansson, D. Van Ban, Wood stiffness and strength as selection traits for sawn timber in *Acacia auriculiformis*, Canadian Journal of Forest Research 40 (2) (2010) 322–329.

[4] L. Schimleck, J. Matos, R. Trianoski, J. Prata, Comparison of methods for estimating mechanical properties of wood by NIR spectroscopy, Journal of Spectroscopy 2018 (2018).

[5] T. Ma, T. Inagaki, S. Tsuchikawa, Non-destructive evaluation of wood stiffness and fiber coarseness, derived from SilviScan data, via near infrared hyperspectral imaging, Journal of Near Infrared Spectroscopy 26 (6) (2018) 398–405.

[6] X. Wang, Acoustic measurements on trees and logs: A review and analysis, Wood Science and Technology 47 (5) (2013) 965–975.

[7] X. Wang, R. J. Ross, P. Carter, Acoustic evaluation of wood quality in standing trees. Part I. Acoustic wave behavior, Wood and Fiber Science 39 (1) (2007) 28–38.

[8] F. J. Rescalvo, M. A. Ripoll, E. Suarez, A. Gallego, Effect of location, clone, and measurement season on the propagation velocity of poplar trees using the Akaike information criterion for arrival time determination, Materials 12 (3) (2019) 356.

[9] L. Espinosa, J. Bacca, F. Prieto, P. Lasaygues, L. Brancheriau, Accuracy on the time-of-flight estimation for ultrasonic waves applied to non-destructive evaluation of standing trees: a comparative experimental study, Acta Acustica united with Acustica 104 (3) (2018) 429–439.

[10] P. Harris, M. Andrews, Tools and acoustic techniques for measuring wood stiffness, in: Proceedings of the 3rd Wood Quality Symposium: Emerging Technologies For Evaluating Wood Quality for Processing, Forest Industry Engineering Association, Rotorua, New Zealand, 1999.

[11] K. T. Hassan, P. Horáček, J. Tippner, Evaluation of stiffness and strength of Scots pine wood using resonance frequency and ultrasonic techniques, BioResources 8 (2) (2013) 1634–1645.

[12] M. Andrews, Where are we with sonics, in: Workshop 2000. Capturing the Benefits of Forestry Research: Putting Ideas to Work, Wood Technology Research Centre. University of Canterbury New Zealand, 2000, pp. 57–61.

[13] R. J. Ross, B. K. Brashaw, J. Punches, J. R. Erickson, J. W. Forsman, R. F. Pellerin, X. Wang, Diameter effect on stress-wave evaluation of modulus of elasticity of logs, Wood and Fiber Science 36 (3) (2004) 368–377.

[14] M. Legg, S. Bradley, Measurement of stiffness of standing trees and felled logs using acoustics: A review, The Journal of the Acoustical Society of America 139 (2) (2016) 588–604.

[15] S. Chauhan, J. Walker, Variations in acoustic velocity and density with age, and their interrelationships in radiata pine, Forest Ecology and Management 229 (1) (2006) 388–394.

[16] H. J. Hansen, Acoustic studies on wood, Ph.D. thesis, University of Canterbury. School of Forestry (2006).

[17] S. C. Olisa, M. A. Khan, A. Starr, Review of current guided wave ultrasonic testing (GWUT) limitations and future directions, Sensors 21 (3) (2021) 811.

[18] E. H. Ling, R. H. Abdul Rahim, A review on ultrasonic guided wave technology, Australian Journal of Mechanical Engineering 18 (1) (2020) 32–44.

[19] Z. Wang, J. Liu, K. Wang, C. Fang, L. Wang, Z. Wu, Nondestructive measurements of elastic constants of thin rods based on guided waves, Mechanical Systems and Signal Processing 170 (2022) 108842.

[20] E. Pabisek, Z. Waszczyszyn, Identification of thin elastic isotropic plate parameters applying guided wave measurement and artificial neural networks, Mechanical Systems and Signal Processing 64 (2015) 403–412.

[21] S. Dahmen, H. Ketata, M. H. B. Ghozlen, B. Hosten, Elastic constants measurement of anisotropic Olivier wood plates using air-coupled transducers generated Lamb wave and ultrasonic bulk wave, Ultrasonics 50 (4-5) (2010) 502–507.

[22] H. Fathi, S. Kazemirad, V. Nasir, A nondestructive guided wave propagation method for the characterization of moisture-dependent viscoelastic properties of wood materials, Materials and Structures 53 (6) (2020) 1–14.

[23] H. Fathi, S. Kazemirad, V. Nasir, Lamb wave propagation method for nondestructive characterization of the elastic properties of wood, Applied Acoustics 171 (2021) 107565.

[24] H. Fathi, S. Kazemirad, V. Nasir, Mechanical degradation of wood under ultraviolet radiation characterized by Lamb wave propagation, Structural Control and Health Monitoring 28 (6) (2021) e2731.

[25] H. Fathi, V. Nasir, S. Kazemirad, Prediction of the mechanical properties of wood using guided wave propagation and machine learning, Construction and Building Materials 262 (2020) 120848.

[26] A. H. A. Bakar, M. Legg, D. Konings, F. Alam, Ultrasonic guided wave measurement in a wooden rod using shear transducer arrays, Ultrasonics 119 (2022) 106583.

[27] D. Alleyne, P. Cawley, A two-dimensional Fourier transform method for the measurement of propagating multimode signals, The Journal of the Acoustical Society of America 89 (3) (1991) 1159–1168.

[28] R. Othman, G. Gary, R. Blanc, M. Bussac, P. Collet, Dispersion identification using the Fourier analysis of resonances in elastic and viscoelastic rods, in: Acoustics, Mechanics, and the Related Topics of Mathematical Analysis, World Scientific, 2002, pp. 229–235.

[29] J. L. Rose, Ultrasonic guided waves in solid media, Cambridge University Press, 2014.

[30] C. Chree, The equations of an isotropic elastic solid in polar and cylindrical co-ordinates their solution and application, Transactions of the Cambridge Philosophical Society 14 (1889) 250.

[31] L. Pochhammer, Ueber die fortpflanzungsgeschwindigkeiten kleiner schwingungen in einem unbegrenzten isotropen kreis-cylinder. (1876).

[32] R. Davies, A critical study of the Hopkinson pressure bar, Philosophical Transactions of the Royal Society of London. Series A, Mathematical and Physical Sciences 240 (821) (1948) 375–457.

[33] M. Shatalov, J. Marais, I. Fedotov, M. D. Tenkam, M. Schmidt, Longitudinal vibration of isotropic solid rods: from classical to modern theories, Advances in computer science and engineering 1877 (2011) 408–9.

[34] L. Xie, C. Bian, J. Wang, Correction factors of the approximate theories for axisymmetric modes of longitudinal waves in circular rods, Acta Mechanica Solida Sinica (2022) 1–10.

[35] A. E. H. Love, A treatise on the mathematical theory of elasticity, Cambridge University Press, 2013.

[36] R. Bishop, Longitudinal waves in beams, Aeronautical Quarterly 3 (4) (1952) 280–293.

[37] R. Mindlin, A one-dimensional theory of compressional waves in an elastic rod, in: Proceedings of the First US National Congress of Applied Mechanics, 1951, pp. 187–191.

[38] I. Bartoli, A. Marzani, F. L. Di Scalea, E. Viola, Modeling wave propagation in damped waveguides of arbitrary cross-section, Journal of sound and vibration 295 (3-5) (2006) 685–707.

[39] P. Bocchini, A. Marzani, E. Viola, Graphical user interface for guided acoustic waves, Journal of Computing in Civil Engineering 25 (3) (2011) 202–210.

[40] W. E. Tefft, S. Spinner, Cross-sectional correction for computing Young's modulus from longitudinal resonance vibrations of square and cylindrical rods, Journal of Research of the National Bureau of Standards A 66 (1962) 193–197.

[41] J. Zemanek Jr, I. Rudnick, Attenuation and dispersion of elastic waves in a cylindrical bar, The Journal of the Acoustical Society of America 33 (10) (1961) 1283–1288.

[42] S. E. Rigby, A. D. Barr, M. Clayton, A review of Pochhammer–Chree dispersion in the Hopkinson bar, Proceedings of the Institution of Civil Engineers-Engineering and Computational Mechanics 171 (1) (2018) 3–13.

[43] R. Booker, Velocity dispersion of isotropic rods of square cross section vibrating in the lowest-order longitudinal mode, The Journal of the Acoustical Society of America 45 (5) (1969) 1284–1286.

[44] S. Spinner, T. Reichard, W. Tefft, A comparison of experimental and theoretical relations between Young's modulus and the flexural and longitudinal resonance frequencies of uniform bars, Journal of Research of the National Bureau of Standards. Section A, Physics and Chemistry 64 (2) (1960) 147.

[45] T. D. Rossing, D. A. Russell, Laboratory observation of elastic waves in solids, American Journal of Physics 58 (12) (1990) 1153–1162.

[46] Y. Chevalier, J. T. Vinh, Longitudinal vibration of rods: Material characterization and experimental dispersion curves, Mechanical Characterization of Materials and Wave Dispersion: Instrumentation and Experiment Interpretation (2013) 271–303.

[47] D. Brizard, An impact test to determine the wave speed in SHPB: Measurement and uncertainty, Journal of Dynamic

Behavior of Materials 6 (1) (2020) 45–52.

[48] H. Shin, Pochhammer–Chree equation solver for dispersion correction of elastic waves in a (split) Hopkinson bar, Proceedings of the Institution of Mechanical Engineers, Part C: Journal of Mechanical Engineering Science (2021) 0954406220980509.

[49] H. Shin, Manual for calibrating sound speed and Poisson's ratio of (split) Hopkinson bar via dispersion correction using Excel® and Matlab® templates, Data 7 (5) (2022) 55.

[50] GRAS 46BF-1 1/4" LEMO Free-field Standard Microphone Set, `https://www.grasacoustics.com/products/measurement-microphone-sets/traditional-power-supply-lemo/product/686-46bf-1`, Last accessed on 2022-10-17.

[51] B. A. Engineer, The mechanical and resonant behaviour of a dry coupled thickness-shear PZT transducer used for guided wave testing in pipe line, Ph.D. thesis, Brunel University (2013).

[52] G. Carta, Correction to Bishop's approximate method for the propagation of longitudinal waves in bars of generic cross-section, European Journal of Mechanics-A/Solids 36 (2012) 156–162.

[53] R. Mindlin, H. McNiven, Axially symmetric waves in elastic rods, Tech. rep., Columbia University. New York Department of Civil Engineering and Engineering Mechanics (1958).

[54] S. P. Anderson, Higher-order rod approximations for the propagation of longitudinal stress waves in elastic bars, Journal of Sound and Vibration 290 (1-2) (2006) 290–308.

[55] D. Gorham, A numerical method for the correction of dispersion in pressure bar signals, Journal of Physics E: Scientific Instruments 16 (6) (1983) 477.

[56] A. M. Bragov, A. K. Lomunov, D. A. Lamzin, A. Y. Konstantinov, Dispersion correction in split-Hopkinson pressure bar: theoretical and experimental analysis, Continuum Mechanics and Thermodynamics (2019) 1–13.

[57] M. Legg, S. Bradley, Experimental measurement of acoustic guided wave propagation in logs, in: 19th International Nondestructive Testing and Evaluation of Wood Symposium, Rio de Janeiro, Brazil, 2015, pp. 681–688.

Chapter 4

The Effects of Dispersion on Time-of-Flight Acoustic Velocity Measurements in a Wooden Rod

This chapter is republished in accordance with Elsevier's copyright policy. The work presented here is the accepted version of the published article. Therefore, the contents are the same but there may be stylistic differences to the published article.
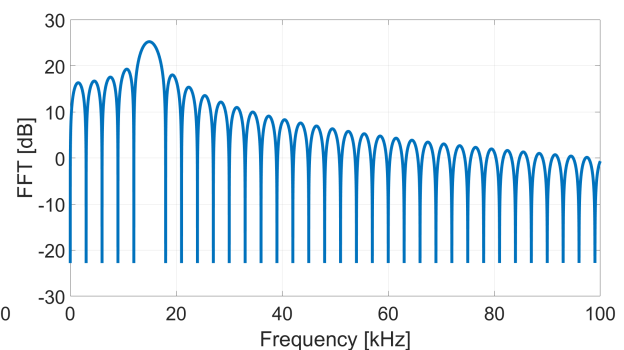
Additional notes:

The figures below show the frequency domain plots for the transmit signals used for simulated experiments in this chapter.
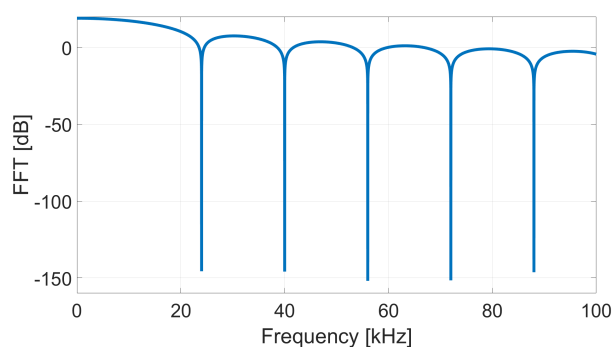
(a) Half cycle of a 8 kHz sine wave

(b) 5 cycles of a 15 kHz sine wave

The Effects of Dispersion on Time-of-Flight Acoustic Velocity Measurements in a Wooden Rod

Adli Hasan Abu Bakar, Mathew Legg*, Daniel Konings, Fakhrul Alam

Department of Mechanical and Electrical Engineering, Massey University, Auckland, New Zealand

Abstract

The stiffness of wood can be estimated from the acoustic velocity in the longitudinal direction. Studies have reported that stiffness measurements obtained using time-of-flight acoustic velocity measurements are overestimated compared to those obtained using the acoustic resonance and bending test methods. More research is needed to understand what is causing this phenomenon. In this work, amplitude threshold time-of-flight, resonance, and guided wave measurements are performed on wooden and aluminium rods. Using guided wave theory, it is shown through simulations and experimental results that dispersion causes an overestimation of time-of-flight measurements. This overestimation was able to be mitigated using dispersion compensation. However, other guided wave techniques could potentially be used to obtain improved measurements.

Keywords: Wood, aluminium, rod, ToF, guided waves, amplitude threshold.

1. Introduction

The measurement of the mechanical properties of wood such as stiffness is important for the forestry industry. The stiffness of wood can be used as a metric to segregate logs into different grades. This can help maximise the profitability and sustainability within the wood industry [1]. The stiffness of timber may be measured using static bending tests, which are considered to be the gold standard. However, ideally, the properties of the wood should be known before it is processed to ensure it is suitable for the end product [2]. Non-Destructive Testing (NDT) techniques [3, 4] have been developed to determine the properties of wood before processing and without damaging them.

The main NDT technique used to measure the stiffness of wood is acoustics since it is simple to use and inexpensive compared to other methods. Wood is an orthotropic material meaning that the mechanical properties are independent in three orthogonal axes. For wood, the acoustic velocity in the longitudinal

---

*Corresponding author
Email addresses: A.Hasan@massey.ac.nz (Adli Hasan Abu Bakar), M.Legg@massey.ac.nz (Mathew Legg),
D.Konings@massey.ac.nz (Daniel Konings), F.Alam@massey.ac.nz (Fakhrul Alam)

direction c_l is often described by

$$c_l = \sqrt{\frac{E_L}{\rho}}, \tag{1}$$

where ρ is the density of the material and E_L is the Modulus of Elasticity (MoE) in the longitudinal direction. The MoE in the longitudinal direction is commonly used to describe the stiffness of wood. This equation is based on fundamental 1D wave theory [5] which does not include factors that can affect the acoustic velocity such as temperature, moisture content, presence of knots, Poisson's ratios and variation in grain angle [6]. There are more complex models for wood which include some of these factors [7, 8]. For example, Legg & Bradley [6] provide a model that includes orthotropic Poisson's ratios. However, the 1D wave theory given in Eqn. 1 is predominantly used in the literature related to wood stiffness. The two most commonly used acoustic methods to measure the stiffness of wood are the resonance and Time of Flight (ToF) methods, as described below. The resonance method can be used on felled logs, while the ToF method can be used on both standing trees and felled logs.

1.1. Acoustic methods and overestimation

The resonance method involves generating longitudinal stress waves by performing a hammer hit at one end of the sample in the direction parallel to the grain. A Fast Fourier Transform (FFT) is performed on the received acoustic signal and resonance frequencies are identified. The longitudinal resonance acoustic velocity can then be calculated using

$$c_{res} = \frac{2Lf_n}{n}, \tag{2}$$

where L is the length of the sample, f_n is the nth resonant frequency and $n = 1, 2, 3....$. Note that flexural resonance techniques have also been used by researchers where the hammer hit is impacted normal to the grain [9].

For wood related studies, the ToF method generally involves two probes which are inserted into a sample separated by a distance d. The acoustic velocity can be calculated using

$$c_{tof} = \frac{d}{T}, \tag{3}$$

where T is the propagation time of a stress wave from one probe to the other. Traditionally, a hammer hit is performed at or near one of the probes to generate longitudinal stress waves. Hammer hit excitation is generally used for NDT measurements of wood properties because it provides a strong excitation signal with a good Signal-to-Noise Ratio (SNR). This is important given the highly attenuative nature of wood, particularly at higher acoustic frequencies. In addition to hammer hit excitation, ultrasonic excitation signals are also used for acoustic velocity measurements in wood [10].

In wood studies, the propagation time T is predominantly obtained by measuring the First Time of Arrival (FToA) of the signal at each receiver probe. For hammer hit excitation, signal peaks are not

commonly used as they can be distorted during propagation, which can lead to large errors. The FToA technique identifies when the signal is first detected at each of the receiver probes and ignores the remainder of the signal. The amplitude threshold method appears to be the main technique used in wood studies to determine the FToA of the received signal. The method is also widely used in ultrasonic NDT to determine the FToA of a propagating signal in order to extract the ToF. This technique measures the time when the signal at each receiver first goes above a chosen threshold value [11, 12, 13]. Alternatively, other FToA methods such as Akaike Information Criterion (AIC) [14], Modified Energy Ratio (MER) [15] and cross-correlation [16] have also been used.

Stiffness measurements obtained using acoustic resonance and ToF have shown good correlations with those obtained using static bending tests. However, the ToF method results have a systematic overestimation in stiffness measurements compared to the values obtained using both static bending tests and resonance. This overestimation is related to the ToF method measuring acoustic velocities which are systematically higher than those obtained using acoustic resonance [6].

Several studies have suggested possible reasons as to why this is occurring. For example, the variation in stiffness from pith to bark [17], the age and diameter of the trees and the difference in wave propagation of the acoustic signals used in the two methods [5]. Despite these suggestions, the exact cause of the overestimation is still not known.

1.2. Guided waves and dispersion effects

For rod-like structures, guided waves are expected to propagate as different types of vibrations, which are called wave modes [6]. Unlike 1D wave theory, guided wave theory considers the dispersion of wave modes. Dispersion is influenced by the mechanical properties and diameter of a sample. Dispersion is caused by the propagation of different frequency components at different velocities. This causes the signal to spread out as it propagates through a medium [18].

Guided wave NDT testing techniques have been used to measure wood properties [19, 20]. However, this is an emerging area of research and there have been relatively few studies on this topic. In our previous paper [21], a 2D FFT method was used to obtain wavenumber-frequency domain dispersion curves for wood and aluminium rod samples. These dispersion curves showed the presence of the fundamental longitudinal, flexural and torsional wave modes in the rod samples. The resonance velocity was found to roughly correlate with the L(0,1) wave mode dispersion curve at low frequencies. However, phase velocities were not calculated from these wavenumber-frequency domain plots since the resulting phase velocities would have had high errors due to the low resolution associated with the 2D FFT method.

Generally, in guided wave testing, ultrasonic transducers are used to generate narrowband excitation signals to reduce the effects of dispersion and limit the number of wave modes excited [22, 23]. Hammer hits or sharp impacts are therefore generally not used in guided wave testing since they generate wide bandwidth

excitation signals and provide less control. This means that there are a limited number of studies on dispersion and guided waves for impact-like excitation.

The Split Hopkinson Pressure Bar (SHPB) is a technique that measures the dynamic mechanical behaviour of materials, particularly at high strain rates, by analysing the shape of signals generated by a sharp impact [24]. Knowledge of guided waves and dispersion has been used to improve the accuracy of these measurements. It has been reported that dispersion can cause signal distortion on SHPB tests on metal samples. This can cause significant changes to the rise time at the start of the measured impact signal [25].

Although the SHPB technique does not use velocity measurements, the findings from this area of research could provide some insights into a potential cause of error in ToF measurements obtained using FToA techniques such as amplitude thresholding. Could the distortion caused by dispersion at the start of the signal affect the accuracy of amplitude threshold ToF velocity measurements?

For the SHPB technique, dispersion compensation methods have been developed to mitigate dispersion effects which have helped to reduce signal distortion and improve the rise time at the start of the signal to give more accurate results [26, 27, 28]. Besides the SHPB technique, dispersion compensation techniques have also been used to reduce the effects of dispersion on ultrasonic guided wave measurements on metal samples [29, 30, 31]. One of these studies, which was performed by Xu et al. [32], has investigated the effect of dispersion compensation on ToF measured values for ultrasonic guided waves. However, these ToF measurements were not obtained using FToA techniques. Instead, the ToF measurements were obtained by measuring the propagation time of the largest peak at the centre of the wave packet for different propagation distances. They reported that more accurate group velocity ToF measurements were obtained after dispersion compensation was performed.

No previous work has been found that has investigated the effect of dispersion on ToF measurements obtained using FToA methods (looking at the start of the signal, not the peak). Additionally, no studies have been found which have utilised dispersion compensation to reduce dispersion effects for acoustic measurements made on wood.

In this study, resonance, amplitude threshold ToF and guided wave longitudinal velocity measurements were performed on thin cylindrical aluminium and wooden rods. The amplitude threshold ToF acoustic velocities were measured before and after dispersion compensation was performed. The results were then compared with acoustic resonance velocities.

1.3. Contributions

The research presented here offers the following contributions. To the best of the author's knowledge, this is the first work to:

(1) Investigate the effects of dispersion on ToF acoustic velocity measurements made using the FToA.

(2) Show that dispersion effects can be a source of overestimation in FToA ToF velocity measurements.

(3) Use dispersion compensation to mitigate the overestimation in the measured FToA ToF velocity measurements. We are not aware of any previous studies that have performed dispersion compensation for wood.

The remainder of the paper is organised as follows. Section 2 describes the wave propagation and dispersion compensation theory. Section 3 describes the methodology, hardware and experimental procedure used. Section 4 presents the results obtained. Lastly, Section 5 provides a conclusion and suggestions for future work.

2. Wave propagation model

The following section outlines a simple wave propagation model that is used in this work to simulate the propagation of the sound waves through the wooden and aluminium rods. Also included is a description of the dispersion compensation technique used in this work. This allows the effects of dispersion on FToA acoustic velocity measurements to be evaluated.

Consider a signal $g(t)$ excited by a transducer, which only generates a single wave mode. The received signal $y(t)$ at a distance d from the transmitter can be modelled in the frequency domain as

$$Y(\omega) = G(\omega)e^{-j\ k(\omega)\ d\ -\ \alpha(\omega)\ d}, \tag{4}$$

where ω is the angular frequency, $G(\omega)$ is the Fourier transform of $g(t)$, $k(\omega)$ is the wavenumber, and $\alpha(\omega)$ is the attenuation [31]. The wave number can be calculated using

$$k = \frac{\omega}{v_{ph}}, \tag{5}$$

where v_{ph} is the phase velocity. The peak of the wave packet will propagate at the group velocity v_{gr}. For a narrowband signal, the distance and time t may be related using

$$d(t) = v_{gr}(\omega_o)\ t, \tag{6}$$

where ω_o corresponds to the central frequency of the narrow band excitation frequency.

For a dispersive material, both the phase and group velocity will be frequency-dependent resulting in dispersion. This causes the signal to spread out as it propagates. The above theory therefore allows dispersive guided wave propagation to be simulated using either theoretical or measured dispersion curves.

Dispersion compensation techniques have been developed to mitigate the effects of dispersion from the received guided wave signals in post-processing [29, 33, 34]. Consider that a received signal $y(t)$ has experienced dispersion. Dispersion compensation can be performed at the i_{th} propagation time t_i in the frequency domain using

$$\hat{Y}(\omega, t_i) = Y(\omega)e^{j(k(\omega)\ d(t_i) - w\ t_i)} \tag{7}$$

where $Y(\omega)$ is the Fourier transform of the received signal $y(t)$ and d is the propagation distance. This performs frequency domain shifting of each frequency component in the signal to correct for changes in phase velocity due to dispersion. Each frequency component of the signal is calculated using Equation 7 and the inverse Fourier transform

$$\hat{y}(t) = \text{IFFT}[\hat{Y}(\omega, t_i)], \tag{8}$$

is used to convert the frequency domain dispersion compensated signal to a time domain version. This will provide the correct dispersion compensation of the received signal $y(t)$ for a sine wave mode at time t_i but will over or under compensate for other times.

To correct the signal for all times, the above process can be performed in a loop, where the i_{th} iteration performs dispersion compensation for the i_{th} time in the signal. This value is saved into a new array, which is the dispersion compensated version of the received signal $y(t)$ for all times. This technique was used in this work to perform dispersion compensation. A more computationally efficient dispersion compensation method can be found in [29].

3. Methodology

3.1. Wood and aluminium rod samples

A radiata pine cylindrical rod with a diameter of 16 mm and a length of 2460 mm was used. The sample was chosen such that it did not have any observable defects. For comparison, measurements were repeated on a 6061-T6 aluminium cylindrical rod with a diameter of 16 mm and a length of 2510 mm. The aluminium sample is an isotropic and homogeneous material whose dispersion curves can be easily obtained since its mechanical properties are known. However, it should be noted that wood is orthotropic, inhomogeneous and highly attenuative particularly at high frequencies.

Figure 1 shows the theoretical dispersion curves for a 16 mm diameter aluminium rod. The dispersion curves were obtained using GUIGUW [35]. The dispersion curves were obtained using the following parameters for a 16 mm diameter aluminium rod: Young's modulus = 68.9 GPa, density = 2,710 kg/m³ and Poisson's ratio = 0.33. This would give a theoretical bulk wave speed of about 6175 m/s for the aluminium sample [6]. We can see that the three fundamental longitudinal, flexural and torsional wave modes are present. However, at higher frequencies or higher sample thickness, higher order wave modes are expected to be present.

3.2. Resonance setup

An 8 oz hammer with a metal head tip was used in the experiment to generate stress waves. For resonance measurements, a hammer hit parallel to the wood grain was performed at one exposed end of the sample to generate longitudinal stress waves. The resulting signal was measured using a GRAS 46BF-1 microphone
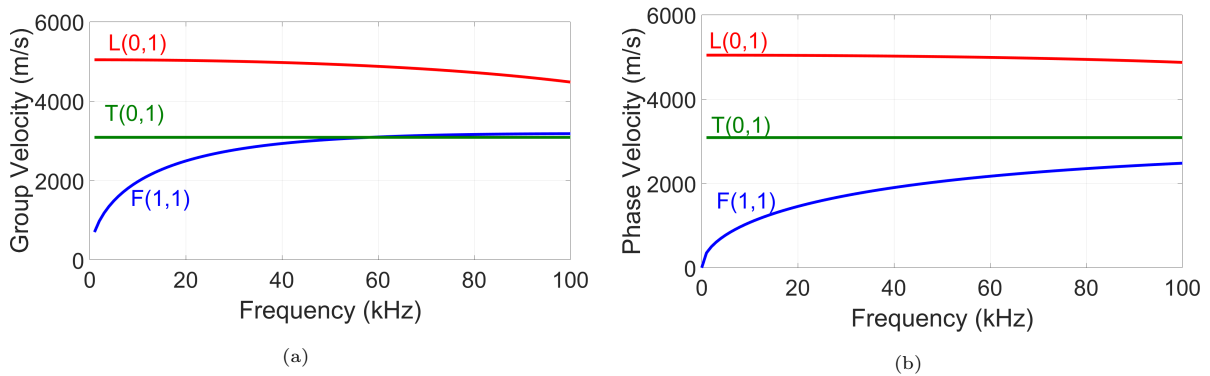
Figure 1: Theoretical dispersion curves for a 16 mm diameter aluminium rod showing the fundamental longitudinal L(0,1), torsional T(0,1) and flexural F(1,1) wave modes plotted as (a) group velocity and (b) phase velocity.

located at the opposite end of the sample relative to the hammer impact. The microphone was connected to a GRAS 26A-1 pre-amp and was powered through a GRAS 12AK power module. The received signal from the microphone was then sampled at 2 MHz using the Analog to Digital Converter (ADC) channels of a Data Translation DT9832 data acquisition module, see Figure 2. The received signal was saved to file and further processed in MATLAB.
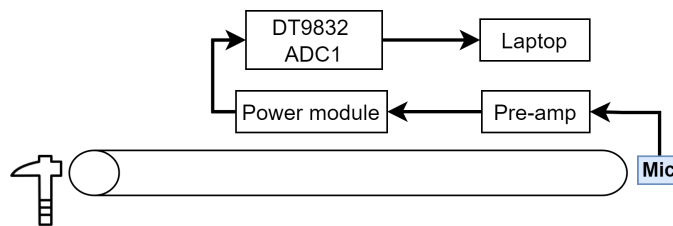
Figure 2: Experimental setup for resonance measurements

.

3.3. Hammer hit (ToF) setup

Traditionally, probes are inserted into a sample to penetrate through the bark and allow coupling of the acoustic signals to the wood. However, in this work we have used shear PZT transducers manufactured by TWI, UK [36] directly coupled to the wood sample by clamping them using springs, see Figure 3. This provides better control over the types of vibrations being measured and transmitted. For example, by aligning the transducers parallel to the grain, we can enhance the transmission and reception of longitudinal vibrations and suppress torsional and flexural vibrations [21, 37].

Two transducers were positioned as shown in Figure 4. The contact faces of the shear transducers were oriented parallel to the grain to enhance the reception of vibrations in the longitudinal direction. A hammer hit was performed at one end of the sample parallel to the grain. The received signal produced by the
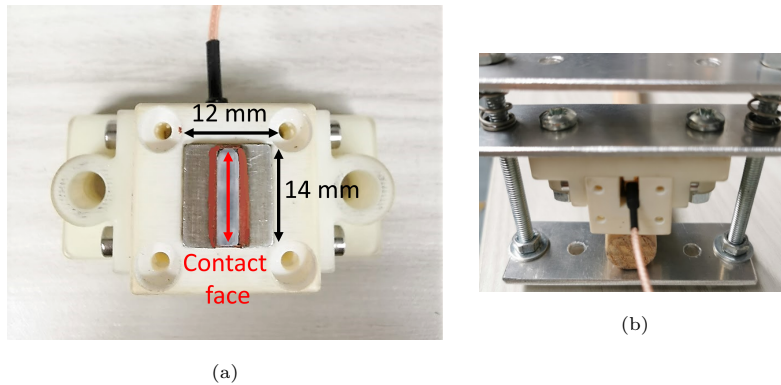
Figure 3: Photo (a) shows one of the transducers used in this experiment. Photo (b) shows the transducer being pushed against a wooden rod sample using springs.

hammer hit has a high amplitude and hence pre-amps were not needed. The transducers were directly connected to the ADCs of the DT9832 and the received signal at RX1 and RX2 were sampled at 2 MHz and saved to file. The recording of the received signal was initiated by pressing a keyboard button just before a hammer hit was manually performed.
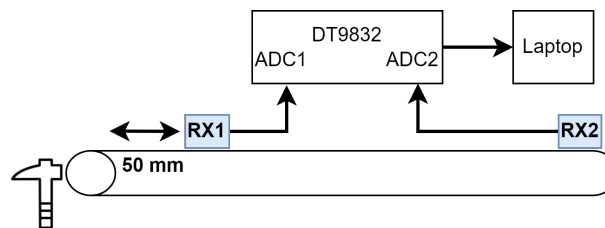

Figure 4: Experimental setup for hammer hit (ToF) measurement.

3.4. Tone burst and guided wave setup

Three shear transducers were positioned and clamped in the configuration shown in Figure 5. The contact faces of the transducers were oriented parallel to the grain to enhance the transmission and reception of vibrations in the longitudinal direction [21]. Note that the positioning of the RX1 and RX2 transducers was the same as for the hammer hit measurements.

The excitation signal applied to transducer TX was created in MATLAB and outputted from an Agilent 33210A Function Generator. To amplify the transmitted signal, a custom-built linear power amplifier capable of amplifying signals up to 400 Vpp was used. The receivers were connected to pre-amps and the received signal at RX1 and RX2 were sampled at 2 MHz using the ADC channels of the DT9832 module, refer Figure 5. The received signals were saved to file for further processing. In contrast to the manual hammer hit recordings, hardware triggering was used to synchronise the transmission of the transmit signal with the
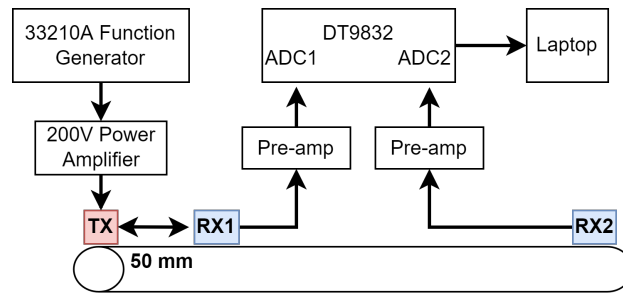
Figure 5: Experimental setup for tone burst and guided wave measurements.

recording of the received signal. Two types of excitation were made using this experimental setup, which are tone burst excitation with and without Hanning window.

Non-windowed tone burst measurements were used for amplitude threshold ToF measurement. These were used as they were narrowband and were more repeatable than hammer hit excitation. The tone bursts were five cycles of a 15 kHz sine wave. These measurements will be referred to as "tone burst measurements" in the following text.

Hanning-windowed tone bursts were used for the guided wave measurements. Windowing helps to reduce the bandwidth of the signal to minimise the effects of dispersion. These measurements used five cycles of a Hanning windowed sine wave with central frequencies ranging from 15 to 50 kHz in 1 kHz increments. These measurements were performed to experimentally measure the phase velocity dispersion curves for the $L(0,1)$ wave mode and will be referred to as "guided wave measurements" in the remainder of the paper.

3.5. Data processing

For resonance measurements, the microphone recordings of hammer hits at the ends of the rods were processed to calculate resonance acoustic velocities for both samples. The FFT of the received signal was used to obtain the resonant frequencies. In most cases, the first or second harmonic is used to obtain the resonance velocity. However, reports in the literature have mentioned that resonance velocities vary depending on which harmonic frequency is used. Also, resonance measurements at lower frequencies are more prone to errors due to frequency resolution issues [38]. To minimise these errors, an average resonance velocity using the lowest five resonance frequency peaks using Equation 2 was obtained for each sample. This was repeated for five measurements and the average was taken as the resonance velocity. Figure 6 below shows the FFT spectra of the wood and aluminium samples obtained from the resonance measurement. The red-marked points correspond to the resonant peaks for the longitudinal wave mode.

ToF velocity measurements were obtained using the FToA amplitude threshold method. The times when the signal at receivers RX1 and RX2 first went above a certain threshold were measured. The difference between these times T was then calculated. The ToF velocity was then calculated using Equation 3. This was performed for both hammer impact and the 15 kHz sine wave tone bursts. The threshold was set to
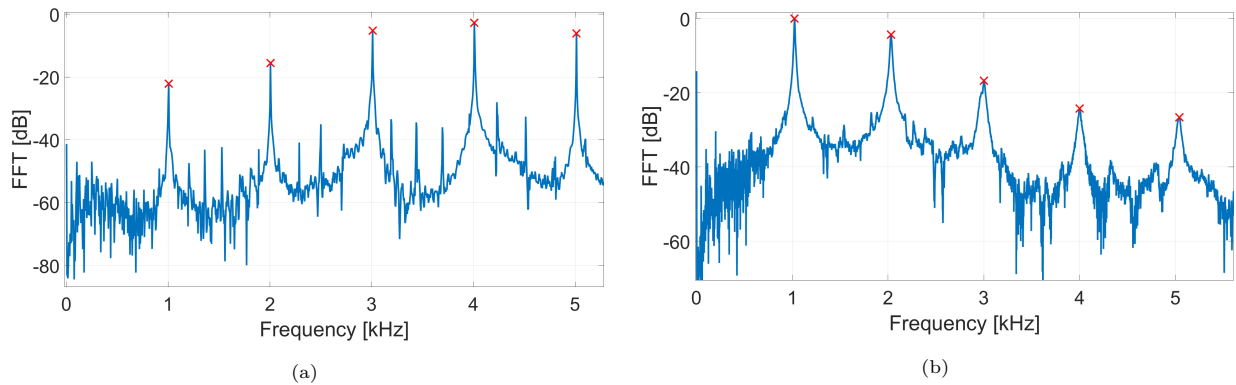
Figure 6: Plots of FFT spectra obtained from resonance measurements for (a) aluminium and (b) wood sample.

0.002 V and 0.02 V for the hammer impacts and tone bursts respectively. These values were chosen as they were approximately three times the standard deviation of the RMS of the noise and did not result in false positives. Note that a lower threshold value was used for the hammer hits as pre-amps were not used for these measurements which resulted in a lower noise. The average of five measurements was taken as the measured ToF acoustic velocity. The measurements were performed without removing the transducers.

Experimentally measured dispersion curves for the fundamental longitudinal L(0,1) wave mode were obtained from the guided wave measurements. These measurements were performed using Hanning windowed sine wave signals with varying transmit frequencies. Phase velocities were obtained from these measurements using a frequency-domain shifting technique. For each transmission, the received signal at RX1 was converted into the frequency-domain using the Fast Fourier Transform (FFT). Equation 4 was then used to simulate the propagation of the RX1 signal by a distance d using an initial phase velocity v_{ph}. The propagated signal was then converted back into the time-domain using the Inverse Fast Fourier Transform (IFFT). The Root Mean Squared Error (RMSE) between the propagated time-domain RX1 signal and the received signal at RX2 was calculated. The phase velocity was iteratively adjusted by 1 m/s until a minimum RMSE was obtained. The velocity value which corresponds to the minimum RMSE was taken as the phase velocity at the central transmit frequency. This process was repeated for a range of central transmit frequencies. Figure 7 shows a block diagram process of measuring the phase velocity from received signal RX1 and RX2.

3.6. Dispersion curves and dispersion compensation

Phase velocity dispersion curves were fitted using the calculated phase velocities of the guided wave measurements performed at various transmit frequencies for both samples. For the aluminium sample, a theoretical phase velocity dispersion curve of the L(0,1) wave mode was obtained using GUIGUW and the parameters mentioned in Section 3.1. The same could not be done for the wood sample as the mechanical
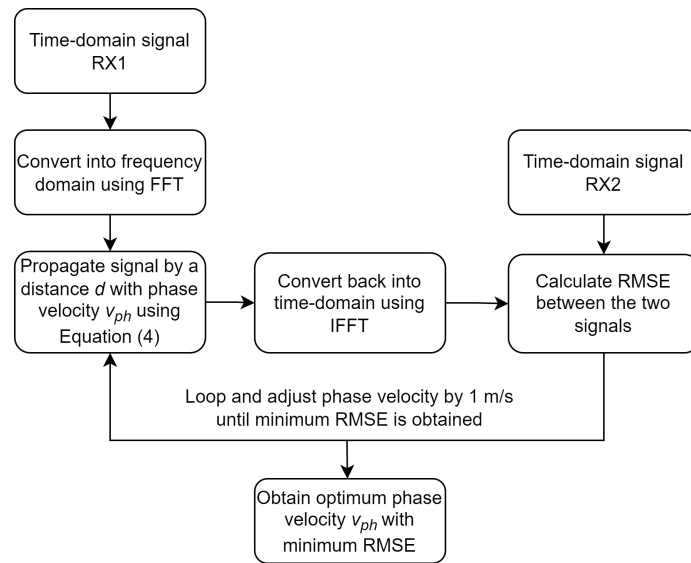
Figure 7: Block diagram process of obtaining phase velocity from guided wave measurements.

properties are not known. However, a curve of best fit was plotted using the following equation

$$c_l = c_o \sqrt{\frac{1 + \alpha_1 \ \alpha_2 \ k^2}{1 + \alpha_1 \ k^2}}, \tag{9}$$

where c_o is the rod velocity, α_1 and α_2 are constants and k is the wavenumber. The optimum values for c_o, α_1 and α_2 were obtained using a non-linear least squares fitting technique. The above equation is based on the correction of the Rayleigh-Bishop theory [39] which approximates the dispersion relation of the fundamental longitudinal wave mode for isotropic bars of any cross-section. The equation was chosen as it is easy to use and gives good approximations at low frequencies.

Using the theoretical and fitted dispersion curves, dispersion compensation was performed on both the simulated and experimental waveforms for the transmitted frequency range using the method described in Section 2. The ToF acoustic velocities were then obtained using the FToA amplitude threshold method. These ToF measurements were obtained both before and after dispersion compensation had been applied to the signals.

3.7. Numerical simulation

Simulations were also performed to evaluate if dispersion was causing any overestimation in amplitude threshold ToF velocity measurements. The advantage of performing these simulations was that it allowed the effects of dispersion to be evaluated without any other external factors being present that could influence the wave propagation.

Two types of excitation signals were used in the simulations. A hammer hit excitation signal was approximated as half of a cycle of a sine wave with frequencies respectively of 2 and 8 kHz for wood and

aluminium samples. These were chosen as the shape was similar to the first cycle of the measured hammer hit signals for these samples. Additionally, a five cycle 15 kHz sine wave was also used.

Using the experimentally measured L(0,1) phase velocity dispersion curves for aluminium and wood, Equation 4 was then used to simulate the propagation of these excitation signals at a distance of 2510 mm for both samples respectively. Figure 8 shows an example of the simulated transmitted and received signals for the aluminium sample.

(a) Half a cycle of a 8 kHz sine wave.
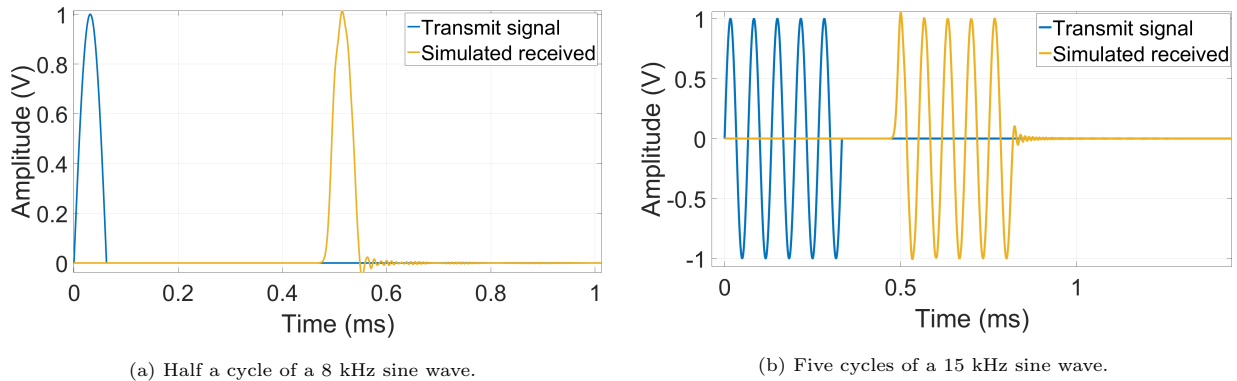
(b) Five cycles of a 15 kHz sine wave.

Figure 8: Plots showing the simulated transmit and received signal using different signal excitation for the aluminium sample.

The FToA of the received signals were then determined from the simulated signals using the amplitude threshold method with a threshold value of 0.01 V. The simulated amplitude threshold ToF acoustic velocity was then measured using Equation 3.

4. Results

Table 1 shows the experimental acoustic velocities obtained using resonance, amplitude threshold ToF and guided wave methods for both aluminium and wood samples, before any dispersion compensation was performed. Note that the resonance and hammer hit ToF acoustic velocities presented in the table are obtained from the average of five measurements. Both tone burst and guided wave measurements produced similar results for each individual recording. Hence the uncertainty of the two measurements was calculated from the sampling resolution. Results from the table show that the acoustic velocities obtained using the amplitude threshold ToF(for both hammer hit and tone burst excitation) and guided waves method were higher than resonance. This is observed for both the aluminium and wood samples. The ToF velocity measurements were outside the uncertainty range for resonance and were approximately 1.8 - 3.2% higher. Guided wave velocities have a lower overestimation (< 1%) relative to resonance and are within the uncertainty of the resonance velocity measurements.

Note that the measured acoustic velocities for the aluminium sample are significantly lower than the expected bulk wave speed of 6175 m/s. This indicates that bulk waves were not being measured and hence

Table 1: Experimental acoustic velocity measurements obtained using different excitation methods for the aluminium and wood samples. The guided wave acoustic velocity represents the phase velocity of a 5 cycle Hanning-windowed 15 kHz sine wave.

Methods	Aluminium (m/s)	Wood (m/s)
Resonance	5036 ± 21	4463 ± 41
Hammer (ToF)	5130 ± 35	4592 ± 33
Tone burst (ToF)	5141 ± 7	4608 ± 7
Guided Waves	5062 ± 7	4508 ± 7

this is not a cause of the overestimation relative to resonance observed for this sample.

4.1. Experimental dispersion curves

Figure 9 shows the guided wave phase velocity measurements obtained for the aluminium and wood samples. Each data point in the figure represents a single measurement obtained using a narrowband excitation signal. This excitation signal was composed of five cycles of a Hanning-windowed sine wave with a central frequency f_o. These measurements were repeated using values of f_o which ranged from 15 to 50 kHz for aluminium and 15 kHz to 40 kHz for wood in 1 kHz increments. The frequency range used for the two materials was different due to the higher attenuation rate in wood at higher frequencies. For the wood sample, the phase velocities for frequencies above 40 kHz could not be measured reliably as the received signals were highly distorted due to attenuation and hence the results were omitted. Overlaid are their respective phase velocity dispersion curves. For aluminium, the theoretical dispersion curve was obtained using GUIGUW. For wood, the dispersion curve was obtained by fitting a curve through the guided wave phase velocity measurements using the method described in Section 3.6. Both dispersion curves are observed to match well with the experimental guided wave measurements. The average error between the measured and theoretical/fitted phase velocities were 5 m/s and 7 m/s for aluminium and wood respectively. The fitted dispersion curve for wood has high R^2 value (0.99) at the frequency range of interest. Figure 9 also shows that the dispersion curve for wood has more curvature compared to aluminium which implies that the wood sample is more dispersive.

Figure 10 shows the wavenumber-frequency domain plots which were presented in our previous paper [21] for the same samples. Overlaid are the guided wave phase velocities and dispersion curves shown in Figure 9 which have been converted into wavenumber using Equation 5. It can be seen that the guided wave measurements and dispersion curves matches well with the L(0,1) wave mode from the wavenumber-frequency plots. Note that the wavenumber-frequency domain plots have relatively low resolution. This would cause dispersion curves obtained from the wavenumber-frequency domain plots to have high variations when converted to phase velocity-frequency domain compared to dispersion curves obtained directly from phase velocity measurements. The error is more prominent at lower frequencies and decreases with increase
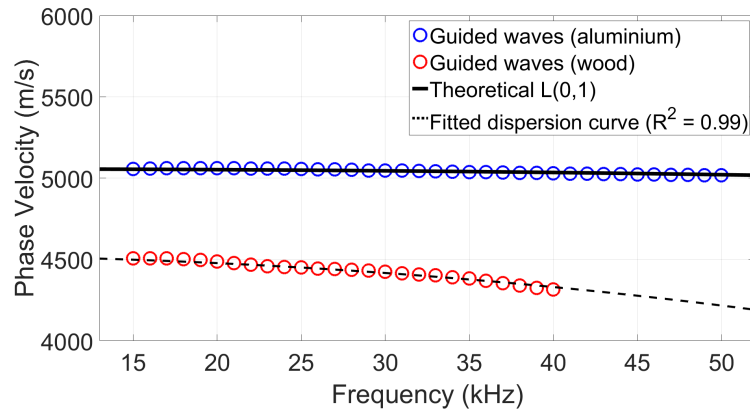
Figure 9: Guided wave phase velocity measurements overlaid with dispersion curves for aluminium and wood sample.

in frequency.

(a) Wavenumber-frequency plot for aluminium
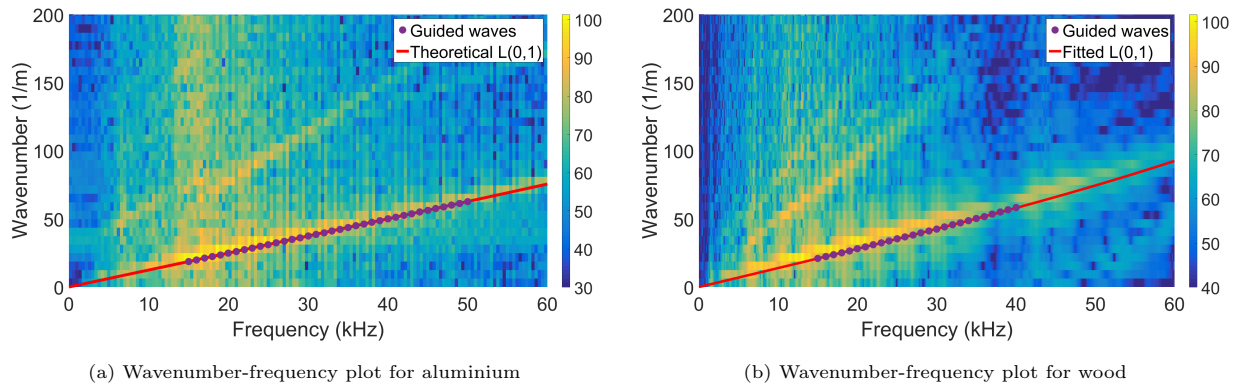

(b) Wavenumber-frequency plot for wood

Figure 10: Wavenumber-frequency plots obtained using the 2D FFT method overlaid with experimental guided wave measurements and fitted dispersion curves.

4.2. Simulated ToF measurements

Simulations were performed using the method described in Section 3.7 to evaluate the effects of dispersion on amplitude threshold ToF measurements and if these effects could be mitigated using dispersion compensation. The received signal at RX1 and RX2 were simulated using the measured dispersion curves of the L(0,1) wave mode shown in Figure 9. Amplitude threshold ToF acoustic velocity measurements were first obtained from the unprocessed simulated signals for the simulated hammer hit and tone burst excitation. Dispersion compensation was then performed in post-processing on the simulated received signal for both RX1 and RX2. Amplitude threshold ToF velocity measurements were then repeated on the dispersion compensated received signals.

Figure 11 shows an example of the simulated received signal for the aluminium sample before and after dispersion compensation has been performed. Note that these plots have been zoomed in to show the first

Table 2: Simulated acoustic velocity measurements for aluminium and wood before and after dispersion compensation. Note that the expected theoretical resonance velocities for aluminium and wood are 5058 and 4526 m/s respectively.

Material	Excitation	Dispersion compensation	
		Before (m/s)	After (m/s)
Aluminium	Hammer	5130	5064
	Tone burst	5141	5072
Wood	Hammer	4592	4538
	Tone burst	4608	4545

arrival of the signal at the RX2 transducer located at the end of the sample, see Figure 5. The plots show that dispersion compensation resulted in a significant difference in rise time at the start of the signal. The dispersion compensated signal has a sharper rise time and is slightly delayed compared to the original signal. However, the phase and rise time were not significantly different at other times. This was also observed for the wood sample. The large difference in rise time at the start of the signal could lead to a difference in amplitude threshold ToF measurement and acoustic velocity measurement of the propagating wave.

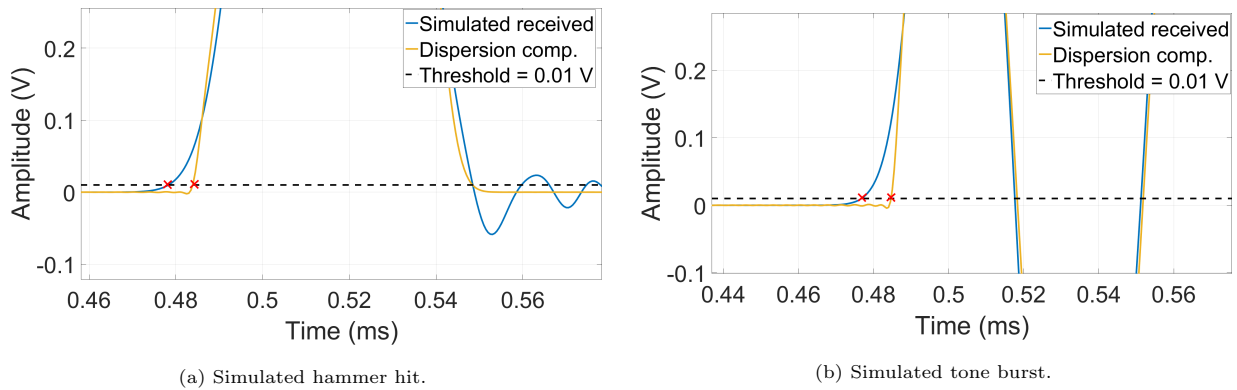(a) Simulated hammer hit.

(b) Simulated tone burst.

Figure 11: Plots showing the simulated received signal for the transducer RX2 located at the end of the sample before and after dispersion compensation for a half-cycle 8 kHz sine wave, meant to roughly approximate a hammer hit, and a 5 cycle 15 kHz tone burst for aluminium.

The simulated signals were processed using the FToA amplitude threshold method to obtain simulated ToF velocity measurements. The measured amplitude threshold ToF velocities of the simulated signals, before and after dispersion compensation, were obtained for the aluminium and wood samples, see Table 2. The results show that the measured acoustic velocities before dispersion compensation was performed were higher than the expected resonance velocity. The results also show a reduction in the simulated acoustic velocities after dispersion compensation was performed making them closer to the expected theoretical resonance values.

4.3. Experimental ToF measurements

Experimental measurements using hammer hit and tone burst excitations were also performed to investigate the effects of dispersion on amplitude threshold ToF measurements. Figure 12 shows the time-domain and frequency-domain spectra of the experimentally received signal from transducers RX1 and RX2 using hammer hit excitation for the aluminium and wood samples. It be seen that the wood sample has higher attenuation with increased frequency compared to the aluminium sample.

(a) Time domain - aluminium

(b) Time domain - wood

(c) Frequency domain - aluminium
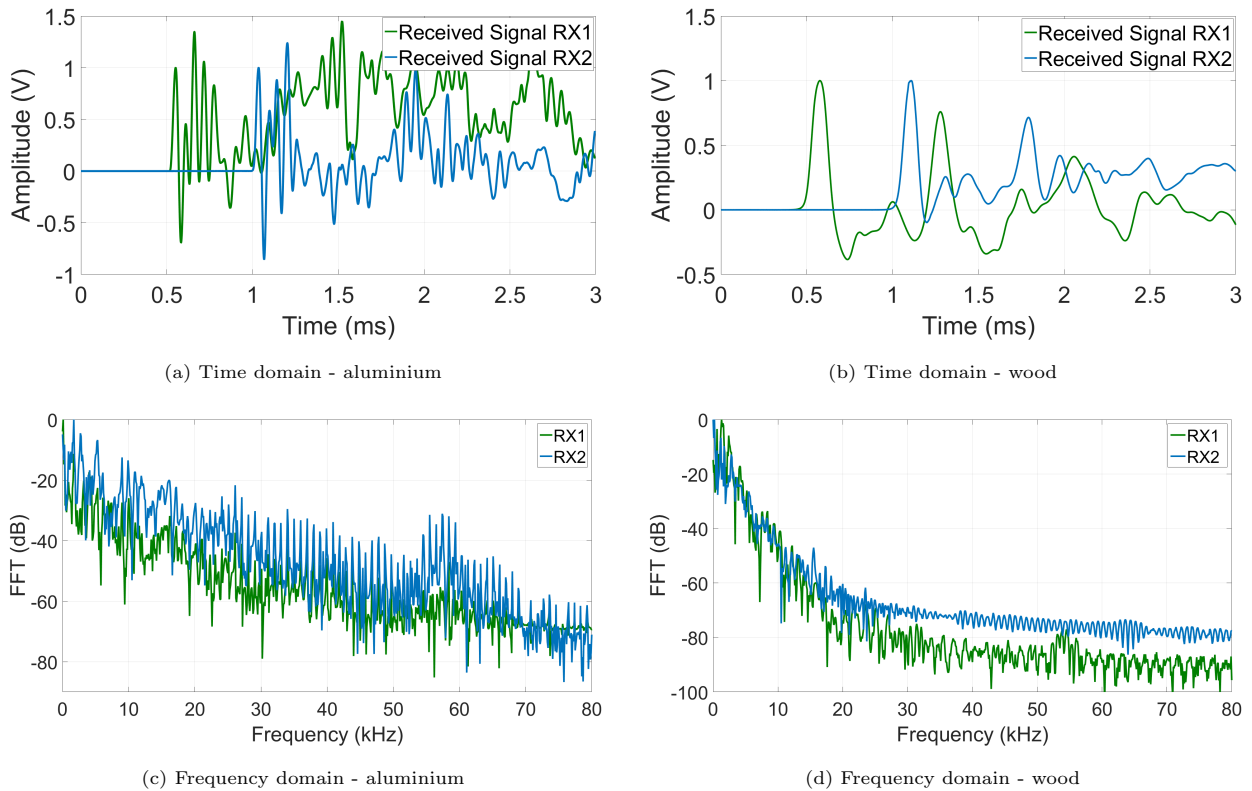
(d) Frequency domain - wood

Figure 12: Plots showing the time-domain and frequency-domain spectra of the received signals at transducers RX1 and RX2 for aluminium and wood samples using hammer hit excitation.

In a similar manner to that used in the simulations, post-processing was performed on the experimental RX1 and RX2 received signals to obtain amplitude threshold ToF measurements. These ToF measurements were obtained both before and after dispersion compensation was performed on the received signals. Figure 13 shows plots of the original received signal and the dispersion compensated signal for the aluminium and wood samples. Note that the arrivals times of the received signal for the hammer hit excitation and tone burst excitation are different as the hammer hit was performed manually without any hardware synchronisation. The results from the figure are similar to what had been observed in the simulations. The plots show that the rise time at the start of the received signal becomes sharper and is slightly delayed for the dispersion compensated signal. Also, the phase and rise time of the received signal before and after disper-

(a) Aluminium - hammer hit.

(b) Aluminium - tone burst.
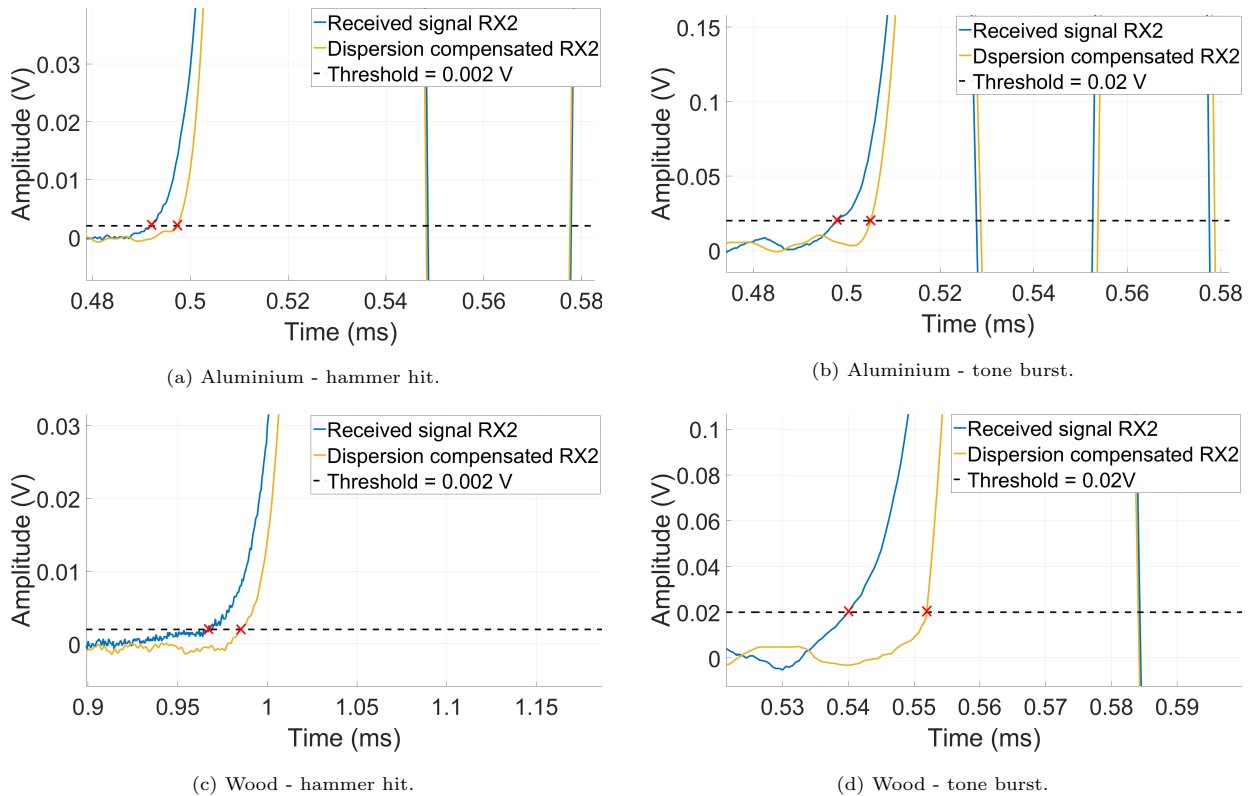

(c) Wood - hammer hit.

(d) Wood - tone burst.

Figure 13: Plots showing the effect of performing dispersion compensation on experimental ToF measurement signals on transducer RX2 for the aluminium and wood samples using a hammer impact and a 5 cycle 15 kHz sine wave tone burst excitation signal.

sion compensation were similar at other times. This was observed for both the hammer hit and tone burst measurements.

The average acoustic resonance velocity for the aluminium and wood samples are 5036 ± 21 m/s and 4463 ± 41 m/s respectively. Table 3 shows the experimental amplitude threshold ToF acoustic velocities measured before and after dispersion compensation was performed on the received signal. The results show that the amplitude threshold ToF measured acoustic velocities for the dispersion compensated signal are smaller than the original dispersed signal and is quite similar to the resonance velocity. This indicates that dispersion compensation was able to reduce the overestimation of the amplitude threshold ToF measurements relative to resonance. Note that the measured acoustic velocity using the tone burst excitation is slightly higher than the hammer impact for both the original and dispersion compensated signal.

Table 3: Experimental amplitude threshold ToF acoustic velocity measurements for aluminium and wood before and after dispersion compensation. Note that the acoustic resonance velocity for the aluminium and wood samples are 5036 $\pm$ 21 m/s and 4463 $\pm$ 41 m/s respectively.

Material	Excitation	Dispersion compensation	
		Before (m/s)	After (m/s)
Aluminium	Hammer	5130 $\pm$ 35	5064 $\pm$ 16
	Tone burst	5141 $\pm$ 7	5072 $\pm$ 7
Wood	Hammer	4592 $\pm$ 33	4476 $\pm$ 33
	Tone burst	4608 $\pm$ 7	4525 $\pm$ 7

5. Conclusion

This work investigates the effects of dispersion on ToF acoustic velocity measurements obtained using the amplitude threshold FToA method. This technique uses the very start of the signal to measure the acoustic velocity and is the most common technique used for ToF acoustic velocity measurements in wood.

Acoustic velocity measurements using amplitude threshold ToF, resonance and guided wave methods were performed on 16 mm diameter wood and aluminium rod samples. The guided wave measurements were used to obtain experimental measurements of the phase velocity dispersion curves for the L(0,1) wave mode. These dispersion curves were used to simulate the wave propagation along the rods and to perform dispersion compensation for both the simulated and experimental data. Dispersion compensation was performed to mitigate the effects of dispersion.

Comparisons were made between the received signal before and after performing dispersion compensation for the simulated and experimental data. The results showed that dispersion caused the received signal to spread out as it propagated. This resulted in the signal arriving earlier at the second transducer and having a lower rise time than the dispersion compensated signal. This distortion at the front portion of the dispersed signal resulted in an overestimation of the measured acoustic velocity relative to resonance when using the amplitude threshold FToA technique. Dispersion compensation mitigated this distortion and hence reduced the overestimation, providing ToF acoustic velocity measurements that were closer to the resonance velocities. The L(0,1) wave mode for the aluminium sample had relatively low dispersion. However, the results showed that overestimation in amplitude threshold ToF measurements can still occur at these low dispersion levels. To the best of the authors' knowledge, this is the first study to have shown that dispersion can cause an overestimation in ToF velocity measurements obtained using FToA techniques.

The study showed that dispersion can be a potential cause of the overestimation of ToF acoustic velocity measurements obtained using the FToA amplitude threshold technique. The same effect is expected to occur for other FToA techniques such as AIC and MER since these techniques also utilise the front portion of the received signal. The dispersion compensation technique can be used to mitigate dispersion effects and

reduce the resulting overestimation of the measured ToF acoustic velocity caused by these effects.

For guided wave testing of metal structures, dispersion effects are usually reduced by using narrow bandwidth excitation signals. There have been a couple of studies that have investigated this technique for wood. For example, Subhani et.al [22] investigated ways to reduce the effects of dispersion in timber utility poles using finite element analysis by selecting the optimum excitation frequency. However, the previous studies did not report any FToA acoustic velocity measurements.

The amplitude threshold ToF velocity overestimation observed in this study was relatively low (less than 3%) compared to the values reported in the literature for standing trees, which ranged from about 7 to 31% for radiata pine [4]. However, this study was performed using thin (16 mm diameter) rods, which had relatively minimal dispersion in the excitation frequency range used for the fastest wave mode, the fundamental longitudinal L(0,1) wave mode.

This study has been performed on a small diameter wood sample. For larger diameter samples such as tree stems, higher dispersion would be expected to occur, which could lead to higher overestimations. Further work should be performed on larger diameter samples to investigate the relationship between the measured dispersion curves and any observed overestimation in ToF acoustic velocity relative to resonance. This should include both broadband and narrowband excitation. The experiments should also be repeated on logs, seedlings and standing trees with varying diameters to determine the practicality of the dispersion compensation technique. Other guided wave techniques should also be investigated which can help obtain improved NDT measurements. Stiffness measurements should also be obtained using the techniques in this study and compared with stiffness measurements obtained using static bending tests.

References

[1] R. L. Dickson, C. A. Raymond, W. Joe, C. A. Wilkinson, Segregation of *Eucalyptus dunnii* logs using acoustics, Forest Ecology and Management 179 (1-3) (2003) 243–251.

[2] H. Heräjärvi, Static bending properties of Finnish birch wood, Wood Science and Technology 37 (6) (2004) 523–530.

[3] R. Meder, A. Thumm, D. Marston, Sawmill trial of at-line prediction of recovered lumber stiffness by NIR spectroscopy of *Pinus radiata* cants, Journal of Near Infrared Spectroscopy 11 (2) (2003) 137–143.

[4] X. Wang, Acoustic measurements on trees and logs: a review and analysis, Wood Science and Technology 47 (5) (2013) 965–975.

[5] X. Wang, R. J. Ross, P. Carter, Acoustic evaluation of wood quality in standing trees. Part I. Acoustic wave behavior, Wood and Fiber Science 39 (1) (2007) 28–38.

[6] M. Legg, S. Bradley, Measurement of stiffness of standing trees and felled logs using acoustics: A review, The Journal of the Acoustical Society of America 139 (2) (2016) 588–604.

[7] C. R. Mora, L. R. Schimleck, F. Isik, J. M. Mahon, A. Clark, R. F. Daniels, Relationships between acoustic variables and different measures of stiffness in standing *Pinus taeda* trees, Canadian Journal of Forest Research 39 (8) (2009) 1421–1429.

[8] H. Maurer, S. I. Schubert, F. Bächle, S. Clauss, D. Gsell, J. Dual, P. Niemz, A simple anisotropy correction procedure for acoustic wood tomography (2006).

[9] K. T. Hassan, P. Horáček, J. Tippner, Evaluation of stiffness and strength of scots pine wood using resonance frequency and ultrasonic techniques, BioResources 8 (2) (2013) 1634–1645.

[10] F. Liu, P. Xu, H. Zhang, C. Guan, D. Feng, X. Wang, Use of time-of-flight ultrasound to measure wave speed in poplar seedlings, Forests 10 (8) (2019) 682.

[11] M. Kaphle, A. C. Tan, D. P. Thambiratnam, T. H. Chan, Identification of acoustic emission wave modes for accurate source location in plate-like structures, Structural control and health monitoring 19 (2) (2012) 187–198.

[12] S. Y. Chong, J.-R. Lee, C. Y. Park, Statistical threshold determination method through noise map generation for two dimensional amplitude and time-of-flight mapping of guided waves, Journal of Sound and Vibration 332 (5) (2013) 1252–1264.

[13] X. Wang, F. Divos, C. Pilon, B. K. Brashaw, R. J. Ross, R. F. Pellerin, Assessment of decay in standing timber using stress wave timing nondestructive evaluation tools: A guide for use and interpretation, Gen. Tech. Rep. FPL-GTR-147. Madison, WI: US Department of Agriculture, Forest Service, Forest Products Laboratory, 2004. 12 pages 147 (2004).

[14] L. Espinosa, J. Bacca, F. Prieto, P. Lasaygues, L. Brancheriau, Accuracy on the time-of-flight estimation for ultrasonic waves applied to non-destructive evaluation of standing trees: A comparative experimental study, Acta Acustica united with Acustica 104 (3) (2018) 429–439.

[15] L. Han, J. Wong, J. Bancroft, et al., Time picking and random noise reduction on microseismic data, CREWES Research Report 21 (2009) 1–13.

[16] G. Emms, B. Nanayakkara, J. Harrington, A novel technique for non-damaging measurement of sound speed in seedlings, European Journal of Forest Research 131 (5) (2012) 1449–1459.

[17] A. Krauss, J. Kúdela, Ultrasonic wave propagation and Young's modulus of elasticity along the grain of Scots pine wood (*Pinus sylvestris L.*) varying with distance from the pith, Wood Research 56 (4) (2011) 479–488.

[18] J. L. Rose, Ultrasonic guided waves in solid media, Cambridge University Press, 2014.

[19] I. A. Veres, M. B. Sayir, Wave propagation in a wooden bar, Ultrasonics 42 (1-9) (2004) 495–499.

[20] S. Dahmen, H. Ketata, M. H. B. Ghozlen, B. Hosten, Elastic constants measurement of anisotropic olivier wood plates using air-coupled transducers generated Lamb wave and ultrasonic bulk wave, Ultrasonics 50 (4-5) (2010) 502–507.

[21] A. H. A. Bakar, M. Legg, D. Konings, F. Alam, Ultrasonic guided wave measurement in a wooden rod using shear transducer arrays, Ultrasonics 119 (2022) 106583.

[22] M. Subhani, J. Li, B. Samali, K. Crews, Reducing the effect of wave dispersion in a timber pole based on transversely isotropic material modelling, Construction and Building Materials 102 (2016) 985–998.

[23] J. El Najjar, S. Mustapha, Understanding the guided waves propagation behavior in timber utility poles, Journal of Civil Structural Health Monitoring 10 (5) (2020) 793–813.

[24] U. Lindholm, Some experiments with the split Hopkinson pressure bar, Journal of the Mechanics and Physics of Solids 12 (5) (1964) 317–335.

[25] D. Gorham, A numerical method for the correction of dispersion in pressure bar signals, Journal of Physics E: Scientific Instruments 16 (6) (1983) 477.

[26] D. Gorham, P. Pope, J. E. Field, An improved method for compressive stress-strain measurements at very high strain rates, Proceedings of the Royal Society of London. Series A: Mathematical and Physical Sciences 438 (1902) (1992) 153–170.

[27] A. Tyas, D. J. Pope, Full correction of first-mode Pochammer–Chree dispersion effects in experimental pressure bar signals, Measurement Science and Technology 16 (3) (2005) 642.

[28] A. Barr, S. Rigby, M. Clayton, Correction of higher mode Pochhammer–Chree dispersion in experimental blast loading measurements, International Journal of Impact Engineering 139 (2020) 103526.

[29] P. D. Wilcox, A rapid signal processing technique to remove the effect of dispersion from guided wave signals, IEEE Transactions on Ultrasonics, Ferroelectrics, and Frequency Control 50 (4) (2003) 419–427.

[30] B. Xu, L. Yu, V. Giurgiutiu, Lamb wave dispersion compensation in piezoelectric wafer active sensor phased-array applications, in: Health Monitoring of Structural and Biological Systems 2009, Vol. 7295, International Society for Optics and Photonics, 2009, p. 729516.

[31] M. Legg, M. K. Yücel, V. Kappatos, C. Selcuk, T.-H. Gan, Increased range of ultrasonic guided wave testing of overhead transmission line cables using dispersion compensation, Ultrasonics 62 (2015) 35–45.

[32] B. Xu, L. Yu, V. Giurgiutiu, Advanced methods for time-of-flight estimation with application to Lamb wave structural health monitoring, in: Proc. International Workshop on SHM, 2009, pp. 1202–1209.

[33] R. Sicard, J. Goyette, D. Zellouf, A numerical dispersion compensation technique for time recompression of Lamb wave signals, Ultrasonics 40 (1-8) (2002) 727–732.

[34] K. Xu, D. Ta, P. Moilanen, W. Wang, Mode separation of Lamb waves based on dispersion compensation method, The Journal of the Acoustical Society of America 131 (4) (2012) 2714–2722.

[35] P. Bocchini, A. Marzani, E. Viola, Graphical user interface for guided acoustic waves, Journal of Computing in Civil Engineering 25 (3) (2011) 202–210.

[36] B. A. Engineer, The mechanical and resonant behaviour of a dry coupled thickness-shear PZT transducer used for guided wave testing in pipe line, Ph.D. thesis, Brunel University (2013).

[37] M. Legg, S. Bradley, Experimental measurement of acoustic guided wave propagation in logs, in: 19th International Nondestructive Testing and Evaluation of Wood Symposium, Rio de Janeiro, Brazil, 2015, pp. 681–688.
URL https://www.fs.usda.gov/treesearch/pubs/49713

[38] D. Brizard, An impact test to determine the wave speed in shpb: Measurement and uncertainty, Journal of Dynamic Behavior of Materials 6 (1) (2020) 45–52.

[39] G. Carta, Correction to Bishop's approximate method for the propagation of longitudinal waves in bars of generic cross-section, European Journal of Mechanics-A/Solids 36 (2012) 156–162.

Chapter 5

Comparison of Stiffness Measurements of Wooden Rods Obtained Using Acoustic Guided Waves and Static Bending Tests

The work presented in this chapter is in preparation for submission to a journal. Some additional experiments have been planned to be included before submission.

Comparison of Stiffness Measurements of Wooden Rods Obtained Using Acoustic Guided Waves and Static Bending Tests

Adli Hasan Abu Bakar, Mathew Legg*, Khalid Arif, Daniel Konings, Fakhrul Alam

Department of Mechanical and Electrical Engineering, Massey University, Auckland, New Zealand

Abstract

Acoustic/ultrasonic guided wave testing has been used in recent years for structural health monitoring of timber utility poles and mechanical property characterization of wood samples. However, previous guided wave studies for wood have only compared stiffness measurements with static bending tests for rectangular wood samples. Additionally, these guided wave stiffness measurements have not been compared with the acoustic resonance and time-of-flight methods that are widely used in the wood industry. This study investigates the use of acoustic guided waves for estimating the dynamic Modulus of Elasticity (MoE) of cylindrical radiata pine rods. These MoE values are then compared with measurements obtained using the traditional acoustic resonance, time-of-flight and three-point static bending methods. The results suggest that dynamic MoE values obtained using the resonance, time-of-flight and guided wave method were on average 6.4%, 11.6% and 9.5% higher compared to static MoE obtained using three-point bending test. Guided wave measurements are observed to offer slight improvement compared to the time-of-flight method.

Keywords: Radiata pine, rod velocity, rod, ToF, guided waves, MoE.

1. Introduction

The ability to measure the mechanical properties of wood can bring benefits to the forestry industry. The stiffness of wood is commonly used to segregate logs which can lead to an increase in efficiency, sustainability and profitability [1, 2]. For example, pre-sorting of logs prior to milling can allow structural sawmills to purchase logs that can maximise grade recovery [3]. Traditionally, static bending tests are used to measure the stiffness of wood and are considered the gold standard. Stiffness measurements obtained from this technique are often referred to as the static Modulus of Elasticity (MoE). The technique involves applying a load onto a sample at a constant rate and measuring the resulting deflection. The MoE is then obtained from the resulting load-deflection curve. The two common bending tests are the three-point and four-point

---

*Corresponding author

Email addresses: A.Hasan@massey.ac.nz (Adli Hasan Abu Bakar), M.Legg@massey.ac.nz (Mathew Legg),
K.arif@massey.ac.nz (Khalid Arif), D.Konings@massey.ac.nz (Daniel Konings), F.Alam@massey.ac.nz (Fakhrul Alam)

bending tests [4]. The main difference between them is the area over which load is applied. For a three-point bending test, stress is applied directly under the center of the loading point while for a four-point bending test, the stress is distributed on a wider area between the loading points. The static bending method is time-consuming and generally breaks the sample, which is costly [5]. To mitigate these issues, various Non-Destructive Testing (NDT) techniques have been developed that can be used to measure the stiffness of wood. These include methods such as Near-infrared (NIR) spectroscopy [6], SilviScan [7] and acoustics [8].

Acoustics is the most popular NDT technique for measuring wood stiffness as it is cost-effective, simple to use and non-destructive [9]. The stiffness of wood obtained using acoustic NDT techniques is commonly referred to as the dynamic MoE. Wood is an orthotopic material meaning that the acoustic velocity and mechanical properties are different in three directions - longitudinal, flexural and torsional. The stiffness of wood is related to the MoE in the longitudinal direction. This is generally described as

$$E_L = \rho \ c_l{}^2, \tag{1}$$

where ρ is the density of the material and c_l is the acoustic velocity propagating in the longitudinal direction. The stiffness and acoustic velocity in the longitudinal direction for wood has been related to various wood properties such as microfibril angle, variation in grain angle, tracheid dimensions and density [10].

The two common acoustic methods used for measuring the stiffness of wood are the resonance and Time-of-Flight (ToF) methods. The resonance method involves generating longitudinal stress waves by performing a hammer hit parallel to the wood grain at one exposed end of the wood sample. A device at one end of the sample is then used to measure the received signal. A Fast Fourier Transform (FFT) is performed on the received signal to identify the resonance frequencies. The longitudinal resonance velocity c_{res} is obtained using

$$c_{res} = \frac{2Lf_n}{n}, \tag{2}$$

where L is the sample length, f_n is the nth harmonic frequency and n is an integer ($n = 1, 2, 3...$).

The ToF method generally involves two transducers that are normally attached to probes. The probes are driven into the timber sample and a hammer hit is performed at one of the probes to generate stress waves. The ToF velocity can be obtained using

$$c_{tof} = \frac{\Delta d}{T}, \tag{3}$$

where Δd is the distance between the two probes and T is the time taken for the stress waves to propagate from one probe to the other. Typically, the ToF method uses the First Time of Arrival (FToA) technique to determine when a signal first arrives at the receiver. This technique only looks at the very first portion of the signal and ignores the remainder.

Both acoustic methods are widely used for NDT testing of wood. The ToF method can be used on both standing trees and felled logs whereas the resonance method can only be used on felled logs. Stiffness

measurements performed at the standing tree stage can help in forest evaluation, forest management and silviculture [11, 12].

Studies have shown good correlations between MoE values obtained using acoustic resonance and ToF methods with static bending tests [13, 14, 15]. However, the literature has shown that acoustic velocity and stiffness measurements obtained using the ToF method are systematically higher compared to resonance and can vary between 7 - 35% [16]. This overestimation is also observed between dynamic MoE values obtained using the ToF method and static MoE values obtained using static bending tests [17]. There have been suggestions as to the potential causes of the overestimation such as log diameter [18], the variation in stiffness from pith to bark [19] and the difference in wave propagation between the resonance and ToF methods [20]. However, the exact cause of the overestimation is still not known. Alternate methods to measure the mechanical properties of standing trees needs to be investigated.

Ultrasonic guided wave testing is another NDT technique which has successfully been used for structural health monitoring of structural materials such as metals and concrete [21]. For wood studies, guided waves (GW) have been used for embedded depth estimation [22] and damage assessment [23] of cylindrical timber utility poles. There have been a few studies that have utilized guided wave techniques to measure the elastic constants for rectangular wood samples [24, 25]. Other studies have also used guided wave techniques to obtain the mechanical properties of rectangular wooden plates and compared them with static bending methods [26, 27, 28]. Guided wave studies used for stiffness estimation of wood have only been performed on rectangular cross-section wood samples, which generate Lamb waves and are different to the rod waves generated in circular cylindrical samples. Furthermore, the dynamic MoE values obtained from the guided wave technique have not been compared with dynamic MoE values obtained using traditional resonance and ToF methods.

In our previous work [29], we proposed a new approach to obtain the rod velocity of wood using multi-frequency guided wave measurements. The rod velocity was then compared with acoustic velocities obtained using the traditional resonance and ToF methods. That study only performed measurements on two wooden samples and compared the acoustic velocities and did not include stiffness measurements obtained using static bending tests. Static bending tests are considered the gold standard for measuring the stiffness of wood. Therefore, in this article, we extend on the previous work by comparing MoE values for fifteen cylindrical wooden rods obtained using traditional resonance, ToF, static bending and guided wave methods. To the best of the author's knowledge, this is the first study to compare stiffness measurements using all four methods for any type of material.

This paper is organised as follows. The methodology and experimental procedure are described in Section 2. The experimental results are discussed in Section 3. Lastly, the conclusion and suggestions for future work are given in Section 4.

2. Materials and method

The objective of this study is to compare MoE measurements obtained using resonance, ToF, guided waves and static bending test methods. To do so, fifteen off-the-shelf cylindrical kiln-dried radiata pine rods with a diameter of 16 mm and length of 2440 mm were obtained. The age and origin of the samples are not known. The samples were chosen such that they were undamaged and did not contain any observable defects. The experimental setup for each method is described in the subsections below. The moisture content of the samples can influence the acoustic wave velocity and static bending test measurements. To mitigate this, all the experimental procedure was performed and measured on the same day.

2.1. Resonance

For resonance measurements, a hammer hit was performed parallel to the wood grain at one end of the rod sample. A GRAS 46BF-1 microphone with a bandwidth of 4 Hz - 100 kHz was used to measure the vibrations [30]. The microphone was positioned at the opposite end of the sample using a clamp. The microphone was connected to a GRAS 26A-1 pre-amp and powered through a GRAS 12AK power module. The received signal was sampled at 2 MHz using the ADC channel from a Data Translation DT9832 data acquisition module. The data was saved to file and processed in MATLAB. The experimental setup can be seen in Figure 1.
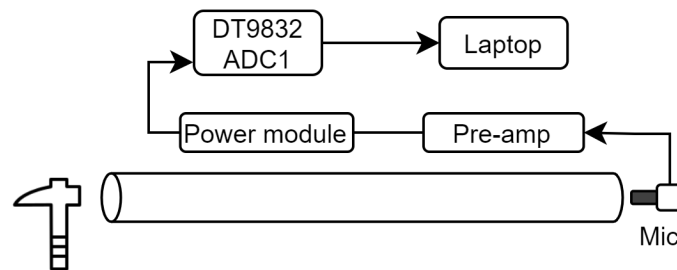

Figure 1: Diagram of the experimental setup for resonance measurements.

A Fast Fourier Transform (FFT) was performed on the received signal and the resonance peaks were identified. Normally, either the first or second harmonic is commonly used. However, in this study, the average velocity obtained from the first and second harmonic is taken as the resonance velocity. The resonance dynamic MoE was then calculated using Equation 1 by substituting the value of c_{res} into c_l.

2.2. Time of flight

Dry-coupled shear PZT transducers were used in this study for excitation/reception of vibrations [31]. The direction of vibration for these shear transducers is parallel to the contact face. This is different from compressional transducers where the direction of vibration is normal to the contact face. The shear
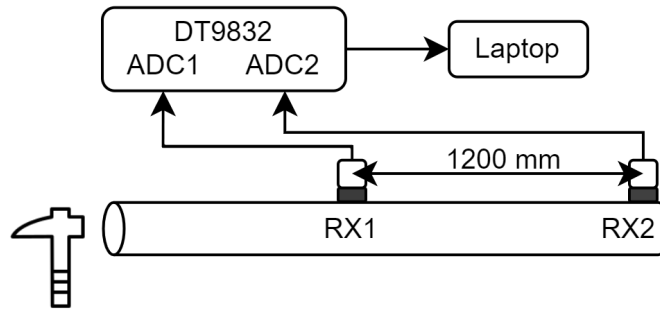
Figure 2: Diagram of the experimental setup for ToF measurements.
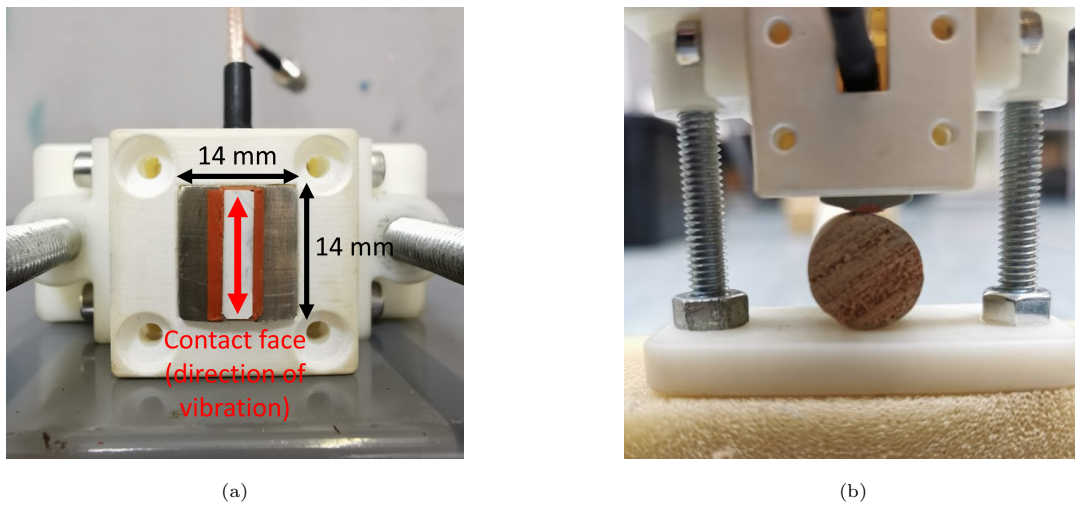

| (a) | (b) |

Figure 3: Photo (a) shows the shear transducer used in the study (with dimensions). Photo (b) shows the transducer being clamped onto a wooden sample.

transducers are broadband and have a flat frequency response for the frequency range of interest. For ToF measurements, two transducers acting as receivers were used and were positioned as shown in Figure 2. The receivers were aligned parallel to the grain to receive longitudinal vibrations and clamped using springs to provide dry coupling, see Figure 3. A hammer hit was performed parallel to the grain at the opposite of the end sample to generate longitudinal vibrations. The recording of the signal was initiated by a keyboard button press just before the hammer hit was performed. At the receiver, the received signals were sampled at 2 MHz using the ADC channels from the DT9832 module. The signal was saved to file and processed using MATLAB.

The amplitude threshold method was used to determine the FToA of the ToF received signals. A fixed threshold value of 0.002 V was used. The threshold value was chosen such that it is 5 times the standard deviation of the noise and did not result in false positives. The average of 10 measurements per sample was taken as the average ToF velocity. This ToF velocity was then used in Equation 1 to obtain the ToF

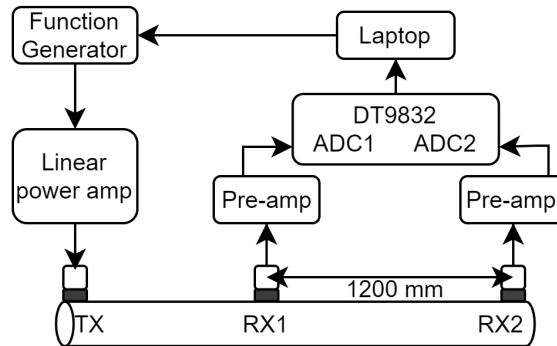dynamic MoE.

2.3. Guided waves

Figure 4: Diagram of the experimental setup for guided wave measurements.

For guided wave measurements, three transducers in a pitch-catch configuration were used. The transducers were positioned as shown in Fig. 4. Five cycles of a sine wave with central frequencies ranging from 15 - 40 kHz were used for excitation. A Hanning window was applied to the signal for narrowband excitation. The signal was created in MATLAB and outputted from an Agilent 33220A function generator. The outputted signal was amplified to 400 Vpp using a custom-built linear power amplifier. To receive the signal, receivers were connected to custom-built pre-amps and sampled at 2 MHz using the ADC channels from a DT9832 module. Hardware triggering was used to synchronise the excitation and reception of the signal.

Guided wave measurements were performed over a range of frequencies and phase velocities were calculated using a frequency-shifting technique. A curve was fitted through the longitudinal L(0,1) phase velocity measurements to obtain the "rod velocity" which is the phase velocity at zero frequency. Refer to our previous paper [29] for a more detailed explanation of this method. The guided wave dynamic MoE was then calculated by using this rod velocity in Equation 1. The traditional ToF method is used in this study. Therefore, the dispersion compensation technique presented in our previous paper [32] was not implemented for both ToF and guided wave received signals.

2.4. Static bending test

For comparison, static MoE measurements of the samples were obtained using three-point bending tests. The tests were performed using an Instron 5967 Universal Testing Machine according to the ASTM D198 standard [33]. Roller supports were positioned near the edges of the sample for support and a span length of 2200 mm was used. Load was applied to the center of the sample at a loading rate of 15 mm/min. The

three-point bending test was performed until an elongation of 100 mm at the midpoint was achieved. The static MoE was then calculated using

$$E_S = \frac{PL^3}{48\Delta I},$$

(4)

where P is the load (N), L is the span length (mm), Δ is the displacement at midspan (mm) and I is the moment of inertia (mm^4). Figure 5 and 6 shows the experimental setup for the three-point bending test on a 16 mm diameter wooden sample. The moisture content of the samples was measured using a MD918 moisture meter and was measured on the same day as the static bending test. The density of the samples was calculated according to the ASTM D2395 standard [34].
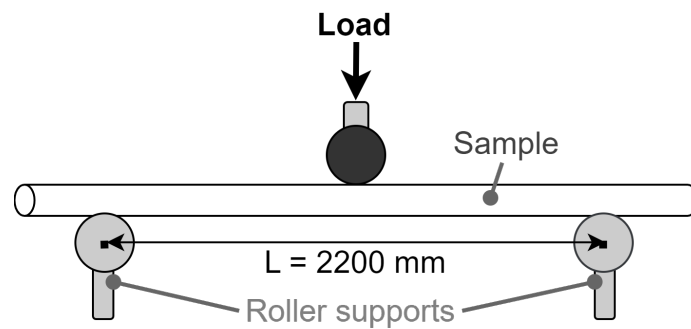
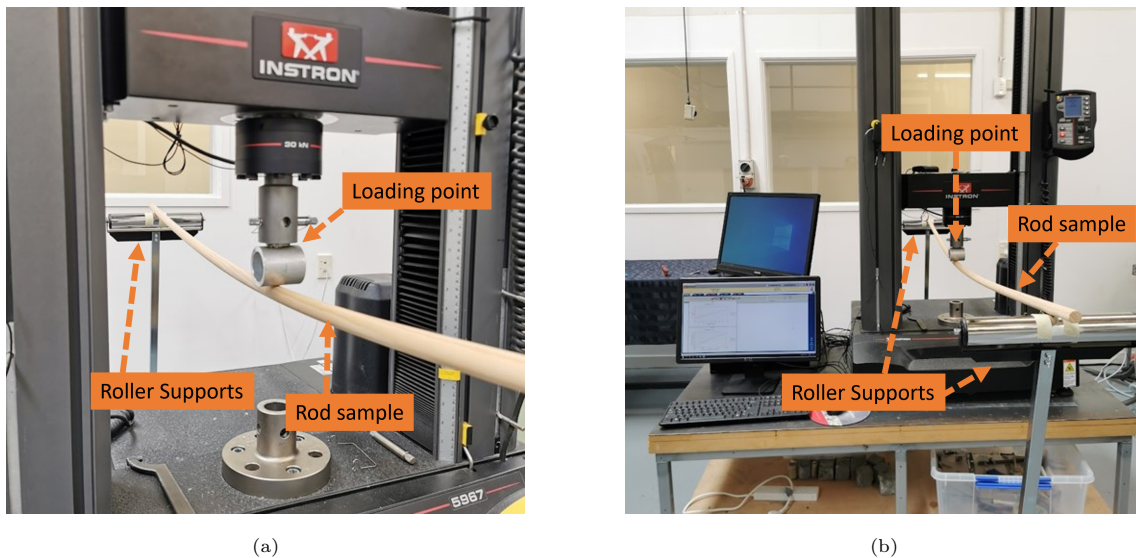Figure 5: Diagram of a three-point static bending test with centre load.

| (a) | (b) |

Figure 6: Experimental setup for three-point bending test using the Instron 5967 Universal Testing Machine.

3. Results

3.1. Wood properties

Table 1 shows the mass, density, acoustic velocity, dynamic MoE and static MoE values obtained for the fifteen radiata pine cylindrical rod samples. The measured moisture content of the samples is approximately 8.5% with no variation between the samples. The measured density of the samples ranges between 395 - 655 kg/m^3, as seen in Table 1. The average density of the samples is approximately 525 kg/m^3 with a standard deviation of 68 kg/m^3. The minimum and maximum values of static MoE obtained were 8.00 and 17.00 GPa respectively whereas the dynamic MoE values ranged from 8.31 - 19.33 GPa. The density and stiffness values obtained in this study are within the range reported in the literature for radiata pine [35].

Table 1: Measured values for varying parameters for the fifteen wooden rod samples where $E_{L(res)}$, $E_{L(ToF)}$ and $E_{L(GW)}$ are the dynamic MoE values for the resonance, ToF and guided wave methods respectively and E_S are the static MoE values.

Sample	Mass (g)	Density (kg/m^3)	Acoustic velocity (m/s)			$E_L(res)$ (GPa)	$E_L(ToF)$ (GPa)	$E_L(gw)$ (GPa)	E_s (GPa)
			Resonance	ToF	GW				
1	248	504	5308	5184	5248	14.21	13.56	13.89	13.59
2	282	574	5621	5805	5754	18.12	19.33	18.99	17.00
3	238	484	5041	5281	5155	12.30	13.50	12.87	11.86
4	322	655	5308	5408	5446	18.45	19.16	19.43	18.73
5	254	517	5356	5592	5446	14.82	16.16	15.32	14.37
6	216	439	4468	4706	4560	8.77	9.73	9.14	8.23
7	230	468	4756	5166	5108	10.58	12.49	12.21	10.05
8	256	521	4917	5118	5068	12.59	13.64	13.38	10.93
9	314	639	5205	5408	5339	17.30	18.68	18.21	16.28
10	272	553	4935	4970	4901	13.48	13.67	13.29	12.32
11	194	395	4588	4598	4588	8.31	8.34	8.31	8.00
12	260	529	5092	5169	5146	13.71	14.13	14.01	13.01
13	268	545	5500	5493	5518	16.49	16.45	16.60	15.69
14	248	504	4684	4830	4832	11.07	11.77	11.78	9.99
15	230	468	4372	4276	4213	8.94	8.55	8.30	8.28
Mean	**225**	**519**	**5010**	**5133**	**5088**	**13.28**	**13.94**	**13.71**	**12.55**
Std. Dev.	**32**	**66**	**367**	**390**	**398**	**3.24**	**3.41**	**3.44**	**3.26**

3.2. Relationship between dynamic MoE and density

Researchers have reported the importance of density to determine wood quality [36, 37]. Figure 7 shows the relationship between dynamic and static MoE values as a function of density. The figure shows a positive linear relationship between the MoE values using all four methods with respect to density.

To quantitatively measure the linear relationship between the MoE and density, Pearson's correlation coefficient (r-value) is used. A positive correlation coefficient indicates the tendency for one variable to increase or decrease together with another variable [38]. Table 2 shows the correlation values between density and the MoE values. The table shows high correlations (0.89 - 0.90) between the two variables. The correlation values obtained in this study are higher than those reported in the literature for radiata pine. Ivkovic et.al [7] and Lindstrom et.al [39] obtained correlation values ranging between 0.39 - 0.71 for radiata pine samples aged between 3 - 8 years old. The low r-value may be due to the inconsistent material properties for juvenile wood. The difference in correlation between MoE and density may also be related to the growth rings and outerwood proportion which could lead to biased results [40]. Previous studies on other tree species have reported strong correlations between density and dynamic MoE. For example, Illic [41] obtained correlations ranging from 0.81 - 0.83 between density and resonance dynamic MoE values. Chauhan and Sethy [42] obtained correlations ranging from 0.73 - 0.74 between density and dynamic MoE obtained using resonance and ToF methods for 8 different wood species. In contrast, some studies have advised against using density alone as a predictor of MoE [43, 44] or have reported no correlation between them [45].
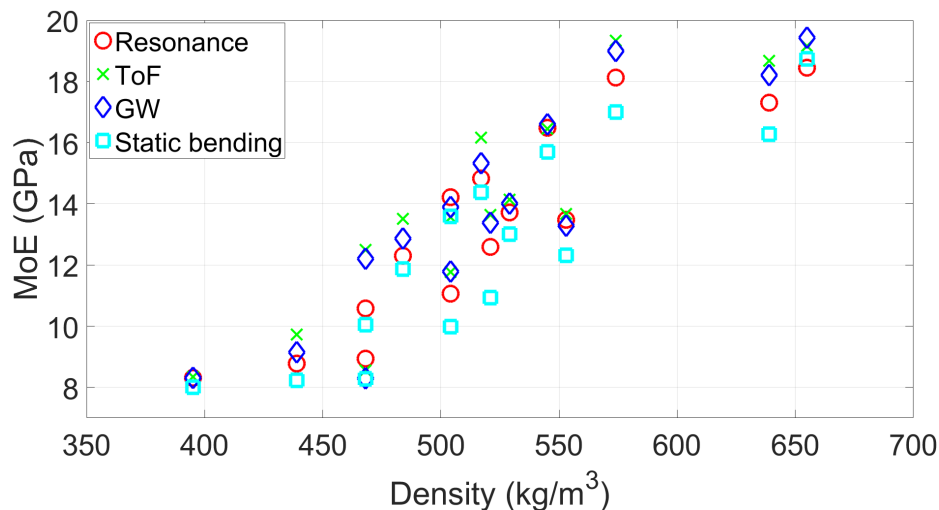

Figure 7: Relationship between MoE values obtained using different methods and density of the samples.

Table 2: Pearson's correlation coefficient between dynamic and static MoE values and density.

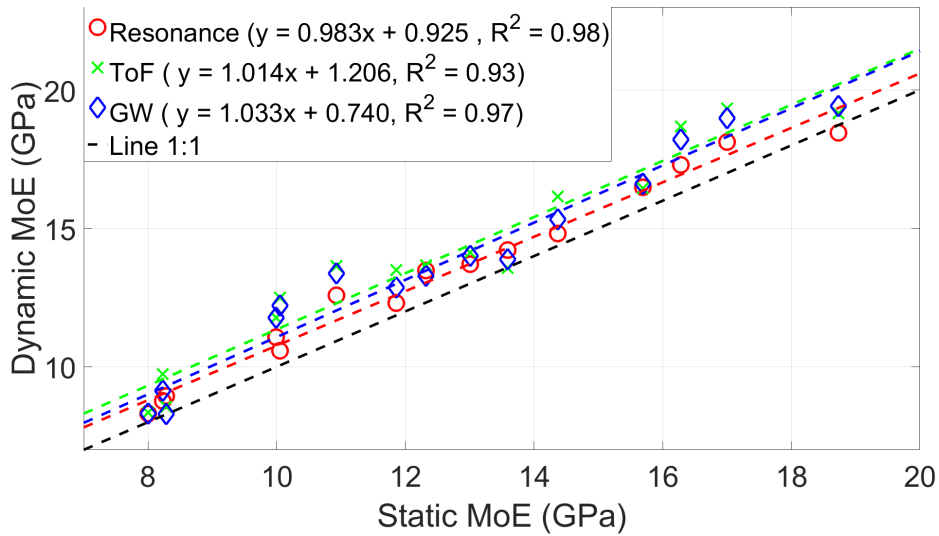|	Density	$E_{L(res)}$	$E_{L(ToF)}$	$E_{L(GW)}$
$E_{L(res)}$	0.90	-	-	-
$E_{L(ToF)}$	0.89	0.97	-	-
$E_{L(GW)}$	0.90	0.98	0.99	-
E_S	0.89	0.99	0.96	0.97

Figure 8: Relationship between dynamic and static MoE for 16 mm diameter wooden rod samples.

3.3. Comparison between static and dynamic MoE

Figure 8 shows the relationship between dynamic MoE and static MoE values obtained for the wooden rod samples. The figure shows good agreement between dynamic MoE values obtained using resonance, ToF and guided wave methods with static MoE values. The coefficient of determination, R^2 value is used to measure the goodness of fit of the regression models to predict static MoE from dynamic MoE values. High R^2 values (0.93 - 0.98) were obtained between the dynamic MoE and static MoE values. The results show that dynamic MoE values obtained using resonance, ToF and guided wave methods are higher compared to static MoE values.

An R^2 value of 0.98 was obtained using the resonance method. Resonance dynamic MoE values were on average 6.4% higher compared to the static MoE values. Similar results were obtained by Lindstrom et.al [40] who performed stiffness measurements using the resonance method on radiate pine samples. The authors obtained an R^2 value of 0.93 and the results from the study show that dynamic MoE values were on average 4 - 7% higher compared to static MoE. Previous studies on other wood species have also obtained resonance dynamic MoE values which were approximately 5 - 10% higher compared to static MoE values

[46, 47]. The resonance dynamic MoE values obtained in this study are consistent with those reported in the literature. More work is needed to investigate the cause of the variation between the resonance dynamic MoE and static MoE values.

Using the ToF method, an R^2 value of 0.93 was obtained. The ToF dynamic MoE values were on average 11.6% higher than static MoE, which is a significant overestimation. This ToF overestimation is expected as it has been reported in the literature for wood [16, 17]. Studies have reported that ToF measurements can vary due to factors such as the ToF tool used [48], the distance between probes [49], the position of probes [50] and the signal strength [51]. The results of this study show relatively small variations in ToF measurements compared to those reported in the literature. This may be because small diameter rod samples were used. We expect higher variations between resonance and ToF measurements in green wood samples due to variation in factors such as moisture content, microfibril angle and temperature.

Guided wave dynamic MoE values were on average 9.5% higher than static MoE values. These results are higher than those reported by Fathi et.al [26, 27] who performed measurements on rectangular wooden plates. The difference may be due to the geometric shape of the samples as cylindrical rods were used in this study. Furthermore, the authors estimated the elastic modulus by measuring the Lamb wave shear velocity and shear modulus. In this study, the longitudinal wave velocity is used to directly measure the elastic modulus. The guided wave method used in this study also produced results that are closer to the ToF method compared to the resonance method. This suggests that similar stress waves are being propagated and measured using both methods. The variation between the ToF and guided wave method may be due to dispersion effects. Dispersion can cause distortion of the ToF received signal which can lead to higher ToF measurements. Dispersion compensation can potentially be used to obtain more accurate ToF measurements as discussed in our previous paper [32]. The difference between guided waves and ToF measurements may be larger for larger diameter samples as it is expected that higher dispersion will be observed in larger diameter samples. However, more work is needed to investigate this.

4. Conclusion

In recent years, guided wave testing has been widely used for structural health monitoring and mechanical property characterization of structural materials. Guided wave testing has also been performed for wood-based materials. However, previous guided wave studies for wood have only compared MoE values obtained using guided waves with static bending tests for rectangular wood samples. In this work, dynamic MoE values obtained using the guided wave technique are compared with traditional resonance, ToF and static bending methods for cylindrical wooden samples. The measurements were performed on fifteen cylindrical radiata pine rods with a diameter of 16 mm and length of 2440 mm.

The rod samples have a density range of 395 - 655 kg/m^3 with an average density of 519 kg/m^3. The

static MoE obtained in this study has a range of 8.00 - 18.73 GPa whereas dynamic MoE has a range between 8.34 - 19.43 GPa. Strong correlations (r-value = 0.89 - 0.90) were observed between dynamic MoE and density, see Table 2. Regressive models for MoE produced high R^2 values, which ranged from 0.93 - 0.98 using the resonance, ToF and guided wave methods.

Table 3: Average difference between dynamic MoE obtained using resonance, ToF and guided wave methods with static MoE obtained using three-point bending test.

Average	$E_{L(res)}$	$E_{L(ToF)}$	$E_{L(GW)}$
Difference (GPa)	0.8	1.4	1.2
Standard deviation (GPa)	0.36	0.84	0.70
Difference (%)	6.4	11.6	9.5

Table 3 shows the average error between dynamic MoE and static MoE. The results show that the resonance, ToF and guided wave methods respectively produced stiffness measurements that were on average 6.4%, 11.6% and 9.5% higher compared to the static bending test respectively. The guided wave method has higher R^2 (0.97) compared to the ToF method ($R^2 = 0.93$). From the results, the best method to be used for stiffness estimation of wood would be the resonance method. This is because resonance dynamic MoE values are closest to the static MoE values which are considered the gold standard for the wood industry. However, this method requires two exposed ends hence it cannot be used on standing trees. Alternatively, the guided wave technique does not require two exposed ends and thus can be performed on standing trees. The guided wave method produces stiffness measurements with lower errors and variation compared to the ToF method. The similarity in measurements between the guided wave and ToF methods suggests that both methods are measuring the same wave mode. The difference may be because the ToF measurements are affected by dispersion effects. The guided wave method used in this study shows potential in obtaining improved stiffness measurements compared to the ToF method but more work is needed.

The measurements performed in this study were limited to 16 mm diameter kiln-dried radiata pine rod samples. Measurements should be repeated on a higher number of samples with varying diameters and sizes. This would help to better determine the errors and uncertainties associated with the proposed guided wave method. The measurements should also be repeated on large log samples, standing trees or seedlings. For large samples and seedlings, the effects of inhomogeneity, moisture content, temperature, microfibril angle, variation in grain angle, presence of knots and higher order wave modes on the proposed guided wave method can be evaluated. The resonance dynamic MoE values found in this study were higher than static MoE values. To determine if there is a bias in static bending measurements, measurements should be repeated on samples with known mechanical properties and using different support length spans. Future work has therefore been planned to perform static bending tests on aluminium rod samples to validate this.

References

[1] A. C. Matheson, R. L. Dickson, D. J. Spencer, B. Joe, J. Ilic, Acoustic segregation of *Pinus radiata* logs according to stiffness, Annals of Forest Science 59 (5-6) (2002) 471–477.

[2] R. Dickson, A. Matheson, B. Joe, J. Ilic, J. Owen, Acoustic segregation of *Pinus radiata* logs for sawmilling, New Zealand Journal of Forestry Science 34 (2) (2004) 175–189.

[3] A. Tsehaye, A. Buchanan, J. Walker, Sorting of logs using acoustics, Wood Science and Technology 34 (4) (2000) 337–344.

[4] M. Babiak, M. Gaff, A. Sikora, Š. Hysek, Modulus of elasticity in three-and four-point bending of wood, Composite Structures 204 (2018) 454–465.

[5] P. Horáček, J. Tippner, K. T. Hassan, Nondestructive evaluation of static bending properties of Scots pine wood using stress wave technique, Wood Research 57 (3) (2012) 359–366.

[6] A. Thumm, R. Meder, Stiffness prediction of radiata pine clearwood test pieces using near infrared spectroscopy, Journal of Near Infrared Spectroscopy 9 (2) (2001) 117–122.

[7] M. Ivković, W. J. Gapare, A. Abarquez, J. Ilic, M. B. Powell, H. X. Wu, Prediction of wood stiffness, strength, and shrinkage in juvenile wood of radiata pine, Wood Science and Technology 43 (3) (2009) 237–257.

[8] Z. Hong, A. Fries, S.-O. Lundqvist, B. Andersson Gull, H. X. Wu, Measuring stiffness using acoustic tool for Scots pine breeding selection, Scandinavian Journal of Forest Research 30 (4) (2015) 363–372.

[9] M. J. Frampton, Acoustic studies for the non-destructive testing of wood, Ph.D. thesis, University of Canterbury (2019).

[10] C.-L. Huang, H. Lindström, R. Nakada, J. Ralston, Cell wall structure and wood properties determined by acoustics—a selective review, Holz als Roh-und werkstoff 61 (2003) 321–335.

[11] X. Wang, P. Carter, R. J. Ross, B. K. Brashaw, Acoustic assessment of wood quality of raw forest materials: a path to increased profitability, Forest Products Journal (5) (2007) 6–14.

[12] X. Wang, R. J. Ross, M. McClellan, R. J. Barbour, J. R. Erickson, J. W. Forsman, G. D. McGinnis, et al., Strength and stiffness assessment of standing trees using a nondestructive stress wave technique, US Forest Service, Forest Products Laboratory: Madison, WI, USA, (2000).

[13] H. Baillères, G. Hopewell, G. Boughton, MOE and MOR assessment technologies for improving graded recovery of exotic pines in Australia (Project No. PNB040-0708), Forest and Wood Products Australia (2009).

[14] C.-M. Chiu, C.-H. Lin, T.-H. Yang, Application of nondestructive methods to evaluate mechanical properties of 32-year-old Taiwan incense cedar *(Calocedrus formosana)* wood, BioResources 8 (1) (2013) 688–700.

[15] C. R. Mora, L. R. Schimleck, F. Isik, J. M. Mahon, A. Clark, R. F. Daniels, Relationships between acoustic variables and different measures of stiffness in standing *Pinus taeda* trees, Canadian Journal of Forest Research 39 (8) (2009) 1421–1429.

[16] X. Wang, Acoustic measurements on trees and logs: a review and analysis, Wood Science and Technology 47 (5) (2013) 965–975.

[17] M. Legg, S. Bradley, Measurement of stiffness of standing trees and felled logs using acoustics: A review, The Journal of the Acoustical Society of America 139 (2) (2016) 588–604.

[18] R. J. Ross, B. K. Brashaw, J. Punches, J. R. Erickson, J. W. Forsman, R. F. Pellerin, X. Wang, Diameter effect on stress-wave evaluation of modulus of elasticity of logs, Wood and Fiber Science (2004) 368–377.

[19] S. Chauhan, J. Walker, Variations in acoustic velocity and density with age, and their interrelationships in radiata pine, Forest Ecology and Management 229 (1-3) (2006) 388–394.

[20] X. Wang, R. J. Ross, P. Carter, Acoustic evaluation of wood quality in standing trees. Part I. acoustic wave behavior, Wood and Fiber Science (2007) 28–38.

[21] M. Mitra, S. Gopalakrishnan, Guided wave based structural health monitoring: A review, Smart Materials and Structures 25 (5) (2016) 053001.

[22] J. El Najjar, S. Mustapha, Condition assessment of timber utility poles using ultrasonic guided waves, Construction and Building Materials 272 (2021) 121902.

[23] U. Dackermann, Y. Yu, E. Niederleithinger, J. Li, H. Wiggenhauser, Condition assessment of foundation piles and utility poles based on guided wave propagation using a network of tactile transducers and support vector machines, Sensors 17 (12) (2017) 2938.

[24] I. A. Veres, M. B. Sayir, Wave propagation in a wooden bar, Ultrasonics 42 (1-9) (2004) 495–499.

[25] S. Dahmen, H. Ketata, M. H. B. Ghozlen, B. Hosten, Elastic constants measurement of anisotropic Olivier wood plates using air-coupled transducers generated Lamb wave and ultrasonic bulk wave, Ultrasonics 50 (4-5) (2010) 502–507.

[26] H. Fathi, S. Kazemirad, V. Nasir, A nondestructive guided wave propagation method for the characterization of moisture-dependent viscoelastic properties of wood materials, Materials and Structures 53 (6) (2020) 1–14.

[27] H. Fathi, S. Kazemirad, V. Nasir, Lamb wave propagation method for nondestructive characterization of the elastic properties of wood, Applied Acoustics 171 (2021) 107565.

[28] H. Fathi, V. Nasir, S. Kazemirad, Prediction of the mechanical properties of wood using guided wave propagation and machine learning, Construction and Building Materials 262 (2020) 120848.

[29] A. H. A. Bakar, M. Legg, D. Konings, F. Alam, Estimation of the rod velocity in wood using multi-frequency guided wave measurements, Applied Acoustics 202 (2023) 109108.

[30] GRAS 46BF-1 1/4" LEMO Free-field Standard Microphone Set, `https://www.grasacoustics.com/products/measurement-microphone-sets/traditional-power-supply-lemo/product/686-46bf-1`, Last accessed on 2022-10-17.

[31] B. A. Engineer, The mechanical and resonant behaviour of a dry coupled thickness-shear PZT transducer used for guided wave testing in pipe line, Ph.D. thesis, Brunel University (2013).

[32] A. H. A. Bakar, M. Legg, D. Konings, F. Alam, The effects of dispersion on time-of-flight acoustic velocity measurements in a wooden rod, Ultrasonics 202 (2022) 106912.

[33] ASTM International, ASTM D198 - 15 - Standard Test Methods of Static Tests of Lumber in Structural Sizes, American Society of Testing and Materials (2015).

[34] ASTM International, ASTM D2395 - 14 - Standard Test Methods for Density and Specific Gravity (Relative Density) of Wood and Wood-Based Materials, American Society of Testing and Materials (2014).

[35] D. Cown, R. Ball, M. Riddell, Wood density and microfibril angle in 10 *Pinus radiata* clones: distribution and influence on product performance, New Zealand Journal of Forestry Science 34 (3) (2004) 293.

[36] R. Bamber, J. Burley, et al., The wood properties of radiata pine, Commonwealth Agricultural Bureaux, 1983.

[37] B. J. Zobel, J. P. Van Buijtenen, Wood variation: its causes and control, Springer Science & Business Media, 2012.

[38] A. K. Sharma, Text book of correlations and regression, Discovery Publishing House, 2005.

[39] H. Lindström, P. Harris, C. Sorensson, R. Evans, Stiffness and wood variation of 3-year old *Pinus radiata* clones, Wood Science and Technology 38 (8) (2004) 579–597.

[40] H. Lindström, P. Harris, R. Nakada, Methods for measuring stiffness of young trees, Holz als Roh-und Werkstoff 60 (3) (2002) 165–174.

[41] J. Ilic, Relationship among the dynamic and static elastic properties of air-dry *Eucalyptus delegatensis* R. Baker, Holz als Roh-und Werkstoff 59 (3) (2001) 169–175.

[42] S. Chauhan, A. Sethy, Differences in dynamic modulus of elasticity determined by three vibration methods and their relationship with static modulus of elasticity, Maderas. Ciencia Y Tecnología 18 (2) (2016) 373–382.

[43] A. Tsehaye, Within-and between-tree variations in the wood quality of radiata pine, Ph.D. thesis (1995).

[44] C. A. Raymond, B. Joe, D. W. Anderson, D. J. Watt, Effect of thinning on relationships between three measures of wood stiffness in *Pinus radiata*: standing trees vs. logs vs. short clear specimens, Canadian Journal of Forest Research 38 (11) (2008) 2870–2879.

[45] J.-P. Lasserre, E. G. Mason, M. S. Watt, J. R. Moore, Influence of initial planting spacing and genotype on microfibril angle, wood density, fibre properties and modulus of elasticity in *Pinus radiata D. Don* corewood, Forest Ecology and Management 258 (9) (2009) 1924–1931.

[46] M. Spycher, F. W. Schwarze, R. Steiger, Assessment of resonance wood quality by comparing its physical and histological properties, Wood Science and Technology 42 (4) (2008) 325–342.

[47] D. W. Haines, J.-M. Leban, C. Herbé, Determination of Young's modulus for spruce, fir and isotropic materials by the resonance flexure method with comparisons to static flexure and other dynamic methods, Wood Science and Technology 30 (4) (1996) 253–263.

[48] Y. Yin, H. Nagao, X. Liu, T. Nakai, Mechanical properties assessment of *Cunninghamia lanceolata* plantation wood with three acoustic-based nondestructive methods, Journal of Wood Science 56 (1) (2010) 33–40.

[49] F. Divos, Acoustic tools for seedling, tree and log selection, The Future of Quality Control for Wood & Wood Products (Edinburgh, UK, 2010), pp. 5-9.

[50] F. Arriaga Martitegui, D. Fernandez Llana, R. Martinez Lopez, M. Esteban Herrero, G. Iñiguez Gonzalez, The influence of sensor placement on in-situ ultrasound wave velocity measurement (Report No. FPL-GTR-239), in: Proceedings of 19th International Nondestructive Testing and Evaluation of Wood Symposium, USDA, 2015.

[51] F. J. Rescalvo, M. A. Ripoll, E. Suarez, A. Gallego, Effect of location, clone, and measurement season on the propagation velocity of poplar trees using the Akaike information criterion for arrival time determination, Materials 12 (3) (2019) 356.

Chapter 6

Conclusion

The ability to measure the mechanical property of wood, particularly stiffness, is an important aspect for the wood industry. It can be used for the segregation of logs into different grades. Additionally, it can also be used for improving breeding trials for juvenile trees which can help improve the profitability, sustainability and efficiency of the industry. Traditionally, the static bending method is used to measure the stiffness of wood. However, this method is costly, time-consuming and can be destructive. Acoustic NDT methods such as the resonance and ToF methods have been developed to mitigate these issues. Both acoustic methods can be used on felled logs and timber samples but the ToF method is the only acoustic method that can be used on standing trees. Literature has reported that the ToF method has a systematic overestimation compared to the resonance and static bending methods. Researchers have suggested the potential causes of the ToF overestimation but the exact cause is still not known.

In recent years, guided wave NDT methods have been widely used for structural health monitoring and mechanical property characterization of metallic structures. There have also been some guided wave studies performed for wood. Most of these guided wave studies have been performed for structural health monitoring of timber utility poles or NDT measurements on rectangular wooden plates. For rectangular plates, guided waves propagate as Lamb waves which are different to rod waves that propagate in cylindrical rods. Additionally, no previous studies have utilised guided wave knowledge to determine the cause of ToF overestimation reported in the literature for wood. Guided wave techniques have also not been compared with the traditional acoustic ToF and resonance methods.

This study is one of the first works to have performed guided wave measurements on cylindrical wood samples. This PhD study resulted in the publication of three peer-reviewed Q1 Journal

Articles, with the fourth one currently in preparation. Additionally, two conference papers have also been published. The results of this study show that guided wave knowledge can be used to improve understanding of wave propagation in wood which has helped to identify a potential cause of the ToF overestimation. Guided wave techniques can also be used to obtain improved NDT measurements for wood. A summary of the main contributions of this study is provided below:

1. The first study to obtain experimental dispersion curves for a wooden cylindrical rod.

2. Enhancement and suppression of desired wave modes can be achieved by utilising ring arrays of shear transducers and varying the transducer orientation.

3. Presented a new approach to measuring the rod velocity of wood by fitting of multi-frequency guided wave measurements.

4. Investigated the effects of dispersion on ToF measurements obtained using amplitude threshold FToA technique.

5. The first work to show that dispersion can be a potential cause of ToF overestimation.

6. The first work to compare acoustic velocity and stiffness measurements obtained using guided waves with traditional acoustic ToF, resonance and static bending methods.

This work shows that guided wave theory can be used to better describe wave propagation in wood. This opens up the pathway for future researchers to implement more complex guided wave techniques for wood. This can help motivate the development of guided wave tools and techniques in order to obtain more accurate NDT measurements for wood. This could lead to improved segregation and breeding opportunities which can increase economic growth. Guided wave techniques can also be used for structural health monitoring of timber structures which can help reduce inspection costs and time.

Future works

Wood is an inhomogeneous material and the acoustic velocity can be affected by factors such as the presence of knots, moisture content, microfibril angle, variation in grain angle and temperature. Additionally, higher order wave modes, which can increase wave propagation complexity, may start to propagate at lower frequency ranges for larger diameter rods, as illustrated in Appendix 1. In order for us to better understand guided wave propagation in wood, it is beneficial to simplify the conditions and reduce the factors that can affect the wave propagation. In this study, we have therefore used small diameter wood samples to simplify the wave propagation. This reduced the effects of inhomogeneity and allowed only the fundamental wave modes to propagate. This could help us to more easily understand guided wave propagation and the effects of dispersion on acoustic velocity measurements in the wood sample.

The diameter of wood samples used in this study is similar to that of juvenile trees and seedlings. The outcome of this study could potentially be used in breeding trials for juvenile trees which can help the wood industry. However, measurements would need to be performed on real juvenile trees and seedlings to see how well the results correlate. In this case, the juvenile trees would be different to the rods used in this study. The juvenile trees have a full ring structure and would be more affected by increase in inhomogeneity, higher moisture content, temperature variation and the presence of reaction wood and knots.

In future work, the experiments should also be repeated on larger diameter samples, logs, and standing trees for a variety of wood species which have different mechanical properties. For large diameter samples, higher dispersion is expected to occur which could lead to higher overestimation. It is also expected that higher order wave modes may start to propagate at lower frequency ranges, as seen in Appendix 1. Additionally, bulks wave are also expected to occur. In this study, higher order wave modes and bulk waves were not measured in the small diameter samples. These waves can travel at higher velocities compared to the fundamental longitudinal L(0,1) wave mode. The ToF method will measure the acoustic signal with the fastest velocity. Therefore, the ToF method could be measuring the arrival times of these waves, which could

lead to an overestimation. Future work should investigate the presence of these waves, under what circumstances they start to propagate and their effects on ToF measurements.

In addition to experimental measurements, Finite Element Analysis (FEA) software such as ANSYS or COMSOL Multiphysics can also be used to perform simulation of guided wave propagation for wood samples. These samples could have varying geometric shapes, diameters, mechanical properties and moisture content. The software can also be used to isolate certain factors which can help improve the understanding of the impacts of specific factors on NDT measurements made on wood. This can further help to identify the potential causes of ToF overestimation.

In this study, shear transducers were clamped onto the sample using springs to provide good coupling. This method would not be practical for large diameter logs and standing trees as it is difficult to set up. Future work should therefore be performed to investigate the practical implementation of the shear transducers in a real-world scenario. This should include mounting, coupling, bark penetration and whether good signal-to-noise ratio can be achieved.

The use of shear transducers in this study allowed the excitation and reception of the torsional wave mode. Currently, there are no guided wave studies that have reported the use of the torsional wave mode for wood. The torsional wave mode is non-dispersive hence dispersion effects will not distort the signal which makes it suitable for NDT. The shear velocity which is the velocity of the torsional wave mode is related to the shear modulus. The ability to measure the shear modulus is also of interest to the wood industry. This can potentially be used to measure the mechanical properties and anisotropy of wood which can help in segregation. In addition, the use of Macro Fiber Composite (MFC) actuators and sensors should also be investigated. The MFCs are thin, flexible and can easily be mounted onto samples compared to the shear transducers used in this study. Some of the MFCs have also been specifically designed to excite and receive torsional vibrations which could provide better signal-to-noise ratio.

The results from this study show that the measured acoustic velocities obtained using the guided wave method are slightly higher compared to the resonance method. This may be due loading of the samples when resonance measurements are performed. The samples were supported using

two foam pads positioned under the sample near each end. Due to the small size of the rods used in this study, it is possible for the samples to be loaded by the foam pads. Any loading on the sample would reduce the resonance frequency which would cause an underestimation of acoustic velocity. However, this would need to be investigated further.

Appendices

Appendix 1

Resonance and ToF velocity calculation

Resonance

Figure 1 shows the resonance received signal in the time and frequency domain. To calculate the resonance velocity, the received signal in the time-domain is converted into the frequency-domain using a Fast Fourier Transform (FFT). The nth resonance harmonic can be obtained from the peaks observed in the frequency-domain signal. The first resonance harmonic is marked with a red cross mark as seen in Figure 1.
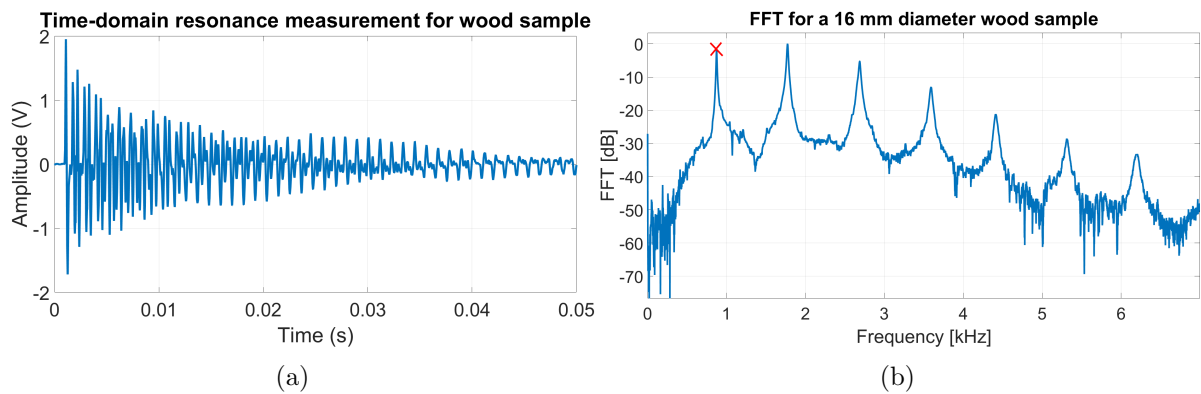
Figure 1: Plots of resonance received signal in the (a) time-domain and (b) frequency-domain for a 16 mm diameter wooden sample.

The resonance velocity can be obtained by using

$$c_{res} = \frac{2L f_n}{n} \tag{1}$$

f_n is the nth resonant frequency where n is an integer $(1, 2, 3 \ldots)$ and L is the length of the specimen. To obtain the resonance velocity from the first harmonic, the following calculations were made. The length of the sample $L = 2.460$ m. At harmonic $n = 1$, the measured resonance

frequency peak $f_n = 873$ Hz. The measured resonance velocity c_{res} is approximately 4295 m/s as seen below.

$$c_{res} = \frac{2 \times 2.46 \ m \times 873 \ Hz}{1} = 4295 \ m/s \qquad (2)$$

Time of Flight

Figure 2 shows a diagram of the experimental ToF setup. RX1 and RX2 are transducers that are separated by a distance and clamped onto the sample. A hammer hit is performed at one end of the sample to generate stress waves.
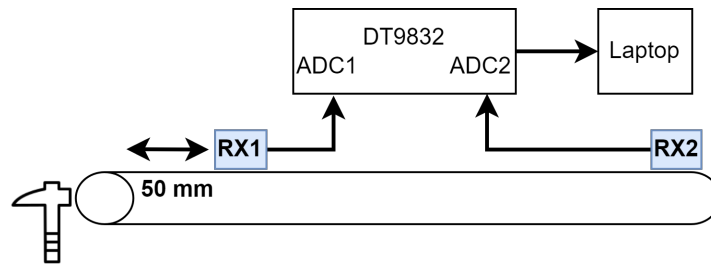
Figure 2: Diagram of ToF experimental setup.

Figure 3 shows ToF received signals for a 16 mm diameter wooden rod. ToF experiments in this study utilize the amplitude threshold technique to measure the First Time of Arrival (FToA) of the received signals. The red-marked crosses in the figure show the FToA of the received signals for RX1 and RX2 using a threshold value of 0.005 V.
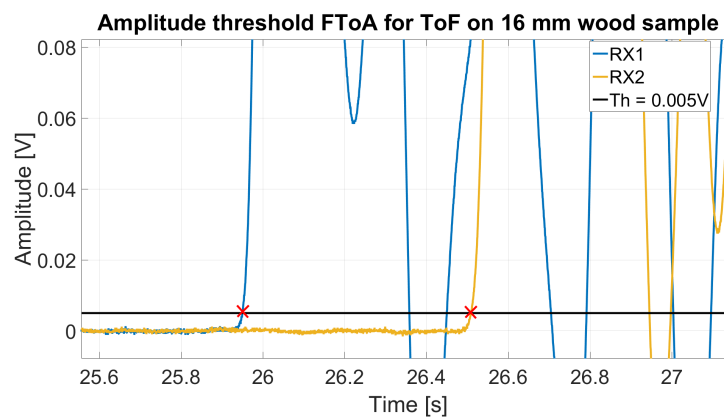
Figure 3: ToF received signals for a 16 mm diameter wooden rod sample.

The ToF velocity can be obtained using

$$c_{tof} = \frac{\Delta d}{T},$$ (3)

where Δd is the distance between two transducers (RX1 and RX2) and T is the propagation time for a stress wave to propagate from one transducer to the other.

From Figure 3, we can calculate the ToF velocity of the sample. Using a threshold value of 0.005 V, the measured FToA at RX1 and RX2 are 25.9500 and 26.5095 ms respectively. The time T taken for the stress wave to propagate from RX1 to RX2 is the difference between the FToA at RX1 and RX2. This is calculated to be 0.5595 ms. The distance Δd between RX1 and RX2 = 1.0 m and $T = 0.5595$ ms. The calculated c_{tof} is approximately 4396 m/s as seen below.

$$c_{tof} = \frac{2.46 \ m}{0.5595 \times 10^{-3} \ s} = 4396 \ m/s$$ (4)

Appendix 2

Guided wave measurements on 101.67 mm diameter aluminium sample

In previous chapters, we have utilised small diameter samples where it is expected that only the fundamental wave modes would be visible at low frequency ranges. However, for larger diameter samples, we would expect higher order wave modes to occur at the frequency range of interest. Some initial measurements were therefore performed on aluminium samples to illustrate the difference in results that would be expected on larger diameter samples. These measurements were performed on an aluminium sample with a diameter of 101.67 mm and a length of 2510 mm, see Figure 1. Aluminium was used because the mechanical properties are known and theoretical dispersion curves can be generated. However, it should be noted that aluminium is isotropic and homogeneous while wood is orthotropic and inhomogeneous.

(a)   (b)

Figure 1: Photos of the 101 mm diameter aluminium sample.

Figure 2 shows theoretical wavenumber-frequency dispersion curves obtained using GUIGUW for 16 mm and 101 mm diameter cylindrical aluminium rods. These were obtained using Young's Modulus of 68.9 GPa and Poisson's ratio of 0.33. For simplicity, only the longitudinal wave modes were plotted while the flexural and torsional wave modes were omitted. Figure 2(a) shows that for the 16 mm diameter aluminium rod, only the fundamental longitudinal wave mode is observed. However, for the 101 mm diameter rod, it can be seen that multiple higher order longitudinal wave modes were observed in addition to the fundamental longitudinal wave

mode, see Figure 2(b).

(a)

(b)
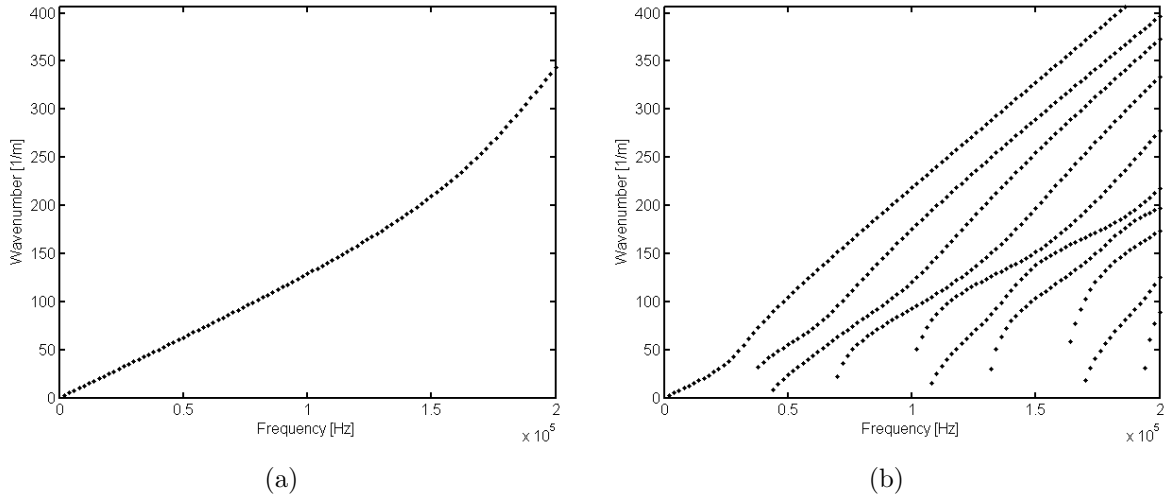
Figure 2: Theoretical wavenumber-frequency domain plots for aluminium sample with diameters of (a) 16 mm and (b) 101 mm.
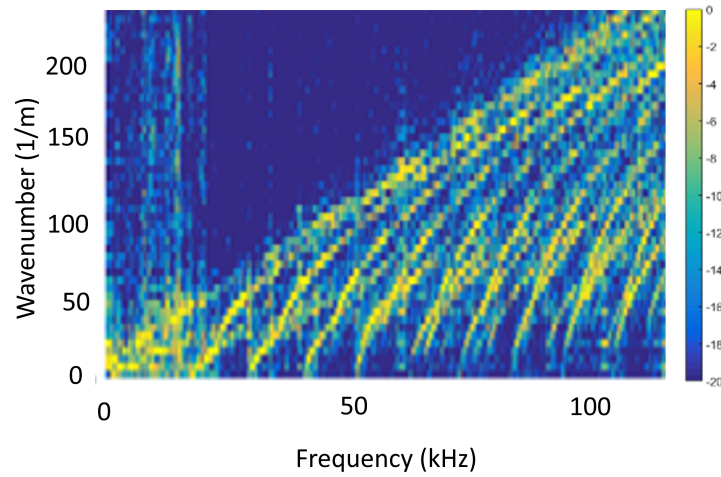

Figure 3: Experimental wavenumber-frequency domain plot for the 101.67 mm diameter aluminium sample.

Initial experimental guided wave measurements were performed on the 101.67 mm diameter aluminium rod. Using the methodology described in Chapter 2, guided wave measurements were made on the aluminium sample with the transducers aligned in the longitudinal direction. A 2D FFT was performed on the guided wave measurements to obtain wavenumber-frequency domain plot, see Figure 3. This figure shows somewhat similar results to the theoretical wavenumber

dispersion curves shown in Figure 1(b). This shows that higher order wave modes are present. In contrast, only the fundamental wave modes were observed for the 16 mm diameter aluminium rod sample as seen in Figure 8 in Chapter 2. This illustrates some of the differences between guided wave measurements performed for large diameter samples. Thus more work will be needed for larger diameter samples. Additionally, improved resolution for the wavenumber-frequency domain plots could be achieved using zero padding.

Appendix 3

Effect of dispersion on measured ToF

Figure 1 shows the phase velocity dispersion curve for aluminium rods with different diameters obtained using GUIGUW. We have also included the dispersion curve for an aluminium rod assuming no dispersion which can be represented as an infinitely thin rod. The phase velocity for a non-dispersive material is a constant phase velocity for all frequencies. The figure shows that as the diameter of the aluminium rod increases, dispersion also increases.
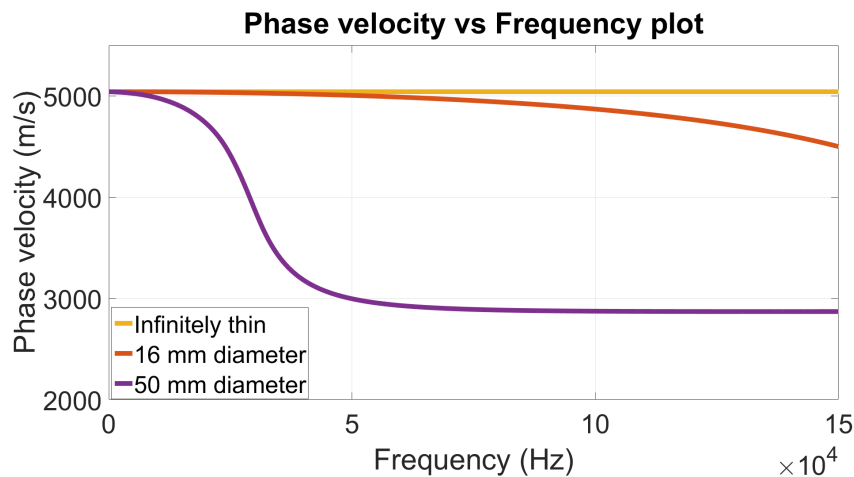
Figure 1: Plot of dispersion curves for aluminium rod with varying diameters.

Using the method explained in Section 3.7 of Chapter 4, simulations were performed on aluminium rods of varying diameters. Figure 2 shows the simulated time-domain received signals when the transmit signal travels a distance of 2.512 m. The figure shows that the rise time of the received signal decreases as the diameter of the aluminium rod increases. This would affect the measured ToF velocity when the amplitude threshold FToA method is used.

The theoretical rod velocity for aluminium can be obtained using

$$c_L = \sqrt{\frac{E_L}{\rho}}, \tag{5}$$

where E_L is the Modulus of Elasticity (MoE) in the longitudinal direction and ρ is the density

of the material. The MoE and density for aluminium 6061 are 68.9 GPa and 2,710 kg/m^3 respectively. Using Equation 5, the theoretical rod velocity for the aluminium sample would be approximately 5042 m/s.
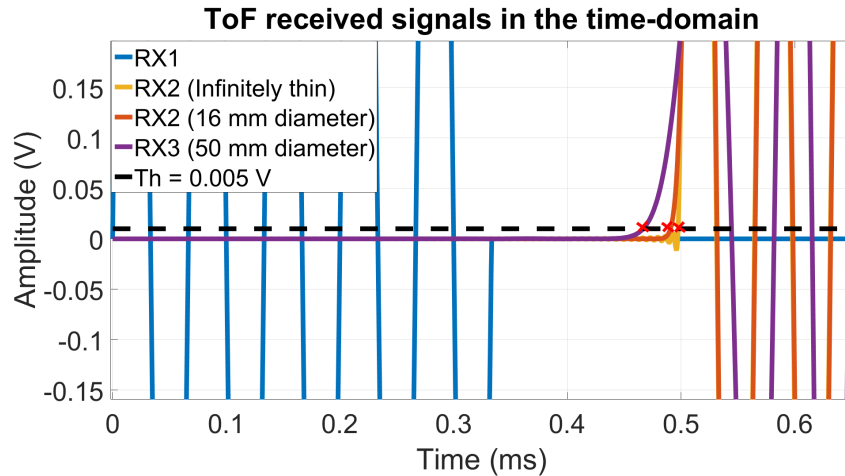

Figure 2: Simulated time-domain received signals for aluminium rods with varying diameters.

Table 1 shows the measured ToF velocity obtained using the amplitude threshold FToA technique for aluminium rods with varying diameters. The measured ToF velocity for the infinitely thin rod is similar to the theoretical rod velocity for aluminium. The table also shows that as the diameter of the aluminium rod increases, the measured ToF velocity also increases. These simulations indicate that dispersion effects which may vary with diameter can potentially cause ToF overestimation when measured using the traditional amplitude threshold method

Table 1: Measuired ToF velocities for aluminium with varying diameters.

Dispersion	ToF velocity (m/s)
Infinitely thin	5042
16 mm diameter	5121
50 mm diameter	5384

Appendix 4

This article was published and presented at the Acoustics 2022: The Nature of Acoustics conference held on 31 Oct - 2 Nov 2022 at Te Papa, Wellington, New Zealand.

Non-destructive testing on a wooden cylindrical rod using guided wave and shear transducer arrays

Adli Hasan Abu Bakar [(1)] and Mathew Legg [(1)]

(1) Department of Mechanical and Electrical Engineering, Massey University, Auckland, New Zealand
m.legg@massey.ac.nz

ABSTRACT

Acoustic methods such as resonance and time of flight techniques have traditionally been used to measure the mechanical properties of wood. Guided wave techniques have been used extensively for non-destructive testing on metallic structures. However, there have only been a few studies that have utilized guided wave techniques for non-destructive testing on wood. In this study, guided wave measurements were performed on wood and aluminium cylindrical rods using a ring array of shear transducers. Enhancement of either the fundamental L(0,1) or fundamental torsional T(0,1) wave modes and suppression of other wave modes could be achieved using the transducer array. The torsional T(0,1) wave mode has not been used for non-destructive testing of wood. The non-dispersive nature of the T(0,1) wave mode makes it a desirable wave mode for wood property estimation. In addition, experimentally measured phase velocity dispersion curves were used to perform dispersion compensation on amplitude threshold time-of-flight received signals. Results suggest that dispersion can be a cause of overestimation in acoustic velocity measured using the time-of-flight method relative to resonance. Dispersion compensation can be used to mitigate this overestimation to obtain more accurate acoustic velocity measurements.

INTRODUCTION

Acoustic technology is a popular Non-Destructive Testing (NDT) technique that is used to measure wood stiffness as it is easy to use and less expensive compared to other NDT methods. The stiffness of wood is related to the Modulus of Elasticity, E in the longitudinal direction and is generally estimated using

$$E = \rho \, v_l{}^2 \qquad (1)$$

where ρ is the density and v_l is the acoustic velocity in the longitudinal direction. The resonance and Time of Flight (ToF) methods are the most common acoustic methods [1]. However, it has been reported that the ToF method has a systematic overestimation in measured acoustic velocity compared to the resonance method [2].

An acoustic signal propagating in a rod-like structure initially propagates as bulk waves. After travelling sufficient distance, guided waves are expected to be generated. These guided waves are composed of different types of vibrations called wave modes which are generally dispersive. The wave modes propagating in rod-like structures are the longitudinal, flexural and torsional wave modes. Dispersion happens when the frequency components in a signal travel at different velocities along a waveguide. As the signal propagates, it spreads out it space and time. Dispersion curves describe the relationship between the velocity of the wave modes with frequency and can be represented in different domains such as phase velocity vs frequency, group velocity vs frequency or wavenumber vs frequency [3].

There are several studies that have performed guided wave measurements in timber samples [4]–[10]. However, no previous study has investigated the effects of dispersion on ToF measurements performed on wood. The effects of dispersion on sharp impacts have been

investigated for isotropic materials using Split Hopkinson Pressure Bar (SHPB) test. It has been reported that dispersion can cause significant changes to the rise time at the start of the measured received signal [11]. Dispersion compensation techniques have been used to reduce the effects of dispersion on guided wave measurements for isotropic materials [12]. However, no previous studies have performed or investigate the effects of dispersion compensation for wood.

This paper investigates the use of shear transducers and guided wave measurements to obtain experimental dispersion curves for a cylindrical wooden rod. This is also the first study to use a ring array of shear transducers for wood. Results indicate that the desired wave modes can either be enhanced or suppressed by changing the alignment and using a ring array of transducers. The non-dispersive torsional T(0,1) wave mode has not been used for non-destructive testing for wood. The T(0,1) wave mode is non-dispersive and makes it suitable for wood property measurement. The systematic overestimation of the ToF method relative to resonance have been reported in literature. The effects of dispersion on ToF measurements for wood has not been investigated. Experimentally measured dispersion curves were used to perform dispersion compensation on ToF measurements. The result suggest that dispersion can be a cause of the overestimation and dispersion compensation can be used to mitigate this.

MATERIALS AND METHODS

A kiln-dried radiata pine rod with a diameter of 16 mm and length of 2460 mm was used. Similarly, an aluminium rod with a diameter of 16 mm and length of 2510 mm was also used for comparison purposes. Shear transducers manufactured by Plant Integrity Ltd [13] were used for transmission and reception. For dry coupling, the
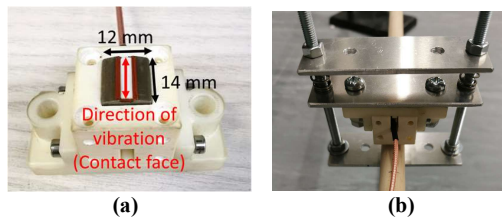
Figure 1. Photo (a) shows a PZT transducer used in the experiment. Photo (b) shows the transducer being pushed against a wood sample.

transducers were clamped onto the sample using springs as shown in Figure 1. The contact faces of the transducers were aligned parallel to the wood grain for longitudinal wave transmission and reception. For torsional wave mode transmission/reception, the contact faces of the transducers were aligned at right angles to the wood grain. A ring array of four transducers was mounted around the sample using the mounting system shown in Figure 2.
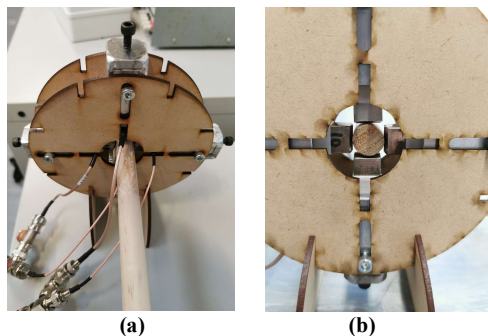
Figure 2. Mounting system for a ring array of transducers around a wood sample

Figure 3 shows the theoretical phase velocity dispersion curve for the aluminium rod sample. These were obtained using GUIGUW using the following parameters. A rod diameter of 16 mm, density of 2,710 kg/m^3, Young's Modulus of 68.9 GPa and Poisson's ratio of 0.33. The dispersion curve shows only the three fundamental wave modes are present. Both the longitudinal L(0,1) and flexural F(1,1) wave modes are dispersive whereas the fundamental torsional T(0,1) wave mode is not.
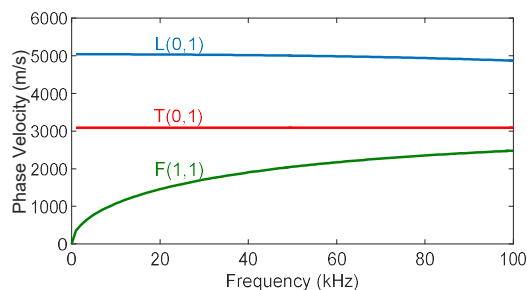
Figure 3. Theoretical phase velocity dispersion curve for 16 mm diameter aluminium.

ToF experimental setup

For wood related studies, the ToF method involves two probes inserted into a sample and separated by a distance d. The acoustic velocity is then measured using

$$v_{tof} = \frac{\Delta d}{T} \qquad (2)$$

where T is the propagation time of the stress wave from one probe to the other. First Time of Arrival (FToA) techniques are commonly used to determine the arrival time of a received signal. The technique only looks at the first part of the signal and ignores the remainder of the signal. The amplitude threshold is the most common FToA method used for NDT testing. The method measures the time at which a signal first goes above a certain threshold value.

For ToF measurements, a shear transducer (RX1) was positioned 50 mm away from end of the sample while another transducer (RX2) was positioned at the opposite end to receive vibrations. A hammer was impacted at one end of the sample (near RX1) parallel to the grain to generate longitudinal vibrations. The signal received from the transducers were then recorded. The transducers were directly connected to the ADC channels of a DT9832 module and sampled at 2 MHz. The amplitude threshold method was used to determine the time T taken for the signal to propagate between the two receivers. The ToF velocity was then calculated using Equation (2). The ToF measurements were repeated 10 times and the average ToF velocity was obtained.

Resonance experimental setup

For resonance measurements, a hammer was impacted parallel to the grain at one end of the sample. A GRAS 46BF-1 microphone was positioned at the opposite end of the sample to measure the received signal. The received signal was sampled at 2 MHz using the ADC channels from a DT9832 module. A Fast Fourier Transform (FFT) was performed on the received signal and the resonance velocities were calculated using

$$v_{res} = \frac{2Lf_n}{n} \qquad (3)$$

where L is the length of the sample and f_n is the nth resonant frequency (where n = 1, 2, 3..). The average of the first 5 harmonics was taken as the resonance velocity.

Guided waves experimental setup

Three transducers were used for guided wave measurements. One transducer acting as a transmitter (TX) was attached at one end of the sample. Another transducer acting as a receiver (RX1) was attached 50 mm away from the transmitter while the other receiver (RX2) was attached at the opposite end of the sample. An excitation signal was created in MATLAB and outputted from an Agilent 33220A Function Generator. A 5 cycle Hanning-windowed sine wave with central transmit frequencies ranging from 15 kHz to 50 kHz was used as the excitation signal. A custom-built 400 Vpp linear power amplifier was used to amplify the transmit signal. The receive transducers were connected to custom-built pre-amps and the received signal was sampled at 2 MHz using the ADC channels of the DT9832 module.

Dispersion curve and dispersion compensation

Assume a signal *g(t)* excited by a transducer that only generates a single wave mode. The received signal *y(t)* at a distance *d* from the transmitter can be modelled in the frequency domain as

$$Y(\omega) = G(\omega)e^{-j\,k(\omega)d - \alpha(\omega)d}, \qquad (4)$$

where ω is the angular frequency, $G(\omega)$ is the Fourier Transform *g(t)*, $k(\omega)$ is the wavenumber and $\alpha(\omega)$ is the attenuation. The relationship between wavenumber and phase velocity v_{ph} is given by

$$k = \frac{\omega}{v_{ph}}. \qquad (5)$$

The phase velocity for each guided wave transmission was calculated using a frequency-domain shifting technique. The received signal at RX1 was converted into the frequency domain using a FFT. Equation (4) was then used to propagate the received signal by a distance *d* using an initial phase velocity v_{ph}. The propagated signal $Y(\omega)$ was then transformed back to the time-domain using an Inverse Fast Fourier Transform (IFFT). The Root Mean Squared Error (RMSE) between the time-domain propagated RX1 signal and RX2 was calculated. The phase velocity v_{ph} was adjusted by 1 m/s until a minimum RMSE was obtained. This was repeated for a range of central transmit frequencies.

A curve was fitted through the calculated phase velocities using Equation (6) which was derived from Ref [15]. Optimum values for c_o, α_1 and α_2 was obtained using a non-linear least squares fitting method.

$$c_l = c_o\sqrt{\frac{1+\alpha_1\alpha_2 k^2}{1+\alpha_1 k^2}}. \qquad (6)$$

Dispersion compensation was then performed on the ToF received signals. Consider a dispersed received signal *y(t)*, dispersion compensation can be performed at the i_{th} propagation time t_i in the frequency domain using

$$\hat{Y}(\omega, t_i) = Y(\omega)e^{j(k(\omega)d(t_i) - \omega\, t_i)}, \qquad (7)$$

where $Y(\omega)$ is the Fourier transform of the received signal *y(t)* and *d* is the propagation distance. This performs frequency domain shifting for each frequency component in the signal for phase velocity correction. Each frequency component of the signal is calculated using Equation (7) and the IFFT is used to convert the frequency-domain dispersion compensated signal to the time-domain [14]. This provides correct dispersion compensation of the received signal *y(t)* at time t_i only. To correct the signal for all times, the above process is performed in a loop where the i_{th} iteration performs dispersion compensation for the i_{th} signal. The product of this iterative process is a dispersion compensated received signal *y(t)* for all times.

Obtaining wavenumber-frequency plots

A similar experimental setup such as the one used for guided waves was used. A transducer acting as a transmitter (TX) was clamped at one end of the rod sample. Another transducer acting as a receiver (RX) was clamped 1000 mm away. A chirp signal ranging from 5 to 100 kHz was used as the transmit signal. The received signal at the receiver (RX) was recorded and saved into an new array in MATLAB. The receiver was reattached 5 mm away from its initial position. The chirp signal was retransmitted and the received signal was recorded and saved. This process was repeated for a total of 201 measurements. The sampled signals from all the measurement positions were arranged in a $201 \times N$ matrix, where *N* is the number of samples. A 2D FFT method [16] was used on the matrix to obtain wavenumber-frequency domain plots. Theoretical dispersion curves for aluminium were overlaid onto these wavenumber-frequency domain plots. This experiment was then repeated using the transmit and receive arrays.

RESULTS

Resonance and Time of Flight

The experimental average resonance and ToF velocities are given in Table 1. The results show that ToF velocities are slightly higher compared to resonance velocities and are not within the measurement error. This is in line with the results reported in literature where ToF measurements are overestimated compared to resonance measurements.

Table 1. Average resonance and ToF velocity.

Material	Resonance velocity (m/s)	ToF velocity (m/s)
Wood	4463 ± 41	4592 ± 33
Aluminium	5036 ± 21	5130 ± 35

Experimentally measured dispersion curves

Aluminium

Figure 4 shows the experimental wavenumber-frequency plots for the aluminium sample obtained using different number of transmitters aligned either in the longitudinal or torsional direction. Theoretical dispersion curves for the aluminium sample were obtained using GUIGUW and overlaid onto the experimental wavenumber-frequency plots. The resonance velocity was converted into wavenumber using Equation (5) and overlaid onto the wavenumber-frequency domain plots. The converted resonance velocity line is observed to align well with the fundamental longitudinal L(0,1) wave mode.

Figure 4(a) shows that using a single transmit and single receive transducer aligned in the longitudinal direction, two dispersion curves that corresponds to the fundamental L(0,1) and F(1,1) wave modes are observed. However, when four transmitters are and a single receiver was used, only a single dispersion curve that aligns with the L(0,1) wave mode is observed, as seen in Figure 4(b).

A similar effect is seen in Figure 4(c) where the F(1,1) and T(0,1) wave modes are observed when a single transmit and single receive transducer are aligned in the torsional direction. Figure 4(d) shows that only the T(0,1) is mainly present when four transmitters were used. These results show that enhancement and suppression of desired wave modes can be achieved using a ring array of shear
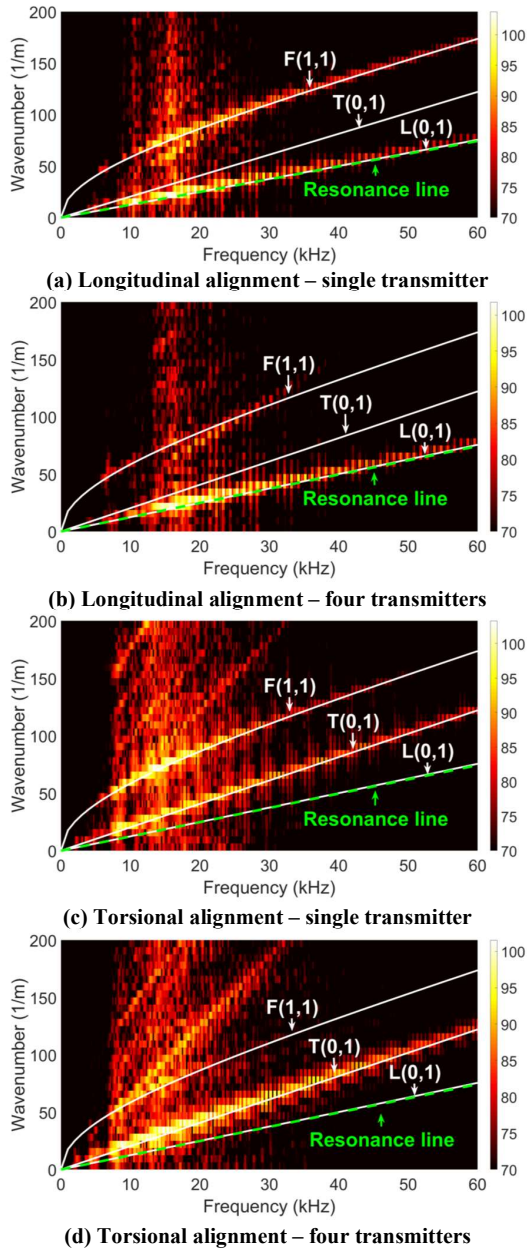
(a) Longitudinal alignment – single transmitter

(b) Longitudinal alignment – four transmitters

(c) Torsional alignment – single transmitter
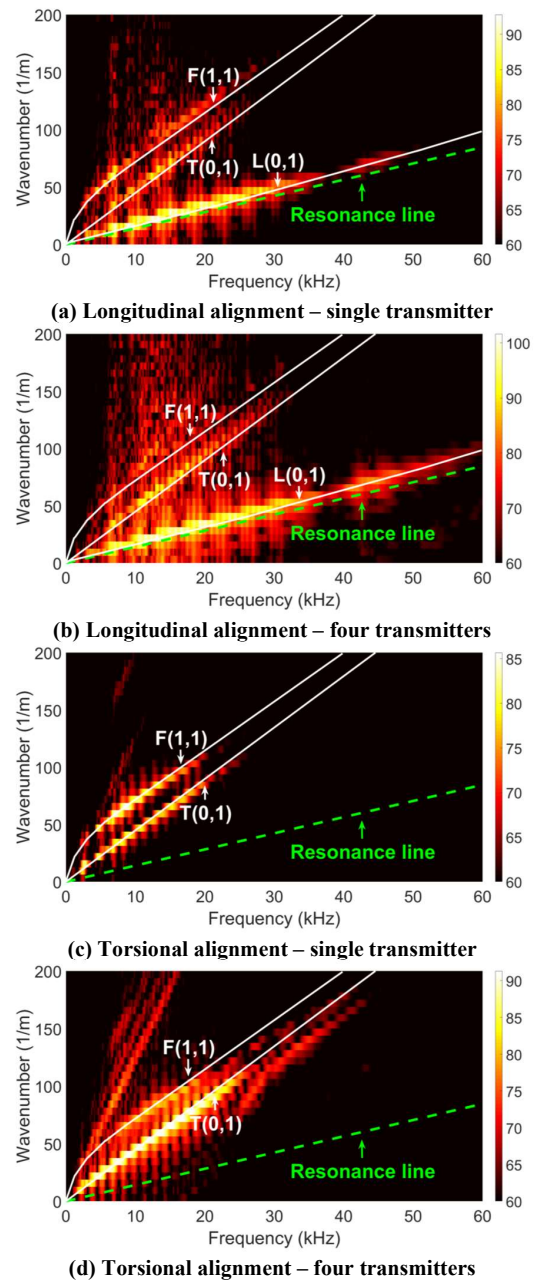

(d) Torsional alignment – four transmitters

Figure 4. Wavenumber-frequency domain plots for the 16 mm diameter aluminium sample using different number and alignment of transducers

transducers. This allows single wave mode excitation/reception to be achieved. Excitation of a single wave mode is desirable as it mitigates the distortion of the received signal which may be a result of the propagation or reflection of other wave modes.

Wood

Figure 5 shows the wavenumber-frequency domain plots for the 16 mm diameter wood sample using different number and alignment of transducers. Three dispersion curves that represent the fundamental longitudinal L(0,1), flexural F(1,1) and torsional T(0,1) wave modes are expected to be observed for the cylindrical wood sample. Curves have therefore been overlaid onto the

wavenumber-frequency domain plots in order to label the observed wave modes.

Similarities are observed between the wavenumber-frequency domain plots for the wood sample in Figure 5 and the aluminium sample in Figure 4. Different wave modes are being excited and measured depending on the alignment of the transducers. The use of a ring array of transducers aligned in either the longitudinal or torsional direction can assist in enhancing the L(0,1) or T(0,1) wave modes and suppressing other unwanted wave modes. A ring array of shear transducers can therefore be used for single wave mode transmission/reception in wood. When

(a) Longitudinal alignment – single transmitter

(b) Longitudinal alignment – four transmitters

(c) Torsional alignment – single transmitter

(d) Torsional alignment – four transmitters

Figure 5. Wavenumber-frequency domain plots for the 16 mm diameter wood sample using different number and alignment of transducers

the transmitters are aligned in the torsional direction, only the torsional T(0,1) wave mode was generated for the wood sample as shown in Figure 5(d). The non-dispersive torsional T(0,1) wave mode can potentially be used for non-destructive testing for wood as it is not affected by dispersion effects.

Dispersion compensation

Dispersion compensation was performed to investigate the effects of dispersion on the ToF received signals. Figure 6 shows the original ToF received signal and the dispersion compensated ToF received signal for the aluminium and wood samples using hammer hit excitation. The results from the figure show significant difference in rise time at the start of the received signal. The dispersion compensated received signal is slightly delayed and the slope of the signal is sharper compared to the original received signal. This phenomena was observed for both the aluminium and wood samples.

(a)

(b)
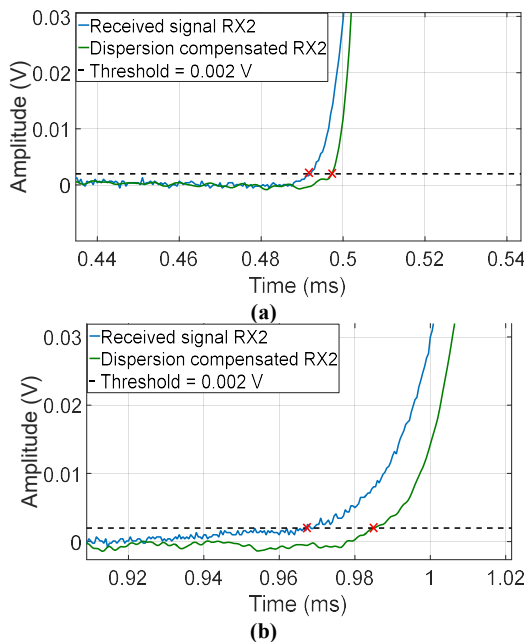
Figure 6. Plot showing the effects of applying dispersion compensation on the received signals for amplitude threshold ToF using hammer hit excitation for (a) aluminium and (b) wood samples

Table 2 shows the amplitude threshold ToF velocities for the wood and aluminium samples before and after dispersion compensation was performed. The results show that a significant reduction in ToF velocity after dispersion compensation was performed on the received signal. The average resonance velocity for wood and aluminium are 4526 m/s and 5036 m/s respectively. The difference between the ToF velocity and resonance velocity for wood was reduced from 1.4% to 0.2% after dispersion compensation was performed. For aluminium, the difference was reduced from 1.8% to 0.5%. This shows that dispersion can be a cause of overestimation for amplitude threshold ToF measurements. The results also show that dispersion compensation can be used to mitigate this overestimation.

Table 2. Amplitude threshold ToF acoustic velocity for 16 mm diameter wood and aluminium sample before and after dispersion compensation.

Material	Before dispersion compensation (m/s)	After dispersion compensation (m/s)
Wood	4592	4538
Aluminium	5130	5064

CONCLUSION

Time of flight, resonance and guided wave measurements were performed on 16 mm diameter cylindrical wooden and aluminium rods using dry-coupled shear PZT transducers. Wavenumber-frequency domain plots were obtained using guided wave measurements and the 2D FFT method. The results show that excitation and reception of the desired wave modes can be achieved by changing the orientation of the transducers in either the longitudinal or torsional direction. Improved measurements were achieved using a ring array of shear transducers. The most significant improvement was most observed when the transducers were oriented in the torsional direction where the torsional wave mode was enhanced and flexural wave modes were suppressed. There are limited studies on the use the torsional wave mode for non-destructive testing for wood.

The overestimation of the ToF method relative to the resonance method has been reported in literature. However, the exact cause of the overestimation is not known. No previous studies have investigated the effects of dispersion on ToF acoustic velocity measurements obtained using amplitude thresholding. In this study, experimental dispersion curves were measured and dispersion compensation was performed on ToF received signals for both aluminium and wood samples. The results show that dispersion can distort the rise time at the start of the received signal. This can affect significantly affect ToF measurements obtained using the amplitude threshold method. The results also show that dispersion compensation can be used to mitigate dispersion effects and reduce the ToF overestimation. This would allow more accurate wood stiffness measurements to be obtained.

Future works could include performing measurements on samples with varying diameters to investigate the relationship between sample diameter and acoustic velocity obtained using resonance, ToF and guided wave measurements. As shown in the results, dispersion effects can be a cause of ToF overestimation. The non-dispersive nature of the torsional wave mode means that it is not affected by dispersion effects. The torsional wave mode could potentially be used to obtain more accurate wood property estimation. More research into guided waves in wood is necessary to determine whether improved measurements of wood properties can be obtained.

REFERENCES

[1] X. Wang, "Acoustic measurements on trees and logs: a review and analysis," *Wood Science and Technology*, vol. 47, no. 5, pp. 965–975, 2013.

[2] M. Legg and S. Bradley, "Measurement of stiffness of standing trees and felled logs using acoustics: A review," *The Journal of the Acoustical Society of America*, vol. 139, no. 2, pp. 588–604, 2016.

[3] J. L. Rose, *Ultrasonic guided waves in solid media*. Cambridge university press, 2014.

[4] H. Fathi, S. Kazemirad, and V. Nasir, "Lamb wave propagation method for nondestructive characterization of the elastic properties of wood," *Applied Acoustics*, vol. 171, p. 107565, 2021.

[5] H. Fathi, V. Nasir, and S. Kazemirad, "Prediction of the mechanical properties of wood using guided wave propagation and machine learning," *Construction and Building Materials*, vol. 262, 2020.

[6] V. Nasir, H. Fathi, and S. Kazemirad, "Combined machine learning-wave propagation approach for monitoring timber mechanical properties under UV aging," *Structural Health Monitoring*, p. 1475921721995987, 2021.

[7] I. A. Veres and M. B. Sayir, "Wave propagation in a wooden bar," *Ultrasonics*, vol. 42, no. 1–9, pp. 495–499, 2004.

[8] U. Dackermann, Y. Yu, E. Niederleithinger, J. Li, and H. Wiggenhauser, "Condition assessment of foundation piles and utility poles based on guided wave propagation using a network of tactile transducers and support vector machines," *Sensors*, vol. 17, no. 12, p. 2938, 2017.

[9] J. D. Holt, S. Chen, and R. A. Douglas, "Determining lengths of installed timber piles by dispersive wave propagation," *Transportation research record*, no. 1447, 1994.

[10] B. Sriskantharajah, E. Gad, S. Bandara, P. Rajeev, and I. Flatley, "Condition assessment tool for timber utility poles using stress wave propagation technique," *Nondestructive Testing and Evaluation*, vol. 36, no. 3, pp. 336–356, 2021.

[11] D. Gorham, "A numerical method for the correction of dispersion in pressure bar signals," *Journal of Physics E: Scientific Instruments*, vol. 16, no. 6, p. 477, 1983.

[12] A. Tyas and D. J. Pope, "Full correction of first-mode Pochammer-Chree dispersion effects in experimental pressure bar signals," *Measurement science and technology*, vol. 16, no. 3, p. 642, 2005.

[13] B. A. Engineer, "The mechanical and resonant behaviour of a dry coupled thickness-shear PZT transducer used for guided wave testing in pipe line," 2013.

[14] M. Legg, M. K. Yücel, V. Kappatos, C. Selcuk, and T.-H. Gan, "Increased range of ultrasonic guided wave testing of overhead transmission line cables using dispersion compensation," *Ultrasonics*, vol. 62, pp. 35–45, 2015.

[15] G. Carta, "Correction to Bishop's approximate method for the propagation of longitudinal waves in bars of generic cross-section," *European Journal of Mechanics-A/Solids*, vol. 36, pp. 156–162, 2012.

[16] D. Alleyne and P. Cawley, "A two-dimensional Fourier transform method for the measurement of propagating multimode signals," *The Journal of the Acoustical Society of America*, vol. 89, no. 3, pp. 1159–1168, 1991.

Appendix 5

This article was published and presented at the Acoustics 2022: The Nature of Acoustics conference held on 31 Oct - 2 Nov 2022 at Te Papa, Wellington, New Zealand.

Experimental measurement of phase velocity of ultrasonic guided waves using wave propagation theory

Adli Hasan Abu Bakar [(1)] and Mathew Legg [(1)]

(1) Department of Mechanical and Electrical Engineering, Massey University, Auckland, New Zealand
m.legg@massey.ac.nz

ABSTRACT

Ultrasonic Guided Wave techniques are commonly used for non-destructive evaluation of rod or plate-like structures. Guided waves propagate as wave modes that are generally dispersive. The phase and group velocities of these wave modes can be described using dispersion curves. However, these dispersion curves are dependent on factors such as the mechanical properties, diameter, cross-sectional shape and temperature of the sample. The 2D FFT method is commonly used to experimentally measure the dispersion curves but has low accuracy. Time-domain techniques have also been used to obtain phase velocity measurements. However, these techniques do not take dispersion effects into account, which can lead to errors. In this work, a technique is presented that measures the phase velocity using guided wave propagation theory, which includes dispersion. The results from this technique are compared to methods such as 2D FFT and zero-crossing.

INTRODUCTION

Ultrasonic Guided Wave (UGW) techniques have been widely used for Non-Destructive Testing (NDT) and Structural Health Monitoring (SHM) of metallic structures such as rods, pipes and plates [1 - 2]. Dispersion curves are useful for UGW as they help to predict and understand the behaviour of different types of vibrations called wave modes. Dispersion curves describe the relationship between phase/group velocity as a function of frequency. The ability to experimentally measure dispersion curves is therefore important for guided wave applications.

There are various methods which can be used to estimate dispersion curves such as the Short Time Fourier Transform (STFT) [3], Continuous Wavelet Transform (CWT) [4], Hilbert-Huang Transform (HHT) [5] and others. These methods are time-frequency analysis (TFA) methods and have limitations such as energy concentration optimization [6] and time-frequency resolution [7]. The most widely used method for dispersion curve estimation is the 2D Fast Fourier Transform (FFT) [8].

The 2D FFT method can be used to identify the presence of wave modes propagating in a medium. The method involves performing a 2D FFT in the time and space domain. The results of the 2D FFT gives a visual representation of the dispersion curves in the wavenumber-frequency domain. However, further processing of the results are needed to extract the phase velocity. The resolution and accuracy of the 2D FFT method is dependent on the number of measurement points and the spacing between them. To obtain high accuracy, a large number of measurement points with very small spacing between them is needed. This increases the complexity of the method making it difficult to obtain accurate results.

Another method which is widely used for phase velocity dispersion curve estimation is the zero-crossing method [9]. The zero-crossing method measures the time instants at which the received signals crosses the zero amplitude line. This method is affected by which zero-crossing instants are used. The TFA methods, 2D FFT and the zero-crossing methods do not take dispersion into account. This can lead to errors when performing phase velocity measurements especially for dispersive wave modes where the signal is distorted due to dispersion effects.

This paper investigates a new method for phase velocity measurement using a frequency-shifting technique. The main feature of this technique is that dispersion of the wave mode is considered when obtaining phase velocity measurements. Initial measurements were performed on a slightly dispersive longitudinal L(0,1) wave mode. Using simulation, a signal was propagated by a distance and the error between the simulated and experimental signal was calculated. The dispersion curve was adjusted until a minimum error between the simulated and experimental signal was obtained. Measurements were performed on a cylindrical 16 mm aluminium rod. A comparison between the proposed method, zero-crossing method and 2D FFT method was also made. Results show that the proposed method has similar performance to the zero-crossing method with an average error of 0.25%.

MATERIALS AND METHODS

Dry-coupled shear PZT transducers made by The Welding Institute (TWI) [10] were used for transmission and
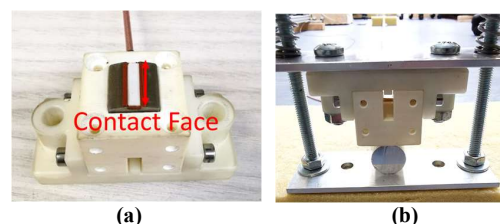

(a)   (b)

Figure 1. Photo (a) shows a PZT transducer used in the experiment. Photo (b) shows the transducer being pushed against an aluminium sample.

reception of acoustic/guided waves. The dimension of the transducer is 12 mm x 14 mm. For coupling, the transducers were clamped onto the sample using springs as shown in Figure 1. Measurements were performed on a 6061-T6 aluminium rod with a diameter of 16 mm and length of 2510 mm. Figure 2 shows the theoretical phase velocity dispersion curves for the aluminium rod sample. These were obtained using GUIGUW assuming a rod diameter of 16 mm, density of 2,710 kg/m³, Young's Modulus of 68.9 GPa and Poisson's ratio of 0.33.
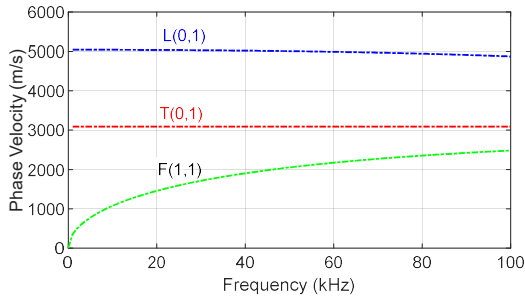
Figure 2. Theoretical phase velocity dispersion curve for 16 mm diameter aluminium rod.

Obtaining wavenumber-frequency plots

Wavenumber-frequency domain plots were obtained using the 2D FFT method described by Alleyne and Cawley [8]. A shear transducer used for transmission (TX) was clamped at one end of the sample while another transducer used for reception (RX) was clamped 1000 mm away. For transmission, a sweep signal ranging from 5 kHz to 100 kHz was generated in MATLAB and outputted from an Agilent 3320A Function Generator. The transmitted signal was amplified to 400 Vpp using a custom-built linear power amplifier. The receiver was connected to a custom-built pre-amp and the received signal was sampled at 2 MHz using the ADC channels from a Data Translation DT9832 module. The received signal was then saved into a new array in MATLAB. The receiver was de-clamped and repositioned 5 mm away from its initial position. The transmission and reception process were repeated until a total of 201 measurement locations were obtained. In MATLAB, the sampled signals were arranged in a $201 \times N$ matrix, where N is the number of samples per measurement location. A 2D FFT was then performed on the matrix to convert from the space-time domain to the wavenumber-frequency domain. Theoretical dispersion curves were then overlaid onto the wavenumber-frequency plot.

Guided waves experimental setup

For guided wave measurements, a pitch-catch configuration was used. The configuration consists of three transducers, one acting as a transmitter and two acting as receivers. The transmitter (TX) was clamped at one end of the rod sample. One receiver (RX1) was clamped 50 mm away from the transmitter and the other receiver (RX2) was clamped at the other end of the rod sample. For transmission, 5 cycles of a Hanning-windowed sine wave with central frequencies ranging from 20 kHz to 50 kHz in steps of 1 kHz were used. The

excitation signal was created in MATLAB and outputted from an Agilent 33220A Function Generator. The signal was then amplified to 400 Vpp using a custom-built linear power amplifier. The receivers were connected to custom-built pre-amps and the received signal was sampled at 2 MHz using the ADC channels from a DT9832 module.

Phase velocity measurement

Phase velocity measurements were obtained using the zero-crossing method and a frequency shifting technique. Details of the methods will be discussed in the following subsections.

Zero-crossing

The phase velocity of the guided wave measurements were obtained using the zero-crossing technique [9]. First, an initial threshold value was defined to window the received signal at the region of interest. The windowed signal was resampled from 2 MHz to 10 MHz using a spline interpolation. This was done to increase the resolution. The time at which the signal crosses the zero amplitude line before and after the threshold value were determined. The zero-crossing instants $t_1(x_n)$, $t_2(x_n)$, $t_3(x_n)$ and $t_4(x_n)$ are obtained, as seen in Figure 3.
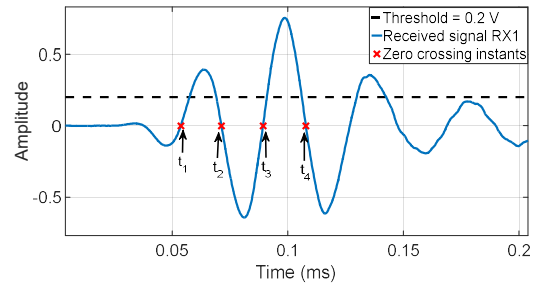

Figure 3. Zero-crossing instants for received signal at RX1 using a 5 cycle 40 kHz Hanning-windowed sine wave as the transmit signal.

The zero-crossing instants were determined for each measurement location x_n for both receiver RX1 and RX2. The phase velocity was calculated using

$$v_{ph} = \frac{x_{n_2} - x_{n_1}}{t_m(x_{n_2}) - t_m(x_{n_1})} \qquad (1)$$

where m = 1, 2, 3 or 4. From the zero-crossing instants, the first, second and third half periods ($T_{0.5,1}, T_{0.5,2}, T_{0.5,3}$) are obtained using

$$T_{0.5,i}(x) = t_{i+1}(x) - t_i(x), \qquad (2)$$

and the equivalent frequencies for the phase velocities were calculated by

$$f_{0.5,i}(x) = 0.5/T_{0.5,i}. \qquad (3)$$

Proposed method

Phase velocity measurements were also obtained using a frequency-domain shifting technique. For each guided wave signal transmission, a Fast Fourier Transform (FFT) was performed on the received signal $g(t)$ at RX1 to convert the received signal into the frequency-domain

111

$G(\omega)$. Simulated propagation of the converted signal $G(\omega)$ by a distance d (distance between receivers RX1 and RX2) was performed using the equation

$$Y(\omega) = G(\omega)e^{-j\,k(\omega)d - \alpha(\omega)d}, \qquad (4)$$

where ω is the angular frequency, $Y(\omega)$ is the Fourier transform of the propagated received signal RX1, $k(\omega)$ is the wavenumber and $\alpha(\omega)$ is the attenuation. The wavenumber was converted into phase velocity using

$$k(\omega) = \frac{\omega}{v_{ph}(\omega)}, \qquad (5)$$

where $v_{ph}(\omega)$ is the phase velocity. After propagation, the signal $Y(\omega)$ was converted back into the time domain $y(t)$ using an Inverse Fast Fourier Transform (IFFT). The difference between the simulated propagated time-domain RX1 signal $y(t)$ and the received signal at RX2 was obtained by calculating the Root Mean Squared Error (RMSE). The phase velocity $v_{ph}(\omega)$ was iteratively adjusted by 1 m/s until a minimum RMSE was obtained . This corresponds to the measured phase velocity for that central transmit frequency. This was repeated for each guided wave transmission. Figure 4 shows a block diagram of the phase velocity measurement process. Figure 5 shows an example of the time-domain plots for the propagated and received signal. The phase of the simulated propagated RX1 signal is observed to match well with the received signal at RX2.
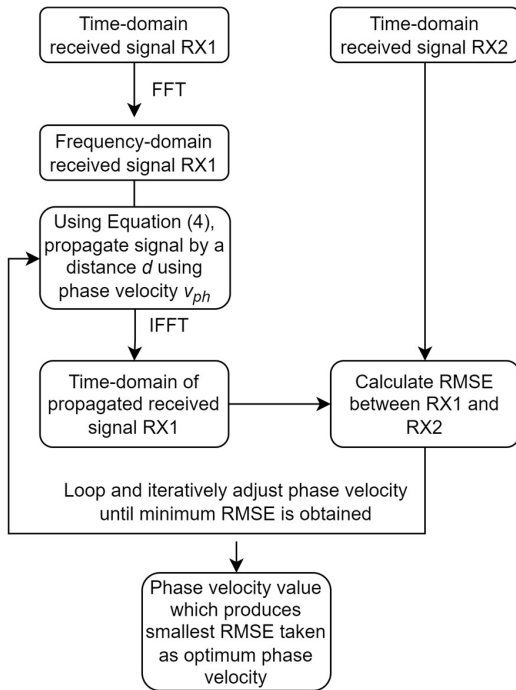
Figure 4. Block diagram of the proposed frequency-shifting technique
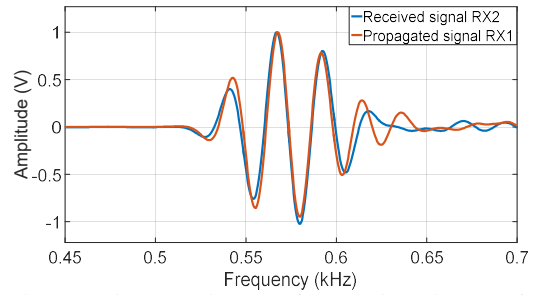
Figure 5. Time-domain plots of the received signal RX2 and propagated signal RX1 using 5 cycles of a 40 kHz Hanning-windowed sine wave as the transmit signal
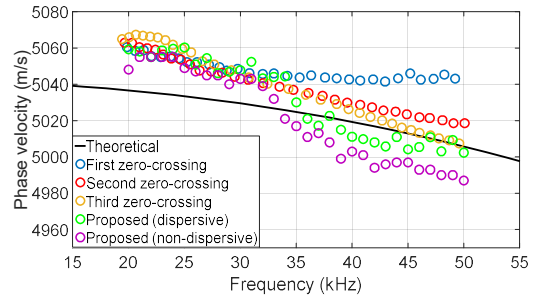
Figure 6. Phase velocity measurements obtained using varying methods.

RESULTS

Comparison with zero-crossing

Figure 6 shows phase velocity measurements obtained using the zero-crossing, proposed method and theoretical phase velocity of the L(0,1) wave mode obtained using GUIGUW. For the zero-crossing method, the first, second and third zero-crossings were used. The figure shows that the first, second and third zero-crossing produces similar phase velocities at low frequencies. However, as the frequency increases, the first zero-crossing starts deviating away from the second and third zero-crossing.

For comparison, using the proposed method, phase velocity measurements were obtained by including and excluding dispersion of the simulated signal. To include dispersion, theoretical phase velocity dispersion curve of the L(0,1) wave mode was used. To exclude dispersion, a constant phase velocity was used for all frequencies. The figure shows that more accurate results were obtained using the proposed method when dispersion was included. Higher variations are observed using the proposed method compared to the zero-crossing method.

Table 1 shows the experimental errors of different methods compared to the theoretical dispersion curve. The largest average error is obtained using the first zero-crossing method which is approximately 0.48%. The smallest average error was obtained using the proposed method by including dispersion which was approximately 0.25%. The difference in accuracy between the two methods is not significant.

Table 1. Experimental errors for phase velocity measurements using different methods relative to theoretical phase velocity.

Technique	Mean difference (m/s)	Standard deviation (m/s)	Average percentage difference (%)
First zero-crossing	24.5	5.4	0.48
Second zero-crossing	15.9	5.5	0.31
Third zero-crossing	15.2	12.0	0.30
Proposed (with dispersion)	12.5	8.1	0.25
Proposed (without dispersion)	15.1	4.5	0.30

Comparison with 2D FFT method

In this subsection, results from the second zero-crossing are used as it provides the best performance compared to the first and third zero-crossing. Phase velocity measurements obtained from the second zero-crossing and the proposed method (with dispersion) were converted into wavenumber domain using Equation (5). The converted values were overlaid onto the wavenumber-frequency domain plot, as seen in Figure 7. The figure shows that the zero-crossing and proposed method align well with the theoretical L(0,1) wave mode and overlaps with the experimental dispersion curve. Note that the 2D FFT method can only provide a qualitative measure of the dispersion curve as it has low resolution. The resolution of the 2D FFT method is limited and is affected by the number of measurement points and the distance between each measurement point. A single pixel in the y-axis when converted from wavenumber to phase velocity would lead to large errors. In this study, the calculated pixel resolution in the y-axis is 6.22 m^{-1}. At the wavenumber of interest at 30 kHz, the calculated resolution in terms of phase velocity is approximately 714 m/s.
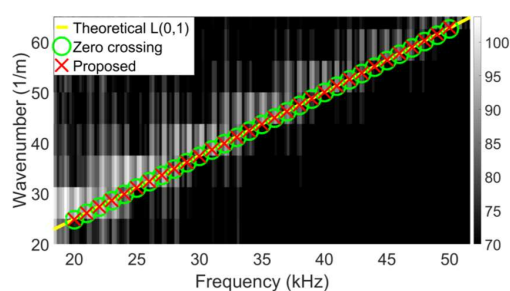
Figure 7. Wavenumber-frequency plot of 2D FFT method overlaid with those obtained using different method.

CONCLUSION

A frequency shifting technique is proposed which includes dispersion for phase velocity measurement. Comparison was made between the proposed method, zero-crossing method and 2D FFT method. Results indicate difference in phase velocity measurement when different zero-crossing instants are used. The performance of the proposed method is observed to be similar to the zero-crossing method. No significant difference was observed using the proposed method when dispersion was excluded. This may be due because the L(0,1) wave mode is only slightly dispersive at the frequency range used in this study. The proposed method aligns well with results obtained using the 2D FFT method. However, the 2D FFT method has low resolution which results in high uncertainties.

Note that in this study, the proposed method was used on a slightly dispersive wave mode. There is potential for the method to be used for more dispersive wave mode where dispersion effects and distortion of the signal are more palpable. Phase velocity measurement techniques that do not include dispersion are expected to be less effective when used on dispersive signals. Future works should include performing measurements at higher frequencies where dispersion effects are more significant or on more dispersive wave modes such as the flexural wave mode. The proposed method has the potential to be used to provide more accurate phase velocity measurements which could lead to improved NDT measurements.

REFERENCES

[1] M. Mitra and S. Gopalakrishnan, "Guided wave based structural health monitoring: A review," *Smart Materials and Structures*, vol. 25, no. 5, p. 053001, 2016.

[2] S. C. Olisa, M. A. Khan, and A. Starr, "Review of current guided wave ultrasonic testing (GWUT) limitations and future directions," *Sensors*, vol. 21, no. 3, p. 811, 2021.

[3] B. Zhao, O. Basir, and G. Mittal, "Estimation of ultrasound attenuation and dispersion using short time Fourier transform," *Ultrasonics*, vol. 43, no. 5, pp. 375–381, 2005.

[4] S. Aeron, S. Bose, and H.-P. Valero, "Automatic dispersion extraction using continuous wavelet transform," in *2008 IEEE International Conference on Acoustics, Speech and Signal Processing*, 2008, pp. 2405–2408.

[5] Y. Zhang, S. Wang, S. Huang, W. Zhao, and others, "Mode recognition of Lamb wave detecting signals in metal plate using the Hilbert-Huang transform method," *Journal of Sensor Technology*, vol. 5, no. 01, p. 7, 2015.

[6] E. Sejdi'c, I. Djurovi'c, and J. Jiang, "Time-frequency feature representation using energy concentration: An overview of recent advances," *Digital signal processing*, vol. 19, no. 1, pp. 153–183, 2009.

[7] M. Niethammer, L. J. Jacobs, J. Qu, and J. Jarzynski, "Time-frequency representations of Lamb waves," *The Journal of the Acoustical Society of America*, vol. 109, no. 5, pp. 1841–1847, 2001.

[8] D. Alleyne and P. Cawley, "A two-dimensional Fourier transform method for the measurement of propagating multimode signals," *The Journal of the Acoustical Society of America*, vol. 89, no. 3, pp. 1159–1168, 1991.

[9] L. Mazeika, L. Draudviliene, and E. Zukauskas, "Influence of the dispersion on measurement of phase and group velocities of Lamb waves," *Ultrasound*, vol. 64, no. 4, pp. 18–21, 2009.

[10] B. A. Engineer, "The mechanical and resonant behaviour of a dry coupled thickness-shear PZT transducer used for guided wave testing in pipe line," 2013.

STATEMENT OF CONTRIBUTION
DOCTORATE WITH PUBLICATIONS/MANUSCRIPTS

We, the candidate and the candidate's Primary Supervisor, certify that all co-authors have consented to their work being included in the thesis and they have accepted the candidate's contribution as indicated below in the *Statement of Originality*.

Name of candidate:	Adli Hasan Bin Abu Bakar
Name/title of Primary Supervisor:	Mathew Legg

In which chapter is the manuscript /published work: 2

Please select one of the following three options:

◉   The manuscript/published work is published or in press

- Please provide the full reference of the Research Output:

A. H. A. Bakar, M. Legg, D. Konings, F. Alam. Ultrasonic guided wave measurement in a wooden rod using shear transducer arrays. Ultrasonics 119 (2022) 106583 doi:10.1016/j.ultras.2021.106583

○   The manuscript is currently under review for publication – please indicate:

- The name of the journal:

- The percentage of the manuscript/published work that was contributed by the candidate: 80.00

- Describe the contribution that the candidate has made to the manuscript/published work:

The candidate conducted the experiments, performed data collection and analysis and produced the first draft of the manuscript.

○   It is intended that the manuscript will be published, but it has not yet been submitted to a journal

Candidate's Signature:	*[signature]* Digitally signed by Adli Hasan DN: C=NZ, CN=Adli Hasan, Email=a.hasan@massey.ac.nz Reason: I am the author of this document Location: your signing location here Date: 2022.12.13 19:03:49+13'00' Foxit PDF Reader Version: 11.0.0
Date:	13-Dec-2022
Primary Supervisor's Signature:	Mathew Legg Digitally signed by Mathew Legg DN: cn=Mathew Legg, c=NZ, email=m.legg@massey.ac.nz Date: 2022.12.15 12:40:06 +13'00'
Date:	15-Dec-2022

This form should appear at the end of each thesis chapter/section/appendix submitted as a manuscript/publication or collected as an appendix at the end of the thesis.

MASSEY UNIVERSITY
TE KUNENGA KI PŪREHUROA
UNIVERSITY OF NEW ZEALAND

**GRADUATE
RESEARCH
SCHOOL**

STATEMENT OF CONTRIBUTION
DOCTORATE WITH PUBLICATIONS/MANUSCRIPTS

We, the candidate and the candidate's Primary Supervisor, certify that all co-authors have consented to their work being included in the thesis and they have accepted the candidate's contribution as indicated below in the *Statement of Originality*.

Name of candidate:	Adli Hasan Bin Abu Bakar
Name/title of Primary Supervisor:	Mathew Legg

In which chapter is the manuscript /published work: 3

Please select one of the following three options:

◉   The manuscript/published work is published or in press

- Please provide the full reference of the Research Output:

A. H. A. Bakar, M. Legg, D. Konings, F. Alam. Estimation of the rod velocity in wood using multi-frequency guided wave measurements. Applied Acoustics 202 (2023) 109108 doi: 10.1016/j.apacoust.2022.109108

◯   The manuscript is currently under review for publication – please indicate:

- The name of the journal:

- The percentage of the manuscript/published work that was contributed by the candidate: 80.00

- Describe the contribution that the candidate has made to the manuscript/published work:

The candidate conducted the experiments, performed data collection and analysis and produced the first draft of the manuscript.

◯   It is intended that the manuscript will be published, but it has not yet been submitted to a journal

Candidate's Signature:	*Digitally signed by Adli Hasan DN: C=NZ, CN=Adli Hasan, E=a.hasan@massey.ac.nz Reason: I am the author of this document Location: your signing location here Date: 2022.12.13 19:04:00+13'00' Foxit PDF Reader Version: 11.0.0*
Date:	13-Dec-2022
Primary Supervisor's Signature:	Mathew Legg *Digitally signed by Mathew Legg DN: cn=Mathew Legg, c=NZ, email=m.legg@massey.ac.nz Date: 2022.12.15 12:41:46 +13'00'*
Date:	15-Dec-2022

This form should appear at the end of each thesis chapter/section/appendix submitted as a manuscript/ publication or collected as an appendix at the end of the thesis.

STATEMENT OF CONTRIBUTION
DOCTORATE WITH PUBLICATIONS/MANUSCRIPTS

We, the candidate and the candidate's Primary Supervisor, certify that all co-authors have consented to their work being included in the thesis and they have accepted the candidate's contribution as indicated below in the *Statement of Originality*.

Name of candidate:	Adli Hasan Bin Abu Bakar
Name/title of Primary Supervisor:	Mathew Legg

In which chapter is the manuscript /published work: 4

Please select one of the following three options:

◉ The manuscript/published work is published or in press

- Please provide the full reference of the Research Output:

A. H. A. Bakar, M. Legg, D. Konings, F. Alam. The effects of dispersion on time-of-flight acoustic velocity measurements in a wooden rod. Ultrasonics (2022) 106912 doi:10.1016/j.ultras.2022.106912

◯ The manuscript is currently under review for publication – please indicate:

- The name of the journal:

- The percentage of the manuscript/published work that was contributed by the candidate: 80.00

- Describe the contribution that the candidate has made to the manuscript/published work:

The candidate conducted the experiments, performed data collection and analysis and produced the first draft of the manuscript.

◯ It is intended that the manuscript will be published, but it has not yet been submitted to a journal

Candidate's Signature:	*Digitally signed by Adli Hasan DN: C=NZ, CN=Adli Hasan, Email=a.hasan@massey.ac.nz Reason: I am the author of this document Location: your signing location here Date: 2022.12.13 19:04:11+13'00' Foxit PDF Reader Version: 11.0.0*
Date:	13-Dec-2022
Primary Supervisor's Signature:	Mathew Legg *Digitally signed by Mathew Legg DN: cn=Mathew Legg, c=NZ, email=m.legg@massey.ac.nz Date: 2022.12.15 12:42:13 +13'00'*
Date:	15-Dec-2022

This form should appear at the end of each thesis chapter/section/appendix submitted as a manuscript/ publication or collected as an appendix at the end of the thesis.

STATEMENT OF CONTRIBUTION
DOCTORATE WITH PUBLICATIONS/MANUSCRIPTS

We, the candidate and the candidate's Primary Supervisor, certify that all co-authors have consented to their work being included in the thesis and they have accepted the candidate's contribution as indicated below in the *Statement of Originality*.

Name of candidate:	Adli Hasan Bin Abu Bakar
Name/title of Primary Supervisor:	Mathew Legg

In which chapter is the manuscript /published work: 5

Please select one of the following three options:

○ The manuscript/published work is published or in press

- Please provide the full reference of the Research Output:

○ The manuscript is currently under review for publication – please indicate:

- The name of the journal:

- The percentage of the manuscript/published work that was contributed by the candidate: 80.00

- Describe the contribution that the candidate has made to the manuscript/published work:

The candidate conducted the experiments, performed data collection and analysis and produced the first draft of the manuscript.

◉ It is intended that the manuscript will be published, but it has not yet been submitted to a journal

Candidate's Signature:	*[signature]* Digitally signed by Adli Hasan DN: C=NZ, CN=Adli Hasan, E=a.hasan@massey.ac.nz Reason: I am the author of this document Location: your signing location here Date: 2022.12.15 12:37:47+13'00' Foxit PDF Reader Version: 11.0.0
Date:	15-Dec-2022
Primary Supervisor's Signature:	Mathew Legg Digitally signed by Mathew Legg DN: cn=Mathew Legg, c=NZ, email=m.legg@massey.ac.nz Date: 2022.12.15 12:42:46 +13'00'
Date:	15-Dec-2022

This form should appear at the end of each thesis chapter/section/appendix submitted as a manuscript/ publication or collected as an appendix at the end of the thesis.

MASSEY UNIVERSITY
TE KUNENGA KI PŪREHUROA

UNIVERSITY OF NEW ZEALAND

GRADUATE RESEARCH SCHOOL

STATEMENT OF CONTRIBUTION
DOCTORATE WITH PUBLICATIONS/MANUSCRIPTS

We, the candidate and the candidate's Primary Supervisor, certify that all co-authors have consented to their work being included in the thesis and they have accepted the candidate's contribution as indicated below in the *Statement of Originality*.

Name of candidate:	Adli Hasan Bin Abu Bakar
Name/title of Primary Supervisor:	Mathew Legg

In which chapter is the manuscript /published work:	Appendix 4

Please select one of the following three options:
.

● **The manuscript/published work is published or in press**

- Please provide the full reference of the Research Output:

A. H. A. Bakar and M. Legg. Non-destructive testing on a wooden cylindrical rod using guided wave and shear transducer arrays, in Acoustics 2022 - The nature of acoustics, Wellington, New Zealand, 2022.

○ **The manuscript is currently under review for publication – please indicate:**

- The name of the journal:

- The percentage of the manuscript/published work that was contributed by the candidate: 80.00

- Describe the contribution that the candidate has made to the manuscript/published work:

The candidate conducted the experiments, performed data collection and analysis and produced the first draft of the manuscript.

○ **It is intended that the manuscript will be published, but it has not yet been submitted to a journal**

Candidate's Signature:	*[signature]* Digitally signed by Adli Hasan DN: C=NZ, CN=Adli Hasan, Email.hasan@massey.ac.nz Reason: I am the author of this document Location: your signing location here Date: 2023.07.01 17:26:35+12'00' Foxit PDF Reader Version: 11.0.0
Date:	01-Jul-2023
Primary Supervisor's Signature:	Mathew Legg Digitally signed by Mathew Legg DN: cn=Mathew Legg, c=NZ, email=m.legg@massey.ac.nz Date: 2023.07.01 19:04:30 +12'00'
Date:	1-Jul-2023

This form should appear at the end of each thesis chapter/section/appendix submitted as a manuscript/ publication or collected as an appendix at the end of the thesis.

STATEMENT OF CONTRIBUTION
DOCTORATE WITH PUBLICATIONS/MANUSCRIPTS

We, the candidate and the candidate's Primary Supervisor, certify that all co-authors have consented to their work being included in the thesis and they have accepted the candidate's contribution as indicated below in the *Statement of Originality*.

Name of candidate:	Adli Hasan Bin Abu Bakar
Name/title of Primary Supervisor:	Mathew Legg

In which chapter is the manuscript /published work: Appendix 5

Please select one of the following three options: .

(●)   The manuscript/published work is published or in press

- Please provide the full reference of the Research Output:

A. H. A. Bakar and M. Legg. Experimental measurement of phase velocity of ultrasonic guided waves using wave propagation theory, in Acoustics 2022 - The nature of acoustics, Wellington, New Zealand, 2022.

(○)   The manuscript is currently under review for publication – please indicate:

- The name of the journal:

- The percentage of the manuscript/published work that was contributed by the candidate: 80.00

- Describe the contribution that the candidate has made to the manuscript/published work:

(○)   It is intended that the manuscript will be published, but it has not yet been submitted to a journal

Candidate's Signature:	*[signature]* Digitally signed by Adli Hasan DN: C=NZ, CN=Adli Hasan, E=a.hasan@massey.ac.nz Reason: I am the author of this document Location: your signing location here Date: 2023.07.01 17:29:18+12'00' Foxit PDF Reader Version: 11.0.0
Date:	01-Jul-2023
Primary Supervisor's Signature:	Mathew Legg Digitally signed by Mathew Legg DN: cn=Mathew Legg, c=NZ, email=m.legg@massey.ac.nz Date: 2023.07.01 19:05:04 +12'00'
Date:	1-Jul-2023

This form should appear at the end of each thesis chapter/section/appendix submitted as a manuscript/ publication or collected as an appendix at the end of the thesis.